Photovoltaics International

Edition 38

As-grown bulk lifetime

University of New South Wales on an issue of increasing relevance for c-Si cell performance

One-roof manufacturing

The gold standard for module reliability and consistency?

Bifacial PERC+ cells and modules

ISFH on the status and prospects for industrial implementation

Bifacial performance

Fraunhofer ISE researchers present new tools for calculating bifacial cell-to-module lossses

Mono PERC

TongWei's roadmap for mass-produced, high-efficiency mono crystalline PERC cells

Diamond-wire-sawn silicon etching

Fraunhofer ISE on the state-of -the-art in multi-Si texturing

www.pv-tech.org PV TECH

While every effort has been made to ensure
the accuracy of the contents of this journal,
the publisher will accept no responsibility for
any errors, or opinion expressed, or omissions,
or for any loss or damage, consequential or
otherwise, suffered as a result of any material
here published.

Cover image: Hanwha Q CELLS' solar cell
production line

Image courtesy of Hanwha Q CELLS

Printed by Buxton Press

Foreword

Welcome to the 38th edition of Photovoltaics International. There is every sign that 2018 is going to be a huge year for the industry as manufacturers continue investing in new tools and technologies. We will doubtless see many of the innovations whose evolution has been documented in these pages becoming increasingly mainstream.

The Institute for Solar Energy Research Hamelin (ISFH) and Meyer Burger Technology AG present a novel bifacial module architecture (p.46). Their technical paper describes a PERC+ bifacial module with 18 Smart Wire connections to the Ag front and Al rear fingers.

Sticking with bifacial solar, Fraunhofer ISE takes a wide-ranging look at a number of challenges surrounding the technology's leap to widespread deployment. The institute's researchers model the cell-to-module losses and offer a system-level assessment of bifacial gains with a view to improving yield predictions for bifacial plants (p.87).

A second paper from Fraunhofer ISE looks at another of the hot topics dominating solar manufacturing right now. Diamond-wire sawing is becoming increasingly prevalent but the trade-off for its materials savings is the smooth surface it leaves behind. Fraunhofer looks at the range of texturing options on offer and the commercial tools already in the market (p.56).

The University of New South Wales, Trina Solar and BT Imaging give a suggestion for predicting the variation in multicrystalline cell performance by measuring the bulk lifetime of ingots (p.34).

We also have a look at PV recycling and lifecycle management from First Solar (p.26), PI Berlin's assessment of PID issues in thin-film solar (p.75) and TongWei presents a roadmap for PERC cells with 22% efficiency (p.67).

Finally, we must end with a tribute to Professor Stuart Wenham who sadly passed away on 23 December 2017 after a short battle with cancer. He was an influential figure among the University of New South Wales' prolific PV research team. Their work has facilitated cost reductions measured not in percentage points but in orders of magnitude. In addition to the giant contribution that he made to the field, the warmth of tributes from close colleagues and friends is evidence of the contribution he made with his character and personality.

John Parnell
Head of Content
Solar Media Ltd

Editorial Advisory Board

Photovoltaics International's primary focus is on assessing existing and new technologies for "real-world" supply chain solutions. The aim is to help engineers, managers and investors to understand the potential of equipment, materials, processes and services that can help the PV industry achieve grid parity. The Photovoltaics International advisory board has been selected to help guide the editorial direction of the technical journal so that it remains relevant to manufacturers and utility-grade installers of photovoltaic technology. The advisory board is made up of leading personnel currently working first-hand in the PV industry.

Our editorial advisory board is made up of senior engineers from PV manufacturers worldwide. Meet some of our board members below:

Stand the test of Time

EUPD RESEARCH
TOP BRAND PV
MODULES
NETHERLANDS
2017

EUPD RESEARCH
TOP BRAND PV
MODULES
GERMANY
2017

SUNTECH

网址: *www.suntech-power.com*

Contents

31

73

84

CONFERENCE
PVCELLTECH

13-14 March 2018
Penang, Malaysia

In just two years, PV CellTech has become the must-attend event to understand the roadmaps of the leading cell producers.
Don't miss being part of this exclusive group of technology experts in 2018!

"PV Celltech addresses the important questions in PV and Solar Media is able to attract high level CTO's to this event to discuss these questions and condenses it all into 2 days with enough time for discussions"
Holger Neuhaus, SolarWorld

"No other event brings together the leaders from the leading manufacturers. The one, not to be missed, conference for cell producers"
Peter Cousins, SunPower

"PV Celltech will, or has, become the leading conference bridging technology and manufacturing"
Don Cullen, Macdermid Enthone

"Wonderful! High velocity, intense, interactive and loads of learning. Thank you"
Paul Gupta, IndoSolar

#PVCELLTECH

celltech.solarenergyevents.com

To get involved either as a speaker, partner or attendee please email: marketing@solarmedia.co.uk

PVTECH   Photovoltaics International   SOLAR MEDIA
EVENTS | PUBLISHING | RESEARCH

Product reviews

Materials: **DKEM**

DKEM has developed DK92K metallization paste to solve different passivation technology challenges for PERC solar cells

Product Outline: DK92K has been developed to be compatible with different passivation technologies and processes for PERC solar cells.

Problem: The consistency of performance and productivity of PERC technology is not expected to be well achieved with different passivation technologies such as ALD (spatial ALD and time-based dual-side passivated ALD), PECVD (remote plasma and direct plasma) as well as other non-AlOx passivation solutions because of the intrinsic limitation of conventional front-side silver paste. One of the challenges for time-based dual-side passivated ALD technology is the need to etch the SiNx/AlOx stacked layer to form a good Ohmic contact with the emitter due to the mismatch between front-side silver paste and dual-side passivated AlOx and the significant increase of series resistance and ratio of EL darkness of cells and modules.

Solution: DKEM's DK92K paste is claimed to lower firing temperatures by 10-15 degrees C compared to DKEM's previous DK91B paste. The DK92K paste is claimed to demonstrate a superior process window and compatibility with different contact requirements and diversified passivation technologies and processes. Specifically for dual-side passivated ALD, a breakthrough of front-side silver paste has been achieved with improved Ohmic contact. Furthermore, DK92K paste could solve the wrap-around deposition issue of AlOx on the front-side of PERC cells and rear-side of n-PERT cells if the passivation process is not fully optimized.

Applications: Metallization of PERC cells.

Platform: DK92K front-side silver paste for black silicon multicrystalline PERC cells and monocrystalline PERC solar cells provides superior low-temperature firing property and contact window enlarged to >120 Ohm/sq and >100 Ohm/sq, respectively.

Availability: Currently available.

Materials: **Heraeus**

Heraeus launches SOL9651D paste for diamond-wire-cut multicrystalline solar cells

Product Outline: Heraeus Photovoltaics has introduced a new paste specifically designed for diamond-wire-cut (DWC) multicrystalline solar cells.

Problem: The SOL9651D series front-side silver paste was developed by Heraeus in response to the growing industry adoption of DWC multicrystalline solar cells with a specially textured surface. Industry analysts expect DWC cells to have 80% market share by the end of 2018. When products like DWC quickly emerge to become the de-facto industry choice for cell manufacturers, it is critical that the right paste be ready and capable to deliver.

Solution: For companies using DWC cells, SOL9651D is specifically designed to provide a wide range of capabilities and benefits, including: raising the conversion efficiency of DWC cells by >0.1% as well as superior busbar adhesion and reliability on DWC cells with additive/MCCE/RIE-texturing techniques. It has ultra-fine-line compatibility for additional efficiency gain on specially textured DWC cells, while providing a balanced metallization contact and Voc with efficiency improvement.

Applications: Single and double screen printing as well as knotless screens packages.

Platform: The new glass chemistry was developed to provide excellent adhesion of SOL9651D, which allows customers to optimize their busbar design for better electrical performance and cost reduction, especially on DWC/black-silicon texturing. Additionally, this paste series has a wide firing window, which makes the paste specifically suitable for PERC solar cells. It shows superior adhesion for PERC and is compatible for both multi- and monocrystalline wafers. As testified by customers, SOL9651D Series has outstanding (light-induced degradation (LID) performance by reducing the negative impact of irradiation of the charge carrier lifetime.

Availability: Available since October 2017.

PV Modules: **HT-SAAE**

HT-SAAE's HyperC PV module series reaches 300W with mono PERC performance

Product Outline: Shanghai Aerospace Automobile Electromechanical Co., (HT-SAAE) has introduced a new lineup of high-efficiency monocrystalline PV modules under its 'HyperC' Series brand. The HyperC PV module series adopt the PERC technology developed by HT-SAAE, making the cell efficiency for mass production of up to 21.2%.

Problem: High-efficiency PV modules are increasingly being used for residential rooftop PV systems as incentives typically have declined under FiT (feed-in tariffs). PERC technology plays a major role in enhancing cell efficiency and adding value to PV modules. On the premise that costs can be controlled and savings maintained, it can significantly improve module performance and reduce the cost of power generation, leading to additional electricity benefits and higher return on investment.

Solution: The HyperC Series PV modules feature five-busbar cell technology, advanced surface treatment processes, anti-PID cells and high reliability encapsulation material. They come with lower series resistance, higher cell conversion efficiency and higher power output per unit, according to the company.

Applications: Residential, commercial and utility-scale power generation.

Platform: The HyperC includes techniques developed and deployed with the company's 'HIGHWAY' series such as PERC cell technology with five busbars and lower series resistance with output power of 300W and above for a 60-cell module. The HyperC PV modules have passed triple high quality control EL tests and bring together anti-PID and anti-micro-crack characteristics.

Availability: Currently available.

inter solar

connecting solar business

Join the world's leading exhibition series
for the solar industry

INTERSOLAR
EVENTS
2018

www.intersolar-events.com

JUNE 20–22, 2018, MUNICH, GERMANY

THE WORLD'S LEADING
EXHIBITION FOR THE SOLAR INDUSTRY
www.intersolar.de

JULY 10–12, 2018, SAN FRANCISCO, USA

NORTH AMERICA'S PREMIER EXHIBITION
AND CONFERENCE FOR THE SOLAR INDUSTRY
www.intersolar.us

AUGUST 28–30, 2018, SÃO PAULO, BRAZIL

SOUTH AMERICA'S LARGEST EXHIBITION
AND CONFERENCE FOR THE SOLAR INDUSTRY
www.intersolar.net.br

DECEMBER 11–13, 2018, MUMBAI, INDIA

INDIA'S LARGEST EXHIBITION AND
CONFERENCE FOR THE SOLAR INDUSTRY
www.intersolar.in

SUMMIT

INTERSOLAR SUMMIT USA
APRIL 4, 2018, NEW YORK
www.intersolar-summit.com

FOLLOW US

News

Gintech, NSP and Solartech to merge and drop merchant business model

Three of Taiwan's merchant solar cell and module producers, Gintech Energy Corp, Neo Solar Power (NSP) and Solartech Energy have officially announced plans to merge and exit the 'foundry' business model they were founded on.

The three companies said in a joint statement that as they were dealing with a "highly competitive and increasingly concentrated market, the companies believe that Taiwanese manufacturers should come together to form a solar flagship company with a competitive edge on the global market and build a flourishing and prosperous integrated platform".

To comply with Taiwanese laws, the three companies said that they had agreed that NSP would be the surviving company after it merges with the other two partners.

The companies hope to have a legally binding merger agreement signed by the end of December, 2017 and to complete a merger process within the third quarter of 2018.

After the proposed merger, Dr. Sam Hong (NSP) and Dr. Wen-whe Pan (Gintech) are expected to serve as the Chairman and CEO of UREC, respectively.

Under UREC, the new company would have wafer, cell, module and downstream capabilities, in line with the vertically integrated business model as well as manufacturing operations in China and South East Asia.

Credit NSP

NSP, Gintech and Solartech are to merge and undergo a major shift in business model.

COMPANY STRATEGY

LONGi highlights strategic goals at inaugural PV ModuleTech

LONGi Green Energy Technology, the largest integrated monocrystalline manufacturer, revealed its key strategic goals for 2019 at the inaugural PV ModuleTech conference held in Kuala Lumpur, Malaysia, in November.

In a key presentation, "The mono transition to high performance PERC and bifacial modules as the industry standard", Dr. Qiangzhong Zhu, assistant vice president at LONGi Solar, highlighted its drive to provide the solar industry with the products to back up the transition to monocrystalline technology.

With its recent marketing launch of PV 3.0, encompassing the next wave of high-performance, high-reliability and high energy yield modules and systems, Dr. Zhu noted that PV 3.0 also embraces cost competitiveness and, with p-type mono PERC technology, could achieve conversion efficiencies of around 24.5%.

Such will be the transition to mono PERC that LONGi believes modules with mono cells may make up over half of all module capacity by 2020, providing around 61GW of supply, and that most of the modules would be using mono cells with PERC technology.

However, according to Dr Zhu, to achieve these goals, high-quality wafers are important for PERC efficiency gains topping 24% targets. Using a third-party demo plant in Taizhou, China had demonstrated that the energy yield of its Hi-MO1 mono-PERC module was about 3% higher than a polycrystalline module. The energy yield gain of Hi-MO1 was said to be mainly attributable to better low irradiation performance and improved temperature coefficient.

ReneSola exits solar manufacturing

China-based PV manufacturer and downstream project developer ReneSola has officially completed the divestment of its integrated solar manufacturing operations to its chairman and CEO to focus exclusively on downstream business development.

Xianshou Li, chairman and CEO of ReneSola noted that the transaction transformed ReneSola into a pure-play solar downstream player with very little debt.

ReneSola recently said in releasing second quarter 2017 financial results that its late-stage downstream project pipeline was around 480MW with plans for PV power plants in the US, U.K, Turkey, Japan, Canada, France, Poland Thailand, and China, while its early stage projects stood at around 1GW.

The company plans to build and sell around 100MW of projects overseas in 2018 and build and retain around 400MW in China.

JA Solar leaving NASDAQ in all-cash transaction

'Silicon Module Super League' (SMSL) member JA Solar is following another SMSL member, Trina Solar in leaving the NASDAQ and going private via an all-cash transaction led by its founder, chairman and CEO, Baofang Jin.

JA Solar said that it would be acquired by an investor consortium, primarily by Jin and other controlling shareholders in an all-cash transaction, which the company said implied an equity value for JA Solar of approximately US$362.1 million.

Jin and its 'Rollover Shareholders' within the buyer group are funding the acquisition with a loan of US$160 million from CSI Finance Limited part of CITIC Bank China and Credit Suisse, Singapore Branch.

JA Solar is leaving the NASDAQ exchange and going private.

PI Berlin creates Indian subsidiary, acquires SolarBuyer

PV consultancy PI Berlin has formed a subsidiary based in Delhi, India, due to a high demand for laboratory testing and quality assurance in solar projects and equipment.

Much has been said about quality issues in India, particularly given that roughly 90% of the modules used in the market are imported from China, with selection often heavily price-driven. Some studies have found significant drops in module performance in India in just the first three years.

In a release, PI Berlin said the arid deserts and tropical forests of the subcontinent make inspection of components and system design "extremely challenging". The company added that its services can identify errors made during plant planning, module production, transport or installation. It also highlighted the need to remedy issues at an early stage before PV projects become operational.

In related news, PI Berlin in mid-December announced the acquisition of the US company SolarBuyer. SolarBuyer is a provider of risk management and quality assurance services for buyers and investors in the solar industry.

Heraeus opens Delhi office to serve Indian market

Metallization paste producer Heraeus Photovoltaics has opened a new office in Delhi and brought on more staff at its Engineering & Technology Centre in Singapore to help focus on the Indian market.

Announcing the launch of a dedicated local sales team at the REI Expo in Delhi, Heraeus said it was also looking to boost its customization of silver pastes for Indian cell manufacturers as well as offering cell optimization consulting.

Ilke Verena Luck, Heraeus global head of new product development and technology, told PV Tech that the Singapore office helps Heraeus be close to its customers as the many markets in Southeast Asia emerge.

Heraeus has a strong market share in India and works closely with Adani, one of the largest manufacturers in India.

POLICY AND MARKETS

ARENA awards AU$29 million to help spur development of PV technology

As part of an initiative by the Australian government, the Australian Renewable Energy Agency (ARENA) awarded a total of AU$29.2 million for 20 research projects to propel the development of PV technology.

The funding was offered to research teams from the University of New South Wales, Australian National University, Monash University and the Commonwealth Scientific and Industrial Research Organisation (CSIRO).

ARENA's third round of R&D funding supports early research designed to both cut costs and boost the efficiency of PV.

Many of these projects will focus on silicon technologies, as a large number of solar panels are currently made using silicon. Other projects will look to develop solar cells using new materials — such as organic photovoltaics and perovskites.

Along with contributions from industry partners and leading institutions from Asia, Europe and the United States, the total value of the projects is approximately AU$102 million.

India proposes US$1.7 billion support for local solar manufacturers and 12GW CPSU scheme

Aiming to make its local solar manufacturers competitive on the global stage, the Indian government has proposed direct financial support of INR110 billion (US$1.7 billion) and a 12GW allocation of public sector tenders mandated to include locally sourced PV equipment.

The Ministry of New and Renewable Energy (MNRE) issued a number of policy support proposals in early December and is now seeking comments from stakeholders by the end of 2017.

Intentions to encourage production of polysilicon, wafers and ingots from scratch, rather than just cells and modules, featured prominently in the proposals.

MNRE divulged that as of 31 July this year, installed capacity of cells and modules in India stood at 3.1GW and 8.8GW respectively. More importantly, it noted that actual capacity utilisation of this stands at just 1.5GW for cells and 2-3GW for modules and it blamed this on "stiff competition from imports".

The ministry also highlighted that current cell manufacturing capabilities are well below the 20GW per annum required for India's downstream targets.

In addition to the INR110 billion of direct financial support, the Indian government has also proposed a 'central public sector undertakings' with a local content carve-out to 12GW, a plan that many local manufacturers have been calling for them to carry out capacity expansions with confidence brought by an "assured DCR [domestic content] component".

The Indian government is introducing financial and policy support for domestic PV manufacturers.

Credit Indosolar

A 'quality order' for cells and modules has also been brought in. In light of this, the DCR will be reviewed annually to mandate a certain percentage of cells in the programme to be of higher quality, with this percentage and level of quality to increase each year.

Global solar demand in 2017 set for 100GW milestone – SolarPower Europe

Solar trade association SolarPower Europe has updated its global solar demand forecast for 2017, expecting to reach the 100GW level for the first time.

SolarPower Europe said that with global demand reaching 100GW, compared to 76.6GW installed in 2016, annual will be more than 30% in 2017.

The trade group had expected only slight demand growth year-on-year, previously guiding installations could reach as much as 80GW in 2017.

The real driver for strong demand in 2017 has come from China.

The trade group said: "China alone has installed around 42GW in the first nine months of 2017 and is likely to add a total of over 50GW in 2017, which would account for more than half of the world's demand for new solar power capacities this year. This constitutes a 45% growth from the 34.5GW China installed last year."

However, SolarPower Europe noted that in its latest analysis estimates, Europe would also be a small contributor to the 2017 growth levels with installations expected to be around 10% higher than in 2016, with at least 7.5GW grid connected.

In 2016, the European market actually declined by around 20% from 2015, to 6.7 GW, according to SolarPower Europe.

Section 201 tariff could halve utility-scale deployment in US: GTM

A US$0.40/W tariff resulting from the Section 201 case would halve utility-scale deployment in the US between 2018-2022, according to GTM Research.

The company also noted however, that the utility-scale sector could ride-out the impacts of a US$0.10/W tariff with a drop of 9% expected.

The International Trade Commission (ITC) will vote on recommended remedies, including potential tariffs on 31 October before President Trump makes his final determination in January next year.

GTM's report attempts to assess the impact on the industry in the event of tariffs.

"First, we estimate that there will be nearly 5GW of solar capacity that is not subject to tariffs, either because it is not subject to the scope of the petition (i.e. thin film) or because both the cells and modules are manufactured in the US, Korea, Singapore, Canada or Australia, all of which may be exempt. In addition, over 2GW of modules have already been procured for 2018 projects, which will temporarily dampen the tariffs' impact on demand."

Singapore, Canada and Australia are currently exempted from any 201 tariffs however the petitioners, SolarWorld Americas and Suniva, are pressing the ITC to close any "loopholes" that would enable products partly manufactured in other countries to be finished in these nations.

GTM, which is openly against the 201 case, also warns that states with emerging residential markets could struggle to overcome the impact of increased module prices.

Manufacturing under one roof: the gold standard for module consistency and reliability?

Finlay Colville | Head of Market Research | Solar Media

Abstract

Having all manufacturing stages – from raw materials to finished modules – located under one roof in the same factory offers the scope to optimize module quality and reliability. Most c-Si module suppliers today use multiple sites in different countries with flexible outsourcing to third parties. Thin-film manufacturing remains the only single-product/single-site technology for solar currently using the one roof approach.

When manufacturing capacities moved from megawatt to gigawatt 10 years ago, the concept of having a fully integrated and automated production site was widely accepted to be the most effective route to capitalize on the economy-of-scale attributes from having all steps in the raw-materials-to-finished-goods value-chain managed under one roof.

This concept was promoted widely in the past with the emphasis being that a single production facility is uniquely positioned to control production costs in-house. It often formed the basis of the marketing approaches taken by turnkey production line suppliers (across both c-Si and thin-film technologies) and from regional groups promoting domestic production with local jobs.

However, approaching the end of 2017 – a year in which the solar industry is expected to ship close to 100GW of modules – the inherent benefits of the fully integrated fab (that addresses the product quality and reliability metrics behind bankability) have been adopted by remarkably few (if any) c-Si based multi-gigawatt-level module suppliers.

This article explains how this situation has

First Solar is one of the few major PV manufacturers operating a genuine one-roof approach to production.
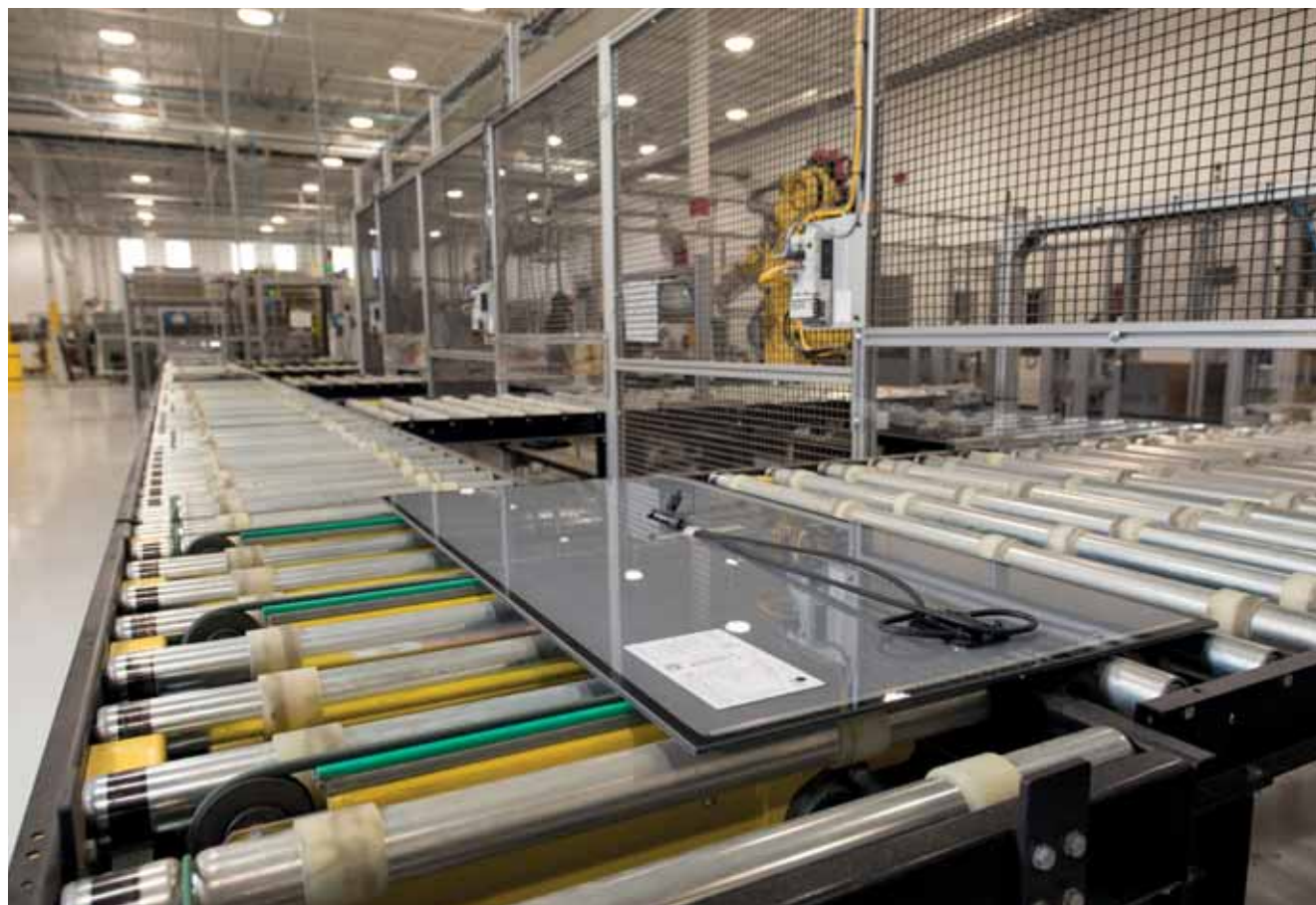
First Solar

Hanwha Q CELLS

Hanwha Q CELLS and JA Solar have the highest percentage of in-house cell and module production of the major suppliers.

evolved; and why the current trend of c-Si module suppliers to run multiple production sites (often across different countries and continents) with strong levels of sub-contracting (frequently changing), is adding to the risk profile of investors and asset owners.

These core themes formed the basis of the inaugural PV ModuleTech 2017 conference in Kuala Lumpur, Malaysia, in November 2017, organized by Photovoltaics International publisher, Solar Media.

What is the one roof/factory model?

Manufacturing solar modules (or panels) remains a highly complex process, with multiple stages in production from raw materials supply (polysilicon chunks for c-Si, glass panels and semiconductor materials for thin film) to finished modules.

Modules are far from commoditized products, a fact often misinterpreted by the industry or miscommunicated across downstream stakeholders. Solar modules have to perform with predictable and reliable performance for 25+ years, often in harsh and demanding environments.

Return on investment, for the homeowner with a kilowatt-sized installation, to a several hundred megawatt utility solar farm, is critically dependent on the choice of modules and module suppliers, and the ability of investors to perform the necessary in-depth technical and commercial auditing of the issues important to manufacturing.

Modules based on c-Si have four basic stages in

the value chain, if we classify polysilicon as the raw material source:

- Ingot pulling (for mono) or casting (for multi)
- Wafer slicing
- Cell production
- Module production

The original concept of the one-roof/factory model for c-Si was based on having all four stages within a single integrated fab. This was proposed mainly to bring down (non-silicon) production costs.

However, this model never came to fruition for c-Si module suppliers, due to many reasons. Perhaps this explains why the c-Si sector generally does not discuss the one-roof model as being important to drive product consistency, quality and reliability, and bankable single bills of materials (BOMs).

The reality of c-Si production today could in fact not be more different, shaped by having discrete companies dominating the ingot/wafer supply chain, and cell/module diversity that has become a complicated and moving target, pushed and pulled by constant trade-related origin of manufacturing-based rules and regulations.

This can be seen clearly across all GW-level c-Si module suppliers today, where ingot and wafer supply is primarily done by different companies, often located in different countries. In fact, ingot pulling/casting and wafer slicing facilities are

typically in different factories or locations even for the major suppliers that have evolved with balanced ingot/wafer capacities.

Outsourced sub-contracting is also employed for each of these stages on a regular basis, especially when market demand and sales pipelines fluctuate, often to companies that most people outside China or Taiwan will not be aware of.

Cell and module c-Si manufacturing is even more diverse, and it is not uncommon for cell and module factories to be concentrated at different manufacturing sites, either hundreds of miles apart in the same country, or located in different countries altogether.

The supply chains for leading c-Si module suppliers become further complicated owing to the high levels of outsourcing to third-party cell and module producers. Many of these third-party producers have evolved quickly across Southeast Asia in an attempt to circumvent made-in-China import barriers for shipping c-Si modules into Europe or the US.

Therefore, when trying to qualify c-Si module suppliers from a technical or commercial due-diligence perspective (factors that underpin bankability), the range of companies making the components of the module – including their respective BOMs, processes, quality checks and financial health – is anything but simple and transparent.

The challenge in terms of module authenticity goes way beyond the name of the company appearing on the final module product being sold. Indeed, for many buyers of c-Si modules, there can be limited documentation provided to clarify if the modules were in fact made in-house by the company selling them, or by tolled or contracted third parties

Hanwha Q CELLS and JA Solar are the leading multi-GW c-Si module suppliers with the highest percentage of in-house produced cells and modules used within their company-branded modules. However, in common with almost all other leading c-Si module suppliers, each has multiple cell and module locations in different countries making a range of c-Si module types (mono, multi, black-silicon, PERC, 60- and 72-cell modules etc.).

This goes a long way to explaining why there are so many organizations, approaches and methodologies involved in third-party module testing, certification, factory auditing and bankability reporting within the c-Si segment of the solar industry today; and indeed why this group of third parties is so vital for module buyers and investors.

It also explains why EPCs, project developers and investors simply have to get more educated on the full audit trail of companies, processes and materials involved in the selection of modules used at their sites.

This is especially true for final asset owners, many of whom enter solely in the secondary market buying completed solar farms, having had no involvement at all in decision-making processes for component supply or build-quality of their acquired assets.

Where thin film differs from c-Si

Thin-film solar manufacturing, where semiconductor layers are deposited on glass panels, remains the one differentiated product offering to the solar industry today. Broadly speaking, there have been three different technical approaches taken by companies over the years: CdTe, CIGS and a-Si.

Attempts by companies to commercialize a-Si based variants went through a brief period many years ago, before limitations on panel efficiencies, high manufacturing costs and equipment reliability ultimately rendered this technology obsolete in the solar industry today. Only two companies succeeded in ramping thin-film approaches to the GW or multi-GW levels in manufacturing: First Solar for CdTe and Solar Frontier for CIGS.

Currently, First Solar is the only company to reach multi-GW levels of thin-film capacity that has been fully utilized with factory/process duplication across multiple sites.

Thin-film production is inherently a single-location manufacturing technology, and as such, it could be argued that First Solar is the only major GW-level solar module producer (across both c-Si and thin-film) that can lay claim to operating the one-roof model, and furthermore rolling out identical factories in different locations with the same production equipment and materials suppliers.

One roof, one process, one BOM and the role of R&D

Another key point inherent to the one-roof concept – that has been somewhat lost during the industry growing from 10GW to 100GW annual demand – relates to the ability to focus R&D efforts and BOM consistency into one manufacturing process or product only, in a repeatable and predictable manner.

The R&D issue is particularly revealing in this respect, as highlighted recently in a piece of analysis undertaken by *Photovoltaics International*'s sister website PV Tech looking at 10 years of R&D spending by 12 key PV module manufacturers [1].

There are many factors driving R&D spending levels, and often it simply comes down to the company's balance-sheet and long-term investment strategy.

However, for years it has been a source of confusion why the vast majority of c-Si module leaders have been allocating R&D budgets in the single-digit percentage levels (of turnover), a figure markedly lower than seen across adjacent technology sectors such as semiconductor and displays.

Perhaps, though, much of this can be traced to the lack of companies that have in-house control over all stages of the value chain in producing 100% of the module components (whether under one roof or not). Add to this product variety across c-Si module types, and it raises the question of where to even allocate R&D efforts, far less what sums are being budgeted.

In looking at the 10-year R&D summary graphic at the company level in the above-cited article (Figure 1), this goes some way to explain why First Solar has been in a position to channel R&D funds at much higher levels than the industry norm.

In the c-Si space, only SunPower (from the companies sampled in the 12 key manufacturers) has had a consistently high level of R&D spending in the last 10 years, with much of this traced back to the one-process approach (IBC cells) and proprietary ownership of all in-house equipment and manufacturing steps, although mainly at the cell stage. SunPower's R&D spending has historically been spread across different technology types, including the dormant CPV efforts and the existing Chinese joint venture project for singulated cell-based modules.

In addition to the ability to focus all R&D spending into one manufacturing process flow, the other main difference in the one-roof approach is having a single BOM for all modules produced. The implications of this are possibly yet to be fully appreciated, but it certainly explains the attention on module encapsulants, for example. If substandard materials are used for encapsulants, module performance in humid (or other harsh) climates can suffer dramatically.

Module BOM traceability is rapidly becoming one of the most discussed, debated and dissected issues for utility-scale solar farms, with asset owners and O&Ms often being the ones burdened by underperforming modules whose failure modes can be traced back to a lack of quality checks for critical materials used in manufacturing.

Are we likely to see any changes going forward?

In looking at the current in-house manufacturing strategies of leading c-Si module suppliers, there does not appear to be any great momentum to adopt a one-roof/factory approach.

The c-Si manufacturing segment, especially cells and modules, is now embroiled in a round of trade cases, including Section 201 in the US and the new MIP rules (extending import conditions on manufacturing cells and modules to Southeast Asia).

There also remains a desire from leading c-Si module suppliers to set annual shipment guidance above in-house effective capacities, necessitating the continued use of outsourcing through third-party OEMs.

In addition, the c-Si technology landscape is
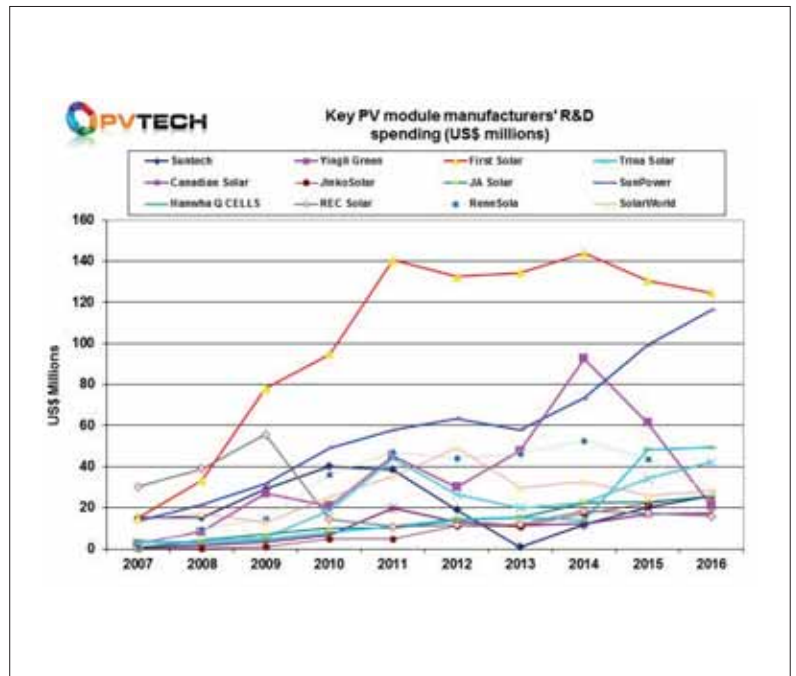
Figure 1. R&D spending levels of 12 major PV module manufacturers from 2007 to 2016.

going through rapid changes from multi to mono, the use of PERC cell types, an increase in the use of 72-cell modules, and even the introduction of glass/glass modules. Therefore, flexibility in supply is almost guaranteed for c-Si module suppliers to retain market-share aspirations.

While the thin-film segment retains a number of small players with limited production capability or global bankability status, this technology segment is certainly going to remain dominated by First Solar, with the company releasing its Series 6 panels in volume next year.

This is an edited version of a blog post that first appeared on www.pv-tech.org

....

References
[1] Osborne, O. 2017, "10 years of R&D spending analysis of 12 key PV module manufacturers", PV Tech, https://www.pv-tech.org/editors-blog/10-years-of-rd-spending-analysis-of-12-key-pv-module-manufacturers

....

About the author

Finlay Colville joined Solar Media in 2015 as head of the new market intelligence activities. Until October 2014, he was vice president and head of solar at NPD Solarbuzz. Widely recognized as a leading authority on the PV industry, he has presented at almost every solar conference and event worldwide, and has authored hundreds of technical blogs and articles in the past few years. He holds a BSc in Physics and a PhD in nonlinear photonics.

News

Planned solar manufacturing capacity expansions bigger than expected in 1H 2017

Global solar PV manufacturing capacity expansion announcements in the first half of 2017 showed a significant increase over the second half of 2016. New plans almost reached the record heights set in the first half of 2016.

The resurgence was overwhelmingly driven by China and the migration to high-efficiency solar cell technologies, compared to a broader geographical split in the prior-year period. Although the second quarter of 2017 surpassed first quarter announcements, major updates to previously reported activity in the last report covering the first quarter of 2017, have also been made.

The first half of 2017 has produced the second (Q2) and fourth (Q1) largest amount of capacity expansion announcements in the history of the solar industry, driven by global end market demand increases that are set to see in excess of 90GW of installations and 100GW of shipments this year. Also fuelling the announcements is the significant migration underway to p-type mono PERC solar cells, although much of what was announced is based on multi-phase multi-year plans, in line with announcements made in the first quarter of 2017.

Credit LONGi

Chinese technology migrations helped explain an increase in capacity expansion announcements in the first half of 2017.

EXPANSIONS

Tongwei initiating 20GW solar cell capacity expansion plans

China-based integrated and merchant PV manufacturer Tongwei Group is starting capacity expansion plans at its subsidiary Tongwei Solar (Hefei) Co at two locations in China at a cost of US$1.8 billion over the next three to five years.

Tongwei has a strategic goal of building a world-class clean energy enterprise and recently opened its high-efficiency monocrystalline solar cell plant in Chengdu, China, with an initial nameplate capacity of 2GW.

The plant also hosts the world's first technically unmanned monocrystalline solar cell production line under the intelligent manufacturing term, 4.0.

Tongwei is investing around RMB12 billion (US$1.8 billion) in total, constructing new cell manufacturing facilities at Hefei Solar's facilities in the Hefei High-tech Industrial Development Zone in Hefei City to provide nameplate capacity of 10GW, while a further 10GW of capacity will be housed in the Southwest Airport Economic Development Zone of Shuangliu District, Chengdu City.

Construction on the new projects is expected to start in November, 2017 and production ramped in phases over the next three to five years.

STRATEGY

Hanwha Q CELLS starts PERC technology migration in China

'Silicon Module Super League' (SMSL) member Hanwha Q CELLS is starting to migrate solar cell capacity at its China-based facilities to PERC technology, highlighting the shift away from standard back side field (BSF) technology for higher conversion efficiencies.

Capital expenditure was being focused in the firm's manufacturing facilities in China to enable the company to have p-type multicrystalline PERC cell production capacity of 1.4GW, while retaining around 1.2GW of BSF production.

Hanwha Q CELLS' in-house cell and module capacity has not increased in 2017 as the company keeps tight control on spending to return to sustainable profitability.

However, with its affiliate Hanwha Q CELLS Korea's expansions in 2017, the group will have access to 8GW of cell and module capacity starting in 2018, up from 6.4GW at the end of the third quarter of 2017.

Hanwha Q CELLS recently reiterated that it expected module shipments in 2017 to be in the range of 5.5GW to 5.7GW.

Meyer Burger to lay off 100 staff in Thun as it shrinks European manufacturing footprint

Leading PV manufacturing equipment supplier Meyer Burger is undertaking another round of cost cutting, product rationalisation and manufacturing restructuring to improve profitability.

Meyer Burger is set to close its manufacturing facility in Thun, Switzerland, which has been the main site for the assembly of its diamond wire wafer cutting tools. The highly successful technology will instead be assembled in China, due to the close proximity to the majority of solar wafer manufacturers.

The shift of diamond wire equipment assembly to China would occur during the course of 2018. The company built the Thun facility, which is also its headquarters in 2012.

It then announced that 100 staff will definitely be let go from its facility in Thun after a consultation procedure was completed on 28 November. However the security of another 60 positions will be dependent on whether

Meyer Burger is planning to lay off 100 staff as part of ongoing restructuring

Credit Meyer Burger

strategic alternatives are found. All the jobs are in manufacturing, logistics, purchasing and production planning.

R&D

Tongwei opens 'world's first' intelligent manufacturing '4.0' solar cell production line

China-based integrated and merchant PV manufacturer Tongwei Group recently opened its completed high-efficiency solar cell plant (S2), which includes the world's first technically unmanned monocrystalline solar cell production line under the intelligent manufacturing term, 4.0.

The S2 plant in Chengdu, China, has an initial nameplate capacity of 2GW, which brings Tongwei's monocrystalline cell capacity to around 3.4GW. The company also has around 2GW of multicrystalline solar cell capacity. The 4.0 cell line is completely unmanned to test intelligent fully automated manufacturing tools and software systems.

Tongwei chose to officially launch the new facility in tandem with a massive ceremony celebrating the company's 35 years of business operations.

The company has also recently completed a 5,000MT polysilicon plant expansion, bringing nameplate production capacity to 20,000MT. However, the company is also undertaking the construction of a new 50,000MT polysilicon plant.

Fraunhofer ISE starts construction of next-gen solar cell laboratory

The Fraunhofer Institute for Solar Energy Systems ISE has started construction of its new 'Centre for High-Efficiency Solar Cells' facility, designed to lead R&D activities in future generations of technology development.

Fraunhofer ISE held a cornerstone ceremony on 4 October 2017 in Freiburg to officially start the construction of the purpose built facility, which is expected to be completed by the end of 2019. German federal and state governments were said to have provided a total of €32.6 million for the new facility.

"We are delighted that in designing the new clean room facilities, we were able to adjust the infrastructure to meet the latest technological challenges," noted institute director Dr. Andreas Bett. "We are grateful to the Federal Ministry of Education and Research (BMBF) and the Federal State of Baden-Württemberg for financing the new laboratory building. With their contributions, they are recognizing the importance of German research activities in the area of photovoltaics."

TUV Rheinland consolidates India testing facilities in state-of-the-art laboratories

TUV Rheinland India, a subsidiary of the TUV Rheinland Group, has opened a new €2.5 million state-of-the-art laboratory at Electronic City in

TUV Rheinland India has opened a new lab in Bangalore to serve India's fast-growing solar market.

Credit TUV

application and R&D centre in Gilching, Germany due to continued demand from a growing customer base.

The new facility includes a wide range of its industrial-grade equipment designed to process different applications in crystalline solar cells, ceramic components, pcb-substrates and other brittle materials such as glass or sapphire.

Earlier in 2017, InnoLas noted that new orders in the first quarter of 2017 exceeded €10 million with the expectation of significant growth during the year, due to the high demand for the Laser Contact Opening (LCO) process for PERC (Passivated Emitter Rear Cell) technology and the increasing interest in LDSE process for advanced P-type solar cells. The company noted the new order intake included a number of key PV manufacturers in Asia, including leading companies in China.

LOCAL MANUFACTURING

India's SECI consults on 'unclear' 20GW solar manufacturing and project capacity plan

Solar Energy Corporation of India (SECI) has issued an expression of interest (EOI) for the setting up of 20GW of vertically integrated solar PV manufacturing capacity in India over the next three years.

In a somewhat muddled EOI, including some contradictory local content target numbers, SECI said it also planned to float a tender for 20GW of solar PV project capacity to be set up by the selected local manufacturers of modules, cells, wafers, ingots and polysilicon. The manufacturers would then supply their own modules to these projects to ensure their own local production is utilized.

There were a number of inconsistencies in the document and it was unclear how a second tender for project development would be carried out. The consultation exercise may allow SECI to clarify some of these thoughts and ideas.

The tentative phasing for setting up the manufacturing capacity is 12 months for modules and cells and 18 months for wafers and ingots from the date of issue of LOI.

Joint ventures, consortiums and companies with existing cell and module capacity, wishing to set up integrated facilities or expand them, will all be eligible to bid in the scheme. 25-year PPAs for the solar projects will be signed with SECI after a tariff-based competitive bidding process.

All projects can be setup in India and the use of available solar parks is permitted. To give even more comfort to the project bidders, SECI will also provide a payment security mechanism. The deadline for submission of EOIs is 11 January 2018.

Out of the 77GW of downstream PV to be tendered by 2020, the Indian government wants local manufacturers to supply a significant proportion of the equipment, to reduce India's overwhelming dependence on module imports from China and Southeast Asia.

Bangalore, India, to provide all testing services under one roof and dramatically reduce turnaround time and accelerate time-to-market for customers.

Growth in PV installations in India is expected to exceed 10GW in 2017 and a number of domestic PV manufacturers are expanding solar cell and module capacity to support India's ambitious plans.

The 14,000 square metre facility in India is the first to combine state-of-the-art laboratories under a single roof. The laboratories include the photovoltaic lab, material testing lab, electrical safety lab, medical lab, battery testing lab and the softlines testing lab.

Key capabilities include X-ray equipment testing, vibration and shock test, wet test and energy efficiency testing. There is a calibration lab for Electromagnetic Interference and Electromagnetic Compatibility testing and measuring equipment, according to TUV Rheinland.

InnoLas invests €3 million in new R&D facility

PV laser technology equipment specialist InnoLas Solutions has opened a new €3 million customer

PV manufacturing capacity expansion announcement plans and analysis for Q3 2017

Mark Osborne, Senior News Editor, Photovoltaics International

Abstract

After the significant upwards revisions made to global solar PV manufacturing capacity expansion announcements in the first half of 2017, which we reviewed in the previous edition of *Photovoltaics International*, the third quarter was characterized by much more tempered plans. The 'Silicon Module Super League' (SMSL) continued to execute on previously announced plans with some adjustments, while others in emerging markets such as Turkey and India retained grandiose nameplate targets though initial ramps remained small.

July review

The month of July proved to be the most active for new capacity expansion announcements in the third quarter of 2017. Total plans reached 3,001MW, which included 1,000MW of new solar cell capacity, a total of 2,000MW of dedicated module assembly and a nominal 1MW advanced integrated manufacturing 4.0 R&D facility in California, opened by SunPower.

Turkish solar company Smart Energy Group was reported to have established a Joint venture with China-based Phono Solar (part of SUMEC) to build and operate an initial 400MW module assembly plant with future plans said to take capacity to 1,200MW. The assembly plant is set to be established in the Gebze Organized Industrial Zone.

Also of note in July was plans by India-based Premier Solar Systems to build a 1,000MW solar cell plant with an overseas business partner.

The company had also announced that it had opened a 200MW fully automated solar module manufacturing facility in Sangareddy, Telangana, India. The module assembly expansion takes nameplate module capacity to 375MW. The company has 50MW of solar cell capacity.

August review

The weakest month for capacity announcements in the quarter was August with only one announcement. India-based Heavy Engineering Corporation announced plans to build a 150MW integrated cell and module assembly plant using both monocrystalline and multicrystalline wafers. Initially, the plant will have a nameplate capacity of 150MW. Modules will be used initially for its in-house downstream PV power plant projects.

There were no dedicated cell or module assembly plant announcements in August and none for thin film.

September review

New announcements rebounded slightly in September. Total new capacity plans totalled around 900MW and were dominated by China-based PV module manufacturer Sunport Power, which officially started production at a 1GW module assembly plant using Eurotron's MWT equipment for

Figure 1. Capacity expansion announcements by product type monthly since January 2014 (MW).

Capacity expansion announcements by product type monthly since January 2014 (MW)

Legend: Thin Film, c-Si Cell, c-Si Module, Integrated cell/module
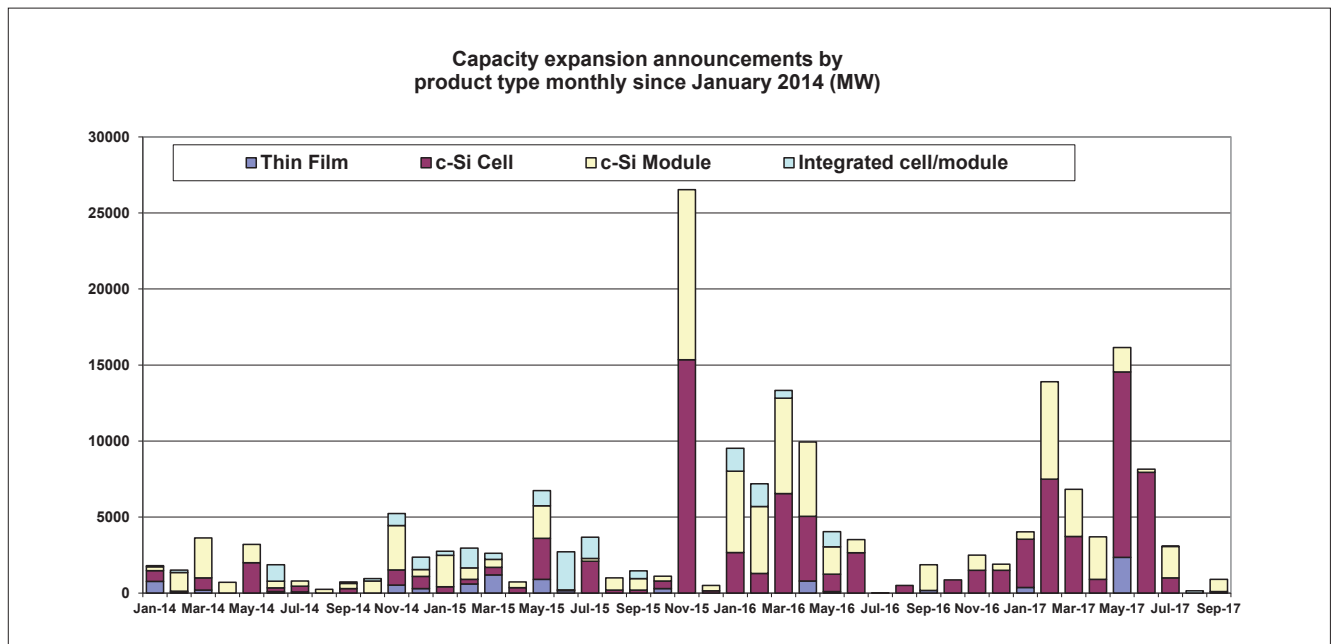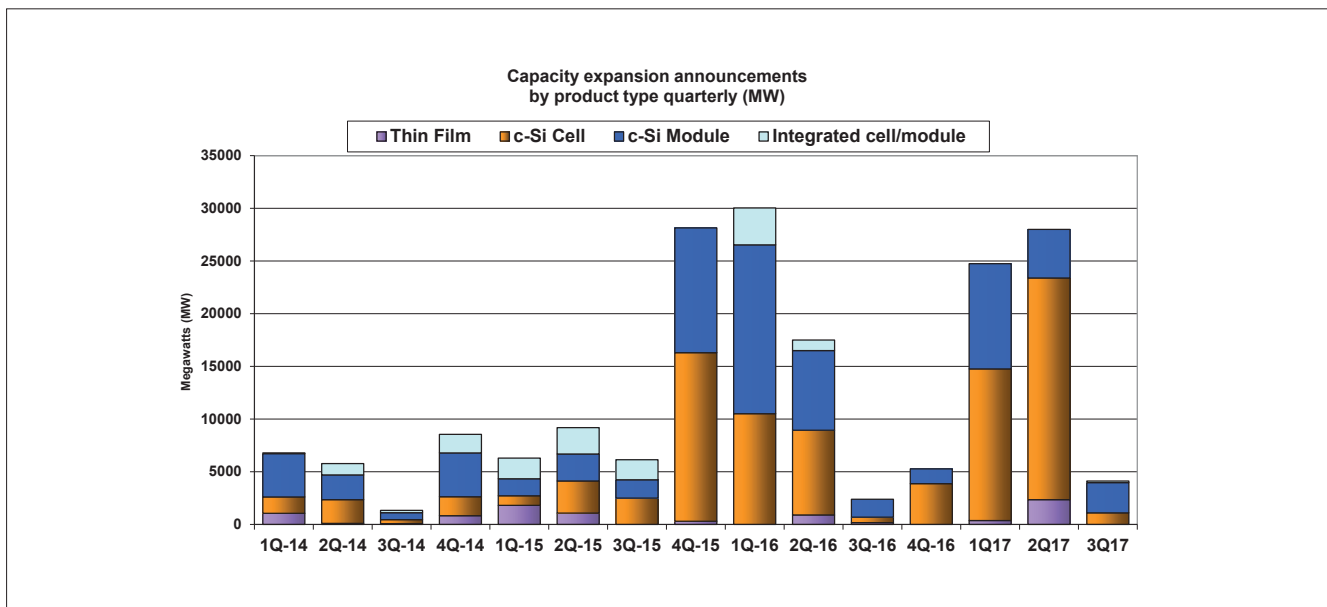
Figure 2. Capacity expansion announcements by product type quarterly (MW).
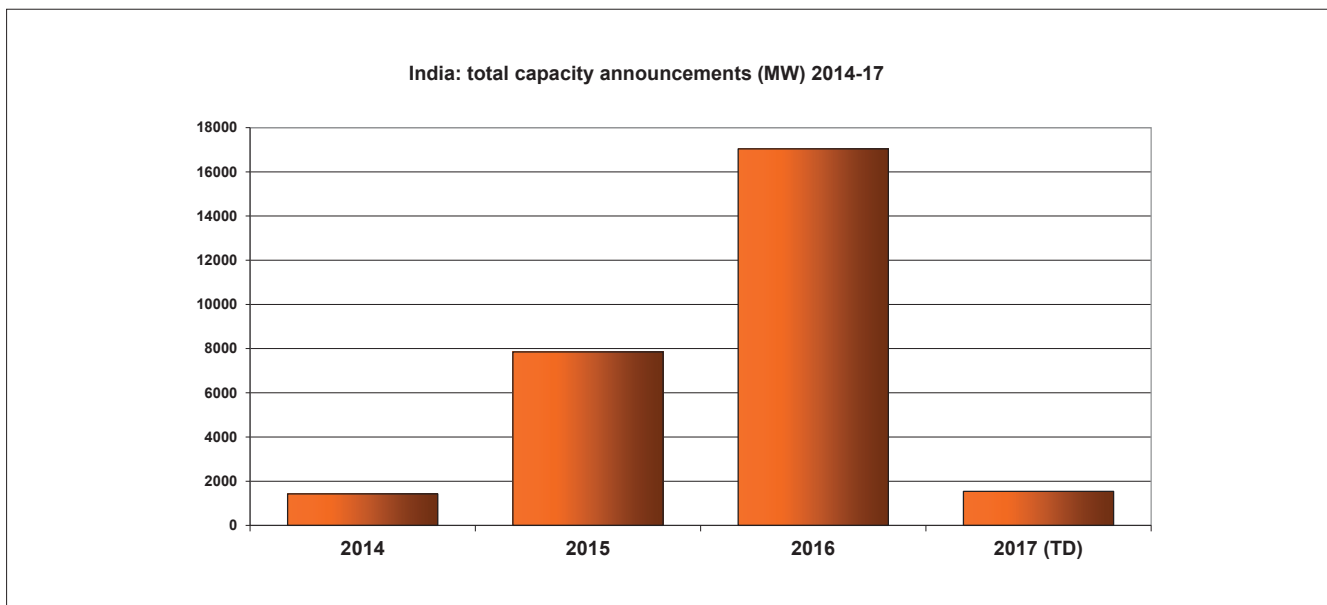
Figure 3. India: total capacity announcements (MW) 2014-17.

back-contact PV modules. The company had initially deployed a 200MW line so the new expansion accounted for 800MW of the total in September.

Also included in September was the first fully automated and unmanned 100MW monocrystalline solar cell line officially opened by Tongwei Group in Hefei, China as part of its most recent 2,000MW new solar cell plant.

Quarterly review

Total third quarter 2017 capacity expansion announcements reached only around 4,122MW, compared to 28,000MW in the previous quarter.

The subdued environment was driven by dedicated module assembly plans, which totalled 2,870MW, while integrated cell and module plans, absent so far in 2017, totalled 151MW. No new thin-film expansion plans were announced in the third quarter.

India review

With a history of solar manufacturing, albeit on a small scale, India has held the promise of becoming a major powerhouse for solar manufacturing, second only to China.

With a downstream PV market in the 6GW range in 2017 and the promise of much higher installation rates through 2022, the gap between capacity expansion announcements and effective nameplate capacity continues to be one of the widest.

Indian government data released in the second quarter of 2017 put solar cell capacity in India at just 3,164MW, yet only 1,667MW as deemed to be operational. A similar situation existed with module assembly capacity: a total of around 8,400MW of capacity was reported to exist in the country, while only around 5,500MW was deemed to be operational.

As seen in the Figure 3 2017 has seen a significant reduction in new announcements compared to the last two years with 2016 peaking at over 17,000MW. In total we have tracked over 27,800MW of announcements in India since 2014.

Building a manufacturing supply-chain base in India that comes even close to meeting domestic demand has proved elusive. A key perennial challenge has been the capital markets but a large proportion of the projects tracked were JVs with China-based companies as well as plans from US and Japan, which have also stalled despite the ability to tap low-cost finance in those countries.

A key emerging challenge that has been cited for manufacturing plans being stalled is related to the low prices tendered on multiple gigawatts of downstream power plant projects. Simply put, the winning bids are lower than potential manufacturing costs in India, not least due to the lack of a highly efficient low-cost manufacturing supply chain in the country that could match that of China.

Having depended on low-cost modules produced in China, India is challenged to compete and JVs with major Chinese producers such as Trina Solar and LONGi Group remain suspended.

However, new efforts by the Indian government to support domestic content requirements through a new wave of government-led downstream projects could become the catalyst required to kick start more effective capacity in India. Uncertainties in trade cases in the US could also make India attractive to supply modules to the US market in 2018 onwards. However, further reforms and a complete and low-cost manufacturing supply chain, coupled to rational tendering, all need to be in alignment before the imbalance between capacity expansion announcements and effective capacity is closed.

Solar 'manufacturing 4.0'

Although the third quarter of 2017 was subdued for capacity expansion plans, it has signalled an important milestone in PV manufacturing. Several facilities were opened in the quarter that relate to the concept of 'manufacturing 4.0', which includes fully automated manufacturing lines and remote operation.

In July, SMSL member GCL System Integration Technology (GCL-SI) announced the establishment and operation of an entirely unmanned module assembly workshop to test intelligent fully automated manufacturing tools and software systems. The workshop is expected to undertake tests for around two years.

The company noted that it was cooperating closely with Chinese domestic equipment manufacturers, and has independently researched and developed a series of intelligent systems, which include a high-speed automated tabbing machine, a high-precision layout machine and a robotic palletizing system. In all, GCL-SI said that 26 separate systems so far developed were industry firsts.

GCL's manufacturing 4.0 workshop.

A key aim of the tests is to achieve a 50% improvement in efficiency, a 60% reduction in online manpower and a 30% reduction in processing costs. Product quality improvement targets were being set at a 21% overall improvement. GCL-SI says its intention is to implement the improvements across its volume manufacturing operations.

In August, SunPower said it had invested around US$25 million in the last 12 months on a new US R&D and pilot line facility located at its headquarters in San Jose, California.

SunPower said the new facility included several high-volume production-sized manufacturing tools, high levels of automation and specialised testing equipment, designed to support its next generation of high-efficiency n-type monocrystalline interdigitated back contact (IBC) solar cells and modules, which are being designed with greater emphasis on lower cost manufacturing.

According to SunPower, over 30 parts suppliers and equipment manufacturers located in the US supplied the facility, which is housing over 100 SunPower engineers and support staff.

In September, as already noted, Tongwei Group opened its completed high-efficiency solar cell plant (S2), which included the world's first technically unmanned 100MW monocrystalline solar cell production line.

The S2 plant in Chengdu, China has an initial nameplate capacity of 2GW, which brings Tongwei's monocrystalline cell capacity to around 3.4GW. The company also has around 2GW of multicrystalline solar cell capacity. The company also has around 2GW of multicrystalline solar cell capacity and recently completed a 5,000MT polysilicon plant expansion, bringing nameplate production capacity to 20,000MT.

Tongwei is investing around RMB12 billion (US$1.8 billion) in total to construct new cell manufacturing facilities at in the Hefei High-tech Industrial Development Zone in Chengdu City to provide nameplate capacity of 10GW, while a further 10GW

Tongwei opened its first 100MW 'manufacturing 4.0' line at its 2GW S2 plant.

of capacity will be housed in the Southwest Airport Economic Development Zone of Shuangliu District, Chengdu City. Construction on the new projects is expected to start in November 2017 and production ramped in phases over the next three to five years.

Tongwei has taken the early lead in China in investing in manufacturing 4.0 capabilities, however much is being done behind the scenes at other major manufacturers and the learning curve is expected to take several years.

SMSL Q3 manufacturing update

JinkoSolar

Leading SMSL member JinkoSolar reported that its in-house annual silicon wafer capacity stood at 7GW at the end of the third quarter, up 1GW from the prior quarter.

Solar cell capacity as expected was 4.5GW, while

module capacity did increase by a further 500MW in the third quarter, reaching 8GW. These are the expected nameplate capacities exiting 2017. Although the company claimed its next wave of expansions had yet to be determined and would be based on market demand dynamics it is highly likely new plans will be announced in the next two quarters.

JinkoSolar is expecting to hit record shipments in 2017, having guided just short of 10GW, indicate almost a 10% global market share of module shipments and is sold out through the first half of 2018.

Canadian Solar

Canadian Solar has made four revisions to capacity expansion plans in 2017 and has also provided initial new expansion plans for 2018.

The SMSL member said it had completed the ramp-up of a new multicrystalline silicon ingot casting workshop at Baotou, China at the end of the third quarter of 2017, with a total annual capacity of 1,100MW, which included capacity relocated from its plant in Luoyang, China.

It also said it expected debottlenecking to push capacity to 1,200MW by the end of 2017, which is in line with the last two updated plans.

Canadian Solar said that it had plans further increase its ingot capacity to 1,720 MW by 30 June 2018, and may expand to 2,500MW if market conditions justify.

Wafer manufacturing capacity had reached 3GW in the third quarter of 2017. The company had previously guided that it expected wafer capacity to reach 4GW at the end the year.

However, Canadian Solar noted that its shift to diamond-wire saw technology, which

Figure 4. JinkoSolar: manufacturing capacity expansions & forecast 2017 (MW).

JinkoSolar: manufacturing capacity expansions & forecast (MW)

■ Ingot/Wafer Production (MW) ■ Cell Production (MW) ■ Module Production

	2015	2016	2017(2Q)	2017(3Q)
Ingot/Wafer Production (MW)	3000	5000	7000	7500
Cell Production (MW)	2500	4000	4500	4500
Module Production	4300	6500	8000	8000
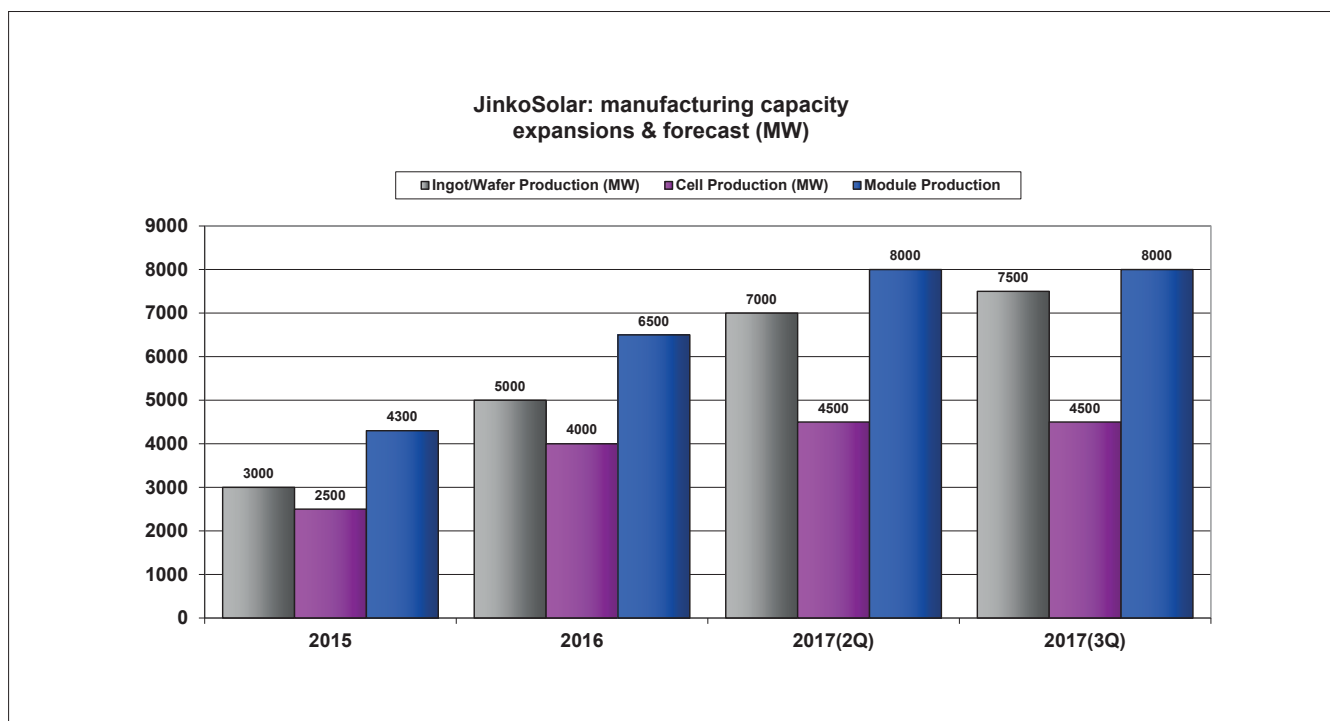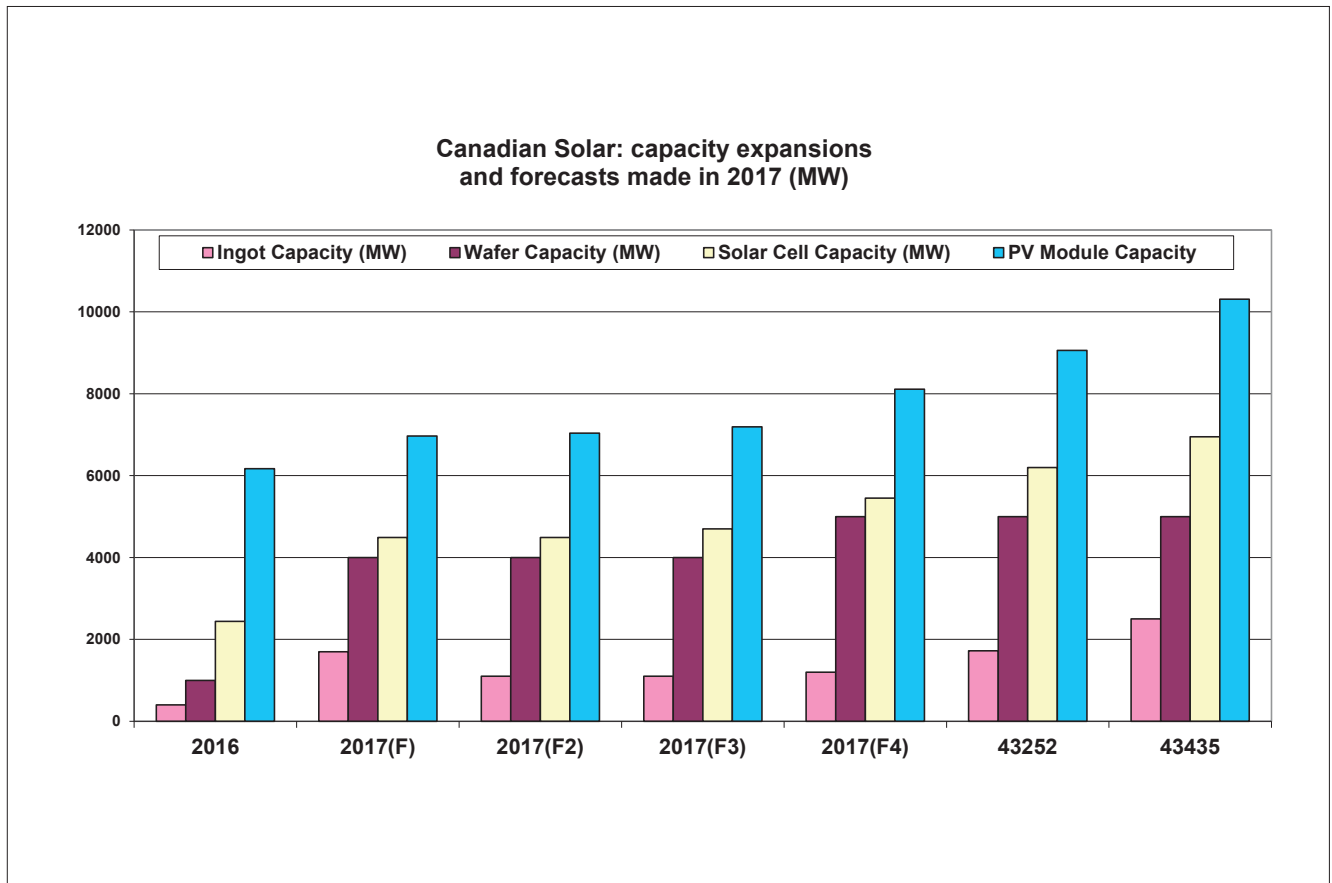
Figure 5. Canadian Solar: capacity expansions and forecasts made in 2017 (MW).

is compatible with its proprietary and highly efficient 'Onyx' black silicon multi-crystalline solar cell technology, helped to significantly offset the recent impact of polysilicon price increases that impact margins and so was planning to add a further 1GW of wafer production to end the year at 5GW.

The company said that its solar cell manufacturing capacity reached 4.7GW at the end of the third quarter of 2017, which was the target in its third revision to its capacity expansion plans.

However, Canadian Solar said that it planned to add additional cell manufacturing capacity at its Funing and Southeast Asia plants by year end, bringing 2017 cell nameplate capacity to 5,450MW, a 750MW increase.

Subject to market conditions Canadian Solar said it planned to add another 1.5GW of cell capacity in 2018 to reach approximately 7GW by the end of 2018.

With respect to PV module manufacturing capacity, Canadian Solar expects that its total worldwide module capacity would exceed 8,110MW by the end of 2017.

Subject to market conditions again, the SMSL member said it planned to add another 1,250MW of module capacity by the end of 2018, bringing nameplate capacity to 10.3GW. Canadian Solar is the first manufacturer to guide nameplate module capacity to reach over 10GW.

JA Solar

JA Solar confirmed that it expected to achieve both cell and module nameplate capacities of around 7,000MW by the end of 2017. JA Solar is on track to achieve full-year module shipments in the region of 6.8GW in 2017, but did not provide an update on 2018 capacity expansion plans.

Hanwha Q CELLS

Hanwha Q CELLS said that it was starting to migrate solar cell capacity at its China-based facilities to passivated emitter rear cell (PERC) technology, highlighting the shift away from standard back side field (BSF) technology for higher conversion efficiencies.

Hanwha Q CELLS noted in its third quarter earnings call that capital expenditure was being focused on its manufacturing facilities in China to enable the company to have PERC cell production capacity of 1.4GW, while retaining around 1.2GW of BSF production. Hanwha's lead manufacturing facilities are in Malaysia and are already 100% PERC.

Its affiliate, Hanwha Q CELLS Korea, is currently adding 1.6GW of cell and module production, which is expected to provide a nameplate capacity of 3.7GW by the end of this year.

"Although the third quarter of 2017 was subdued for capacity expansion plans, it signalled an important milestone in PV 'manufacturing 4.0'"

Hanwha Q CELLS' in-house cell and module capacity has not increased in 2017 as the company keeps tight control on spending to return to sustainable profitability. However, with Hanwha Q CELLS Korea expansions in 2017, the group will have access to 8GW of cell and module capacity starting in 2018, up from 6.4GW at the end of the third quarter of 2017.

Hanwha Q CELLS recently reiterated that it expected module shipments in 2017 to be in the range of 5.5GW to 5.7GW.

GCL System Integration Technology

GCL-SI reported it had ramped its solar cell and module assembly JV plant in Vietnam to around 800MW in the third quarter of 2017.

Critical to the market, the solar cell capacity ramp has been PERC technology with the flexibility to produce p-type multi and p-type mono cells for the residential, commercial and utility-scale markets.

The company said that its total solar cell capacity would reach 2GW by the end of 2017, which would be completely PERC-based technology. Currently, around one-third of production is p-type multi using 'Black Silicon' texturing after wafers (S2 size) are cut with diamond wire. Around a third of production is p-type mono PERC, while a further third of production is flexible to customer demand.

LONGi Group

LONGi Group, which is leading the industry transition to high-efficiency monocrystalline wafers, cells and modules, has actually increased the pace of some of its previously announced plans for 2017.

At the beginning of the year its capacity for wafers had reached 7.5GW and is was expected to reach 12GW by the end of 2017. In the third quarter of 2017, LONGi surpassed the 12GW mark and said it was planning to add further capacity to meet continued strong demand.

LONGi still expects to meet expansion goals of 5GW for solar cells and 6.5GW for modules by the end of the year. However, it does not plan to provide updated plans until issuing its 2017 annual report.

Conclusion

Despite the slowdown in new plans in the quarter, executing on existing plans has been a key theme throughout the year, notably for China-based firms and the majority of SMSL members. Having continued to gain market share in 2017, SMSL members are all expected to announce record annual module shipments in 2017.

Life cycle management and recycling of PV systems

Parikhit Sinha[1,2], **Sukhwant Raju**[1], **Karen Drozdiak**[1] & **Andreas Wade**[1,2]
[1]First Solar; [2]IEA PVPS Task 12

Abstract

Future waste volumes related to exponential growth in photovoltaic (PV) system deployment pose both a waste management challenge and resource recovery opportunity for the PV industry. Active international R&D projects and patent activity have identified mechanical, thermal, chemical and optical methods to delaminate PV modules and extract glass and metals. In addition to lab-scale research, First Solar has demonstrated high-value recycling technology and continuous improvement at a commercial scale. Through implementation of the WEEE Directive, Europe has created the first mandatory market for PV module recycling including the development of PV-specific waste handling and treatment standards. As PV system component prices continue to drop, the financial provisions related to decommissioning, collection and recycling become more relevant to the levelized cost of electricity for PV generation assets. Recent economic analysis indicates that the commercial scrap value of PV power plant decommissioning exceeds decommissioning costs by up to US$0.01-0.02 per watt, further incentivizing recycling over disposal.

Introduction

In 2015, estimated annual global volumes of electronic waste (e-waste) reached a record 43.8 million metric tons and global e-waste generation is expected to increase up to 50 million metric tons by 2018 [1]. Even though solar PV panels significantly differ from typical consumer electronic products, global regulators view PV panels increasingly in the context of e-waste regulations. Solar PV currently accounts for less than 1% of total annual e-waste volumes. However, as PV deployment continues to grow exponentially, cumulative PV waste is expected to amount to 1.7 million-8 million metric tons by 2030, equivalent to 3-16% of total e-waste produced annually today [2]. As global PV demand increases and more modules and systems reach the end of their useful life over the next 10-15 years, recycling will become increasingly important for all PV technologies to ensure that clean energy solutions do not pose a waste burden.

In addition to ensuring compliance with evolving regulatory waste management requirements, PV recycling offers an opportunity to influence project economics in an increasingly commoditized market. As component prices continue to drop, the financial provisions related to decommissioning, collection and recycling become more relevant to the levelized cost of electricity (LCOE) for PV generation assets. These provisions have to be taken into consideration during PV project development, site permitting and when putting PV system components on the market (i.e. PV modules, inverters, other electrical and electronic products).

Voluntary and regulatory approaches to end-of-life management in leading markets

In most countries, PV panels are classified as general or industrial waste and managed in accordance with general waste treatment and disposal requirements [2]. Beyond general waste regulation, voluntary and regulatory approaches have been specifically developed for managing end-of-life PV waste.

The European Union (EU) was the first to adopt PV-specific waste regulations by mandating the recycling of all solar panels under the Waste Electrical and Electronic Equipment (WEEE) Directive (2012/19/EU). Since 2012, the provisions of the WEEE Directive have been transposed into national law by the EU member states, creating the first mandatory market for PV module recycling. In the United States, PV panel disposal is covered under the Resource Conservation and Recovery Act, which is the legal framework for managing hazardous and non-hazardous waste. In 2016, the US Solar Energy Industries Association (SEIA) partnered with PV manufacturers and installer-developers to voluntarily launch a national PV recycling programme, which aims to make affordable PV recycling solutions more accessible to consumers [3].

In Japan, end-of-life PV panels are covered under the general regulatory framework for waste management (the Waste Management and Public Cleansing Act), which defines industrial waste generator and handler responsibilities and waste management requirements including landfill disposal. In 2015, a roadmap for promoting a scheme for collection, recycling and proper treatment of end-of-life renewable energy equipment was developed, followed in 2016 by a guideline promoting proper end-of-life treatment of PV modules including recycling [2].

China has no PV-specific waste regulations but has sponsored R&D on PV recycling technologies through the National High-tech R&D Programme for PV Recycling and Safety Disposal Research under the 12th five-year plan. Directives for
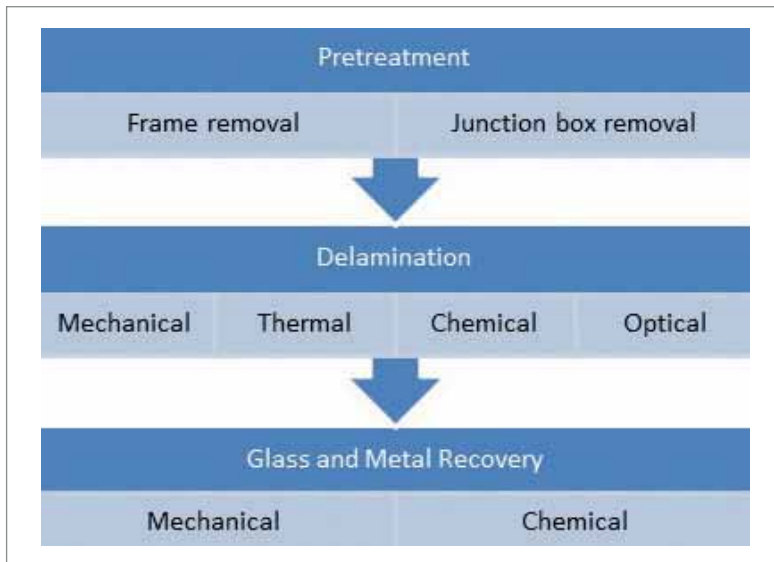
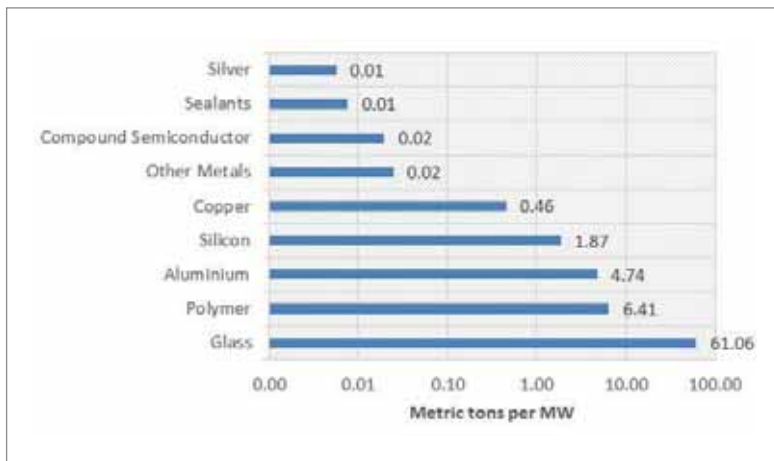**Figure 1. High value PV recycling process steps.**

Figure 2. Average recoverable material fractions of PV Panels in 2030 based on [2].

accelerating the end-of-life management of waste PV modules are also expected in the 13th five-year plan. In India, PV waste is managed by the Ministry of Environment, Forest and Climate Change under the 2016 Solid Waste Management Rules and the Hazardous and Other Wastes (Management and Transboundary Movement) Rules [2].

Internationally, a new sustainability leadership standard for PV modules (NSF 457) includes product end-of-life management criteria covering take-back and recycling.

PV recycling technology

In recent years, R&D projects on PV recycling technology have been sponsored in Europe, China, Japan and Korea, and there has been significant patent activity for both crystalline silicon (c-Si) and thin-film PV module recycling technology in the same regions as well as in the United States [4]. Recycling technology can be categorized as either bulk recycling (recovery of high-mass fraction materials such as glass, aluminum and copper) or high-value recycling (recovery of both bulk materials and semiconductor and trace metals). Bulk recycling is similar to existing laminated glass recycling technology in other industries, and may not recover environmentally sensitive (e.g., Pb, Cd, Se) or valuable (e.g., Ag, In, Te, solar-grade Si) materials in PV modules. High-value PV recycling consists of three main steps: pretreatment to remove the metal frame and junction box, delamination to remove the module encapsulant and recovery to extract glass and metals from the module (Figure 1).

Some common goals in PV recycling technology are to maximize recovery yields, minimize impurities in the products of recycling and minimize capital and operating costs to be competitive with other disposal options. Ensuring worker safety and environmental protection are additional priorities that are implemented through management systems such as OHSAS 18001 and ISO 14001, and air emissions controls and wastewater treatment technology.

In addition to technology, other related considerations that affect the viability of PV recycling are effective collection schemes, predictable waste volumes, customers for the products of recycling and regulations on the handling and transport of waste. These factors can affect commercial decisions on when and where to site PV recycling facilities and whether to operate them in a centralized or decentralized (mobile) manner [5].

The recovery value of a PV module

PV panels typically consist of glass, aluminum, copper and semiconductor materials that can be successfully recovered and reused at the end of their useful life (Figure 2). By mass, today's typical crystalline silison PV panels consist of approximately 76% glass, 10% polymer (encapsulant and backsheet foil), 8% aluminium, 5% silicon semiconductor, 1% copper (interconnectors) and less than 0.1% silver (contact lines) and other metals including tin and lead. Thin-film CIGS and CdTe PV panels consist of higher proportions of glass: 89% and 97%, respectively [2].

Current PV waste volumes remain low as modules have a lifetime of 25 years or more. However, as global PV deployment continues to grow and more modules reach the end of their useful life over the next 10-20 years, PV waste is set to increase nearly 40-fold by 2030 under a normal loss scenario, which assumes a 30-year module lifetime. Leading solar markets including China, the US, Germany, Japan and India (Figure 3) are expected to represent the majority of these projected PV waste streams [2].

By 2030, the recoverable value from recycling end-of-life PV modules is estimated to amount to US$450 million. The recovery value of glass alone has the potential to exceed US$28 million, assuming an average secondary material market price of US$30-50/mt depending on recovery quality of the glass [6].

In Europe, the current raw material recovery rate for recycling PV modules is 65-70% by mass and

is in line with the EU WEEE Directive. CENELEC, the European Committee for Electrotechnical Standardization, has developed a supplementary standard specific to PV panel collection and treatment (EN50625-2-4 & TS50625-3-5) to assist treatment operators. The standard specifies various administrative, organizational and technical requirements aimed at preventing pollution and improper disposal, minimizing emissions, promoting increased material recycling and high-value recovery operations, and impeding PV waste shipments to facilities that fail to comply with standard environmental and health and safety requirements. The standard includes specific depollution requirements whereby the content of hazardous substances in output glass fractions shall not exceed the following defined limit values:

- 1 mg/kg (dry matter) cadmium (Si-based PV); 10 mg/kg (dry matter) cadmium (non-Si-based PV)
- 1 mg/kg (dry matter) selenium (Si-based PV); 10 mg/kg (dry matter) selenium (non-Si-based PV)
- 100 mg/kg (dry matter) lead

The residual value of a PV system at end-of-life

Decommissioning cost modelling

Decommissioning a PV system at end-of-life involves dismantling and disposing of the system. For utility-scale PV projects, local permitting requirements often include stringent decommissioning and land remediation measures [7] [8]. These specify disconnecting the project from the grid, removing the installed features (modules, trackers, electrical wire, inverters, transformers, fencing, O&M building, etc.), and recontouring and revegetating the land to its preconstruction condition. For example, the following utility-scale PV projects in the US and Germany have decommissioning plans containing detailed cost estimates for dismantling, disposal and site restoration.

- Desert Stateline Solar Farm Project (300 MW$_{AC}$ PV project in California) [7];
- Helmeringen I Solar Park (10 MW$_{AC}$ PV project in Germany) [8];
- Silver State South Solar Project (250 MW$_{AC}$ PV project in Nevada) [9].

Costs from these and other representative projects can be aggregated and used to model the present value of the net cost to decommission a PV power plant (NDC$_{PV}$):

$$NDC_{PV} = \frac{[(DC_T + IC_T + MR_T + LF_T) - SV_T - LV_T]}{(1+r)^T}$$

where,

$DC_T + IC_T =$ Direct cost (labour, equipment) and indirect cost of PV plant de-installation, demolition, recovery,

and land reclamation in year T.

$MR_T =$ PV module recycling cost in year T.

$LF_T =$ Landfill disposal cost in year T, including landfill tipping fees and hauling, of non-salvageable material.

$SV_T =$ Scrap value of steel, copper and aluminum recovered during PV solar field and power equipment removal and sold to recyclers at prices prevailing in year T.

$LV_T =$ Value of reclaimed land in year T.

$r =$ Rate of annual discount applied to costs and revenues realized in year T.

In order for net costs to be negative (profitable), the scrap metal value and/or land value must exceed the decommissioning costs. In particular, there are large quantities of steel, copper and aluminum in PV power plants (Figure 4) associated with mounting structures and electrical cables.

Recent economic analysis indicates that the commercial scrap value of PV power plant decommissioning (mainly associated with scrap steel and copper) exceeds decommissioning costs, incentivizing recycling over disposal. Decommissioning cost optimization modelling by Fthenakis et al. [11] estimated a net profit of up to US$1.58 per module area. Monte Carlo analysis by ERM [12] indicated 100% confidence in a net profit from PV plant decommissioning when land value was included and up to 95% confidence in a net profit when land value was excluded, depending on plant design scenarios such as above-ground versus below-ground cabling. High-value recycling scenarios in both studies indicate opportunities to positively influence project economics and the LCOE of a given PV project, with net revenues of up to US$0.01-0.02/W from project decommissioning (excluding land value).

State-of-the-art: the First Solar recycling process

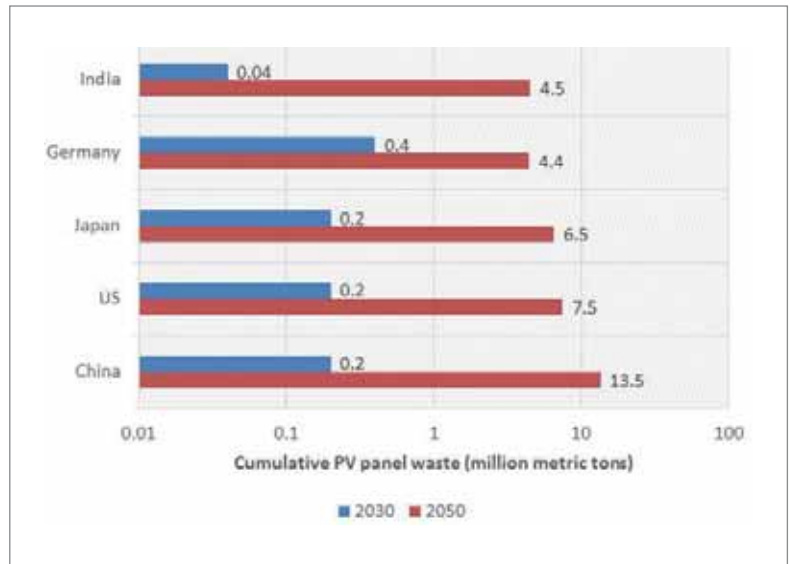In 2005, First Solar established the industry's first voluntary global module recycling programme and
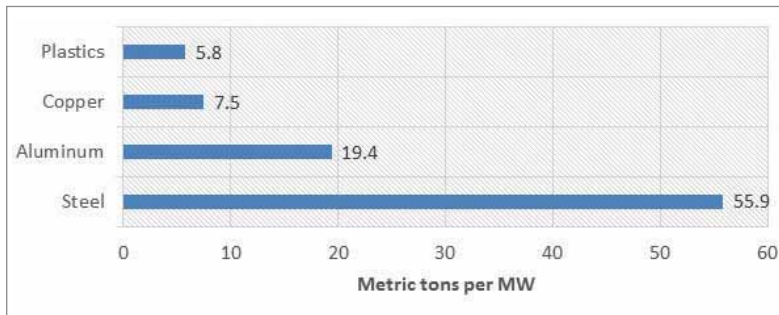
Figure 3. Estimated cumulative PV waste volumes in leading solar markets by 2030 and 2050 (regular loss scenario) [2].

Figure 4. Material fractions of PV power plants [10]. has been proactively investing in

Figure 5. First Solar's first-generation recycling technology based on the mining industry's batch process.

Figure 6. First Solar's second-generation recycling technology based on the chemical industry's batch process.

recycling technology improvements and driving down recycling costs ever since (figures 5-7). In contrast to mechanical recycling processes which focus on recovering major components such as glass, copper and aluminum, First Solar's high-value recycling process is able to recapture more materials while retaining their maximum value so they can be reused in new First Solar modules and new glass or rubber products. First Solar's state-of-the-art PV recycling process recovers more than 90% of the semiconductor material and approximately 90% of glass.

First Solar's first-generation recycling technology was based on the mining industry and involved

moving glass and liquid from process to process with a modest 10 metric tons per day capacity. In 2011, First Solar developed its second-generation recycling technology, which was based on the chemical industry batch process of circulating liquids within scalable reactor columns (30 metric tons per day capacity).

In 2015, First Solar developed its third-generation recycling technology which achieves superior glass and semiconductor purity with reduced capital and operating (chemicals, waste and labour) costs. The continuous-flow process improves the recycling efficiency and throughput, increasing the plant's daily recycling capacity from 30 metric tons to 150 metric tons.

First Solar is proactively investing in recycling technology improvements to drive down overall PV waste collection and recycling costs. By 2018, First Solar recycling plants will have zero liquid waste discharge and will convert most of the incoming PV waste streams into valuable raw materials for other industries.

Conclusions

The responsible life cycle management of PV systems is not only becoming a compliance requirement, e.g. in the European Union where PV module recycling is already mandated by the EU WEEE directive, but also offers opportunities to positively influence project economics and the LCOE of a given PV project by leveraging cost-effective, high-value recycling technologies. In addition to creating value from secondary resources, PV recycling services help de-risk the decommissioning and end-of-life phase for PV asset owners.

References

[1] C. P. Baldé, F. Wang, R. Kuehr and J. Huisman, "The Global E-Waste Monitor", United Nations University, IAS-SCYCLE, Bonn, Germany, 2014.
[2] S. Weckend, A. Wade, G. Heath and K. Wambach, "End-of-Life Management: Photovoltaic Panels", International Renewable Energy Agency (IRENA), International Energy Agency Photovoltaic Power Systems Program Task 12 (IEA PVPS Task 12), Abu Dhabi, Amsterdam, 2016.
[3] E. Butler, "SEIA National PV Recycling Program", in Solar Power International, Las Vegas, 2016.
[4] K. Komoto and J. Lee, "End-of-Life Management of Photovoltaic Panels: Trends in PV Module Recycling Technologies", IEA-PVPS T12-10:2017, 2017.
[5] D. Ravikumar, P. Sinha, T. Seager and M. Fraser, "An anticipatory approach to quantify energetics of recycling CdTe photovoltaic systems", Prog. Photovolt: Res. Appl., vol. 24, pp. 735-746, 2015.
[6] Eurostat, "Recycling – Secondary Material Price Indicator", 2014. [Online]. Available: http://ec.europa.eu/eurostat/statistics-explained/index.php/Recycling_%E2%80%93_secondary_material_price_

indicator#Glass.

[7] Desert Stateline, LLC; LSA Associates, Inc., "Closure, Decommissioning, And Reclamation Plan - Stateline Solar Farm Project San Bernadino County, California", U.S. Bureau of Land Managment, Needles, San Bernadino County, California, USA, 2014.

[8] Schimpf, G. et.al.; Gehrlicher Solar AG, "Untersuchungen zum Recycling einer konkreten PV Anlage", Forum Solarpraxis, Berlin, Germany, 2011.

[9] Silver State Solar Power South, LLC; CH2MHill, "Facility Decommissioning Plan Silver State Solar South Project", Bureau of Land Management, Las Vegas, NV, USA, 2014.

[10] J. E. Mason, V. M. Fthenakis, T. Hansen and H. C. Kim, "Energy Payback and Life-cycle CO2 Emissions of the BOS in an Optimized 3.5MW PV Installation", *Prog. Photovolt: Res. Appl.,* vol. 14, no. 2, pp. 179-190, 2006.

[11] V. Fthenakis, Z. Zhang and J. Choi, "Cost Optimization of Decommissioning and Recycling CdTe PV Power Plants", in *Proc. IEEE PVSC*, Washington D.C., 2017.

[12] A. Cates and R. Stifter, "PV Power Plant Net Decommissioning Cost Model Technical Report", Environmental Resources Management (ERM), San Francisco, CA., 2017.

....

Figure 7. First Solar's third-generation PV recycling technology based on a continuous-flow process.

About the authors

Dr. Parikhit Sinha is a Senior Scientist in the Global Sustainability group at First Solar, where he leads the company's research on environmental product safety and life cycle assessment. He is a member of the International Energy Agency PVPS Task 12 Committee on PV Environmental, Health, and Safety, and a former study director at the U.S. National Academy of Sciences. He has a Ph.D. in atmospheric sciences from the University of Washington, Seattle, and a B.A. in environmental engineering from Harvard University.

Sukhwant Raju is the Global Director of Recycling Operations and Services at First Solar where he leads the development of PV module recycling technology and manages a global recycling team, which currently operates commercial-scale recycling plants in Europe, Asia, and the United States. He has more than 28 years of experience in the chemical and environmental industry and has been involved in the technical design, operations, and business management of chemical treatment, recycling, and hazardous waste management operations at several companies. Sukhwant is a chemical engineer with an Executive MBA degree from David Eccles School of Business at University Of Utah.

Karen Drozdiak is the Sustainability Communications and Analysis Manager at First Solar, where her responsibilities include data analysis, market research, internal and external sustainability communications, and corporate sustainability reporting. She has worked in the PV industry for the past six years and recently participated in the development of the industry's first sustainability leadership standard, led by NSF International and the Green Electronics Council. Karen has a B.A. in History and U.S. Foreign Policy from Columbia University and an M.A. in International Relations and Diplomacy from the Anglo-American University in Prague.

Andreas Wade is the Global Sustainability Director at First Solar where he has been in charge of the company's sustainability program for the past three years. He previously supported business development as Director of Technical Relations and Public Affairs in Europe. Prior to joining First Solar, Andreas designed and implemented the life cycle management strategy for Q-Cells and worked as a process engineer at Shell Exploration and Production. Andreas is the Deputy Operating Agent of the International Energy Agency's PVPS Task 12 Committee and currently also leads the development of a minimum recycling standard for PV modules within the Technical Committee 111X Working Group 6 of CENELEC. Andreas is an environmental process engineer with a M.E. from the Clausthal University of Technology in Germany.

....

Enquiries

Andreas Wade
First Solar
Email: andreas.wade@firstsolar.com

News

Polysilicon supply adequate for 100GW solar market in 2017 - Bernreuter Research

Global solar installations are expected to be in the range of 95GW to 97GW in 2017, while polysilicon supply was more than adequate to meet around 100GW of end market demand, according to Bernreuter Research.

Bernreuter Research said that around 100GW of crystalline solar cells as well as around 5GW of thin-film module production in 2017 was expected. In effect, the solar supply chain has remained in balance and fears of overcapacity occurring in the second half of the year, as per 2016 have been averted, primarily through record demand in China.

China has already installed a record 42GW in the first three quarters of 2017, supporting Bernreuter Research's view and others that that new PV installations in China would exceed 50GW in 2017.

Key demand markets such as the US and India are expected see installations of 12.5GW and 9GW, respectively. According to Bernreuter Research, installs in India have been curtailed, due to higher PV module prices and cancelled shipments from China as string demand in the US and the domestic market offer higher margins.

"Several gigawatts of solar module shipments into the United States will be stockpiled for installation in 2018 to avoid impending tariffs on cell and module imports in the trade case brought up by Suniva and SolarWorld Americas," noted Johannes Bernreuter.

Bernreuter Research expects a global polysilicon output of 460,000 to 465,000 metric tons (MT), including 30,000 MT of electronic-grade material for the semiconductor industry, in 2017.

Credit Wacker Chemie

Polysilicon supply has kept pace with demand through 2017.

MARKET

China pragmatic on raising polysilicon tariffs on Korean imports

An investigation by China's Ministry of Commerce of the People's Republic of China (MOFCOM) on polysilicon dumping by South Korean producers has resulted in only small tariff increases for the largest importers.

MOFCOM's investigation was driven by several domestic polysilicon producers complaining about low prices.

Notably, the world's largest producer, GCL-Poly had not been a petitioner directly neither had Daqo New Energy directly.

New import duties on these companies include; OCI at 4.4%, Hanwha Chemical at 8.9% and Hankook Silicon at 9.5%. Several other polysilicon producers, which according to MOFCOM did not help in their investigations, were slapped with significantly higher import duties. These included an 88.7% tariff on SMP and 113.8% for Woongjin and KAM Corp.

Materials suppliers benefit from increased demand

Taiwan-based materials suppliers benefitted from increased demand for diamond-wire-cut wafers for higher efficiency solar cells that is supporting higher prices in recent months.

Major integrated PV manufacturer Sino-American Silicon (SAS) revenue reached a new peak in September 2017, driven by demand for semiconductor polysilicon and demand for wafers, cells and modules in the solar sector. SAS revenue in September 2017 reached NT$5,663 million (US$187.29 million), up NT$5,180 million in the previous month and was a new record high.

Multicrystalline wafer producer Green Energy Technology (GET) sales continued to trend moderately upwards since the beginning of 2017. GET reported September 2017 revenue of NT$1,137 million (US$37.6 million), an increase of 1.7% over the previous month and a 59% increase over the prior year period. GET noted that the revenue increase was primarily due to wafer ASP's increasing as demand for diamond-wired wafers continued to gain momentum for high-efficiency cells.

Multicrystalline wafer producer Danen Technology Corp's sales have been in recovery mode since a distinct decline in April, 2017. Danen reported September 2017 sales of NT$86.52 million (US$2.86 million) up from NT$75.47 million in the previous month. The company noted price increases on the back of polysilicon price increases for the improvement in sales.

FINANCIALS

REC Silicon sales improve on stronger gases and polysilicon demand

Polysilicon producer REC Silicon ASA benefited from higher sales volumes and ASP increases to report a 23% increase in revenue in the third quarter of 2017.

REC Silicon reported revenue of US$75.5 million in the third quarter, up from US$61.4 million in the previous quarter. Third quarter EBITDA was US$3.6 million compared to US$1.3 million in the previous quarter. The company reported a cash balance of US$88.0 million in the quarter, up by US$16.6 million compared to the second quarter of 2017.

Polysilicon sales volumes increased by 1,131MT to 4,091MT, a 38.2% increase quarter-on-quarter. REC Silicon also noted that the higher than expected polysilicon sales resulted in a reduction in inventory of 1,280MT. Third quarter FBR production was 2,254MT, lower than guidance of 2,290MT.

Amtech's record solar sales continue in fiscal fourth quarter

Specialist PV manufacturing equipment supplier Amtech Systems continues to benefit from major solar order conversion to revenue in its fiscal fourth quarter of 2017.

Amtech reported fiscal fourth quarter 2017 revenue in its solar segment of US$30.1 million, up from US$29 million in the previous quarter and almost double solar segment revenue of US$16.6 million in the second quarter of fiscal 2017.

The solar segment results are the highest seen by Amtech.

Amtech's solar segment order backlog stood at US$81.4 million, down from US$98.2 million in the previous quarter as the company ships orders and new order intake declined to US$9.6 million in the reporting quarter.

The backlog includes deferred revenue and customer orders that are expected to ship within the next 12 months.

Fokko Pentinga, CEO of Amtech, said: "We are pleased to report that shipment of Phase I of the [solar] turnkey order and strong shipments of semiconductor products led to strong financial results in the fourth quarter and fiscal year 2017."

Wacker reports best quarterly polysilicon revenue results since 2012

Major polysilicon producer Wacker Chemie reported its strongest quarter of polysilicon sales since 2012, due to volume growth as the solar industry sets to reach a global end market demand of around 100GW.

Wacker reported third quarter 2017 polysilicon segment sales of €341.7 million, up 35% from the prior year period and the highest since the first quarter of 2012. Sales were also 35% higher than
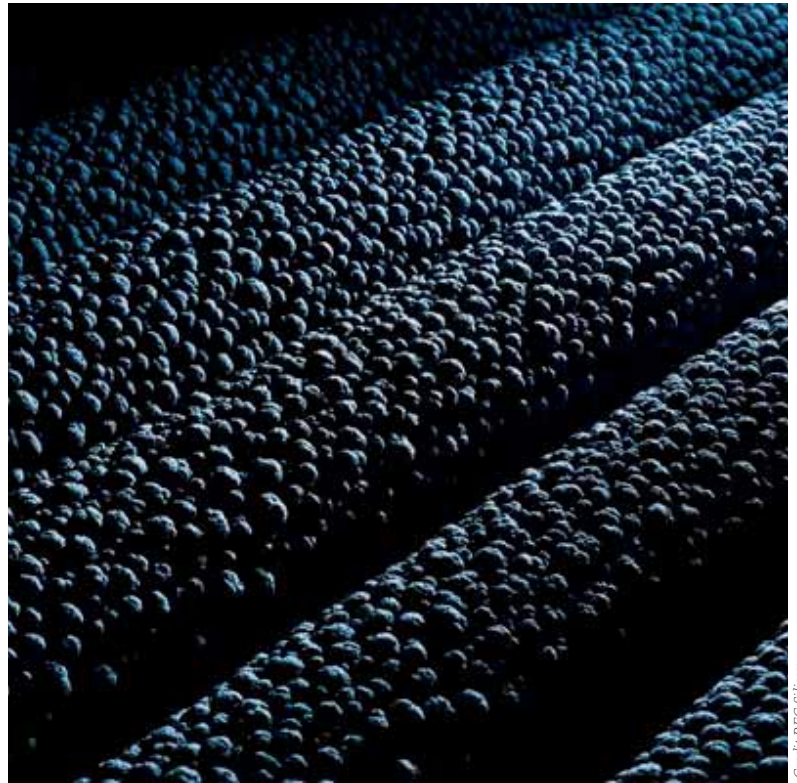
Credit REC Silicon

those reported in the previous quarter.

EBITDA amounted to €85.0 million, compared with €82.3 million in the prior year period and was 19% higher than the previous quarter.

However, EBITDA margins continue to come under pressure, which were 24.9% in the third quarter of 2017, down from 28.9% in the previous quarter and down from 32.5% in the prior year period. Product-mix and inventory effects dampened the EBITDA margin, according to the company.

CAPACITY EXPANSIONS

OCI shifting more polysilicon capacity to serve mono wafer demand

Major Korean-based polysilicon producer OCI Chemical is expanding its production of high-purity polysilicon to meet greater demand for p-type monocrystalline wafers used with PERC technology.

In reporting record third quarter results, OCI said that it would adopt a "two-track strategy" in regards to polysilicon production both in South Korea and the recently acquired facilities in Malaysia.

The company said that its South Korean production of high-purity polysilicon for mono wafers currently only stands at around 42% of capacity. However, this will be increased to around 60% of production capacity in 2018.

OCI has around 52,000MT of polysilicon capacity in South Korea and its average product mix in 2017 for mono-quality polysilicon was said to be only around 35%.

Polysilicon production at its facility in Malaysia, recently acquired from Tokuyama is being expanded from a nameplate capacity of 13,800MT to 16,000MT per annum by the end of 2018, through upgrades and debottlenecking and engineering process improvements.

Daqo to expand polysilicon capacity to 30,000MT

China-based polysilicon producer Daqo New Energy is to increase its capacity at its Xinjiang plant by 7,000MT, which is intended to serve the high-purity needs of monocrystalline solar wafers and the expanding semiconductor sector.

Daqo noted that the Phase 3B expansion plan included the adoption of new designs, processes, technologies and equipment that would further improve the quality and purity of its polysilicon products as well as the ability to conduct further debottlenecking projects that could increase its capacity to 30,000MT per annum, up from 18,000MT to date.

The company said that the project design and initial preparation works for Phase 3B Project would be completed by the end of 2017 and constructions through equipment installations would be completed by the end of 2018. Daqo plans to start pilot production in the first half of 2019 and reach full capacity by the end of the second quarter of 2019.

Already a polysilicon production cost leader, Daqo noted that overall total production cost at the Xinjiang facilities could potentially be decreased to US$7.50/kg. The company is targeting to reduce production costs to around US$8.0/kg by the end of 2018.

DUPONT

Desert Technologies and DuPont enter strategic partnership

PV materials provider DuPont has partnered up with Saudi Arabian manufacturer, developer and EPC Desert Technologies.

Desert Technologies has a regional pipeline of 300MW and plans to ramp its mono module production to 120MW by the end of 2017.

"DuPont is pleased to collaborate with Desert Technologies," said Stephan Padlewski, regional marketing leader, EMEA, DuPont Photovoltaic Solutions. "I believe our collaborative efforts can help accelerate the adoption and growth of long lasting, reliable solar systems in the region that can best withstand the often harsh environment."

As part of the "marketing cooperation agreement", the manufacturer will use DuPont's Tedlar backsheets and use cells featuring its Solamet metalization paste.

Taiwan's Giga Solar paste producer pays DuPont for patents use

Taiwan's leading conductive paste manufacturer Giga Solar Materials Corporation has agreed to pay patent licensing fees to rival, DuPont Photovoltaics.

DuPont said that the agreement was effective on November 15, 2017, although the company added that all other terms of the license agreement, including license fees would remain confidential.

Giga Solar's sales had been impacted by the US anti-dumping duties on cell produced in Taiwan and Chinese module manufacturers securing increasing supply from domestic Chinese cell producers as the Chinese end-market demand has experienced several years of record installations.

Credit DuPont

Solamet paste in production.

As-grown bulk lifetime: Increasingly relevant for silicon solar cell performance

Bernhard Mitchell[1], Daniel Chung[1], Zhen Xiong[2], Pietro P. Altermatt[2], Peter Geelan-Small[1] & Thorsten Trupke[1,3]
[1]University of New South Wales, Sydney, Australia; [2]State Key Laboratory of PV Science and Technology, Trina Solar, Changzhou, Jiangsu, PR China; [3]BT Imaging Pty Ltd, Sydney, Australia

Abstract

This paper investigates the influence of the as-grown silicon material quality on the performance of multicrystalline silicon passivated emitter and rear solar cells (PERCs), using recently developed spectral photoluminescence (PL) imaging techniques at the ingot level (i.e. on silicon bricks), and testing these cells in conjunction with PL measurements on as-cut wafers. The effects of material properties – including bulk lifetime, dislocation density and resistivity – are studied with regard to their correlation to cell output over the whole sample set of three directionally solidified production bricks of widely varying bulk lifetimes and dislocation densities. The data are analysed statistically using a linear mixed model. Bulk lifetime is observed to be correlated to cell performance throughout the studied sample set. The strength of the correlation is determined to be greatest for the material with low dislocation density, where a linear correlation between cell performance and as-grown bulk lifetime is found. There is a clear ongoing trend for increases in cell efficiency and for decreases in the area of dislocations in multicrystalline wafers. Because of this progression, bulk lifetime measured only on the bricks is well suited to predicting the often-dominant material-related variations in cell performance before cell fabrication.

Silicon material quality parameters: bulk lifetime, dislocation density, resistivity

By the end of 2017 it is expected that boron-doped multicrystalline silicon (p-type mc-Si) wafers will have been used in more than 60% of the world's manufactured solar cells [1]. Low-cost mc-Si can be crystallized in large ingots with high throughputs and with less oxygen built into the crystal than in the case of Czochralski-grown monocrystalline silicon (Cz-Si). However, mc-Si contains extended defects (mainly grain boundaries and dislocations) and a higher concentration of metal contaminants. These types of defect usually cause lower as-grown excess carrier lifetimes in mc-Si than in Cz-Si. Both Cz-Si and mc-Si can be affected by degradations of the excess carrier lifetime during module operation in the field [2,3], if defect formation processes are not regenerated or passivated [4,5].

> "A prediction of efficiency from the as-grown silicon material would be extremely valuable in terms of enabling further optimization of production and the identification of R&D priorities."

With improvements in the emitter in standard cells, and with the passivated emitter and rear cell (PERC) being introduced into mass production, bulk recombination is becoming increasingly limiting to achievable cell efficiency [6,7], particularly when using p-type mc-Si wafers [8]. In much of today's mc-Si material, the excess carrier lifetime is limited by dislocations that remain active in the final device, even after gettering and hydrogenation steps [9,10]. However, in recent years the dislocation density of mc-Si has been reduced through advanced engineering of the growth process and the control of the grain size, which (along with improved quartz crucible technology) have also improved bulk lifetimes. As an example, effective lifetimes exceeding 500µs at an injection level of $10^{15} cm^{-3}$ have been measured on p-type mc-Si with surface passivation, after removal of the phosphorus-diffused layers on both sides [11].

A recent study confirmed that a significant proportion of the total variance in mc-Si PERC cell efficiency is due to bulk lifetime [12]. The question arises as to whether much of this variance can be predicted from the as-grown silicon material, noting that the Si material is altered during cell processing, for example by gettering and annealing during phosphorus diffusion and through hydrogen bulk passivation. A prediction of efficiency from the as-grown silicon material would be extremely valuable in terms of enabling further optimization of production (selective processing, sorting, optimization of the crystallization processes, etc.) and the identification of R&D priorities.

The three most important material quality metrics in mc-Si are:

1. Excess carrier bulk lifetime (for simplicity denoted 'lifetime' hereafter)

2. Dislocation area fraction

3. Resistivity

It should be stressed that all measurements of lifetime in this study relate to as-grown material and not to the effective or bulk lifetime of silicon

> "The sPLIR technique defines a new standard for industrial metrology at the ingot level."

after solar cell processing. The dislocation area fraction can be measured accurately on as-cut wafers using PL imaging, while the resistivity can be measured with an eddy-current sensor. However, the bulk lifetime of as-cut wafers cannot be accurately determined from effective lifetime measurements, since the strong surface recombination causes an asymptotic relationship between the bulk and the effective lifetime for values above ~10μs [13]. However, bulk lifetime can be measured on bricks, since this material property is associated with a spectral shift in the PL emission spectrum [14]. Additionally, the resistivity can be readily measured on bricks. It should be noted that the dislocation area fraction across the surface of wafers is not very representative of dislocation area fractions on the side facets of bricks.

Figure 1. Bulk lifetime images of each of the four sides of three bricks, using the spectral PL intensity ratio analysis (sPLIR) [16]. The colour scale ranges from 0 to 300μs and is identical for all images. The weighted average injection level is in the range $1–8\times10^{13}$cm^{-3}, depending on the local lifetime. Each brick facet is approximately 156mm × 315mm in size.
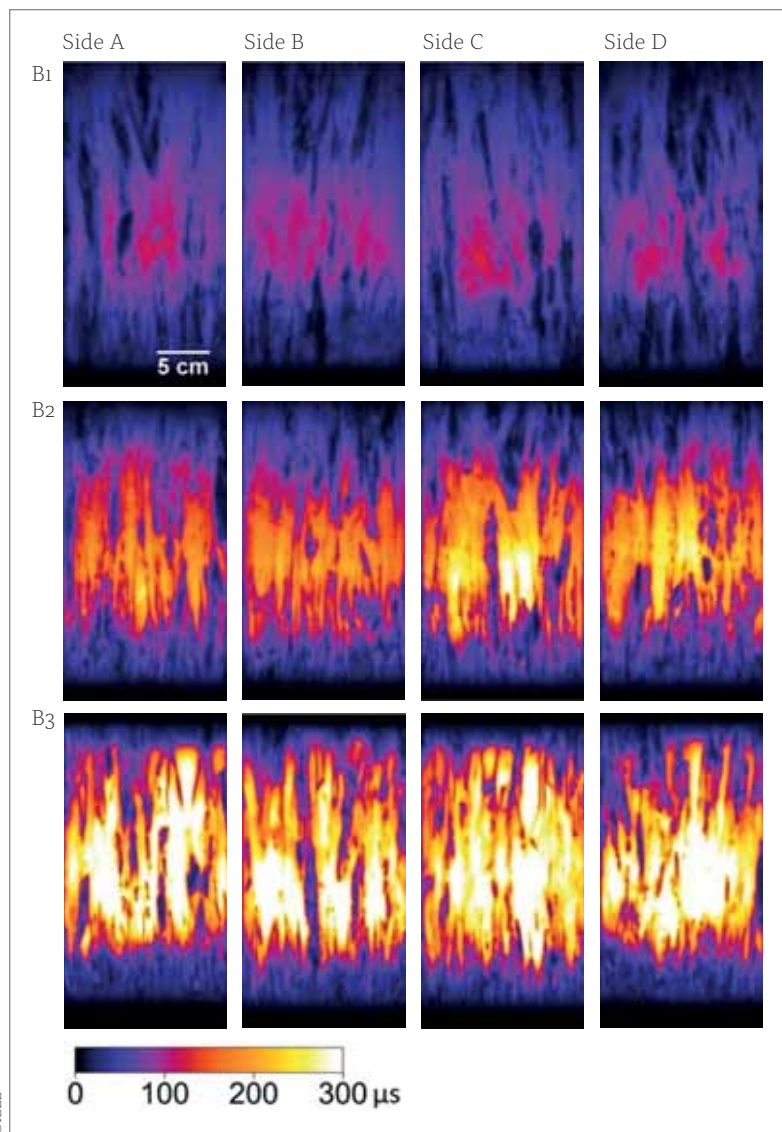
Measurements of dislocation area fractions on as-cut wafer have previously been used to fairly accurately predict cell performance [9]. This approach has worked particularly well for Al-BSF cells, as the performance of these cells is commonly not limited by the bulk lifetime or the respective diffusion length within the larger grains [8,15]. Thus, any variances in cell performance are primarily caused by extended defects, i.e. dislocations and grain boundaries, which act to significantly reduce the lifetime, carrier collection and implied voltage locally. The performance of mc-Si PERC solar cells has been predicted using this approach, but with larger absolute errors, however, because of the stronger influence of bulk lifetime [9]. To the authors' knowledge, predictions of cell efficiencies based on lifetime measurements from PL imaging on bricks have not been published prior to this work. However, Gibaja et al. [16] studied quality metrics based on quasi-steady state photoconductance (QSSPC) measurements on ingots.

The study reported in this paper combines recent advances in ingot PL imaging achieved at UNSW and BT Imaging [17,18], with state-of-the-art high-performance multi material and cell production at Trina Solar [11]. It is shown to what certainty variances in material properties, as measured in silicon bricks, can be used to predict cell performance. In particular, the specific material properties (lifetime, dislocation and resistivity) that have the strongest correlation to cell efficiencies in industrial production are investigated. This paper is an extract of the full paper published by Mitchell et al. [19].

Combining brick, wafer and cell metrology data

Three bricks with a large spread of values in bulk lifetime and dislocation area fractions were selected from the production line at Trina Solar. The bricks originated from different silicon ingots, giving three completely independent samples. Each brick was measured on all four side facets using BT Imaging's LIS-B3 brick inspection tool [20], which utilizes the patented quantitative spectral photoluminescence intensity ratio analysis technique (sPLIR) [14]. In this method, steady-state bulk lifetime images are acquired using a line-scanning photoluminescence (PL) imaging system at an injection level that depends on the bulk lifetime, for example 3×10^{13}cm^{-3} at 1μs and 8×10^{13}cm^{-3} at 500μs, which reflects the depth-weighted average bulk lifetime across the outer 1–3mm of the brick [14]. The sPLIR technique has been developed and refined over the last seven years by UNSW and BT Imaging, and defines a new standard for industrial metrology at the ingot level.

Height-dependent bulk lifetime measurements were made on all four facets of each of the bricks. These bulk lifetime profiles provide a single lifetime value for each wafer position (given as the distance from the bottom of the ingot) by appropriately

averaging the bulk lifetime data over the four sides of the brick. In this study, an image resolution of 320μm per pixel was used to assess the spatially resolved bulk lifetime, resulting in about 1000 data points along the height of the brick. In addition, resistivity measurements along the height profile were taken on all four sides of the bricks.

Fig. 1 outlines the significant spread in material quality that is present across the sampled bricks, with maximum intra-grain bulk lifetimes of up to 120μs in B1, 250μs in B2 and almost 450μs in B3. The appearance of dark features in the bulk lifetime images also indicates that B1 has more dislocations than B2 and B3.

The three bricks were subsequently cropped, polished and sliced into wafers. The wafers were fully tracked, and every fifth wafer was processed into PERC solar cells at Trina Solar. The $I–V$ parameters (I_{sc}, V_{oc}, FF, etc.) of the cells were measured using a production xenon flash lamp $I–V$ tester. The $I–V$ data was then matched with the brick and wafer metrology data as a function of brick number and height.

As-cut wafers were characterized using a BT Imaging QS-W3 wafer inspection tool, and a dislocation value was extracted for every wafer using the tool's proprietary image processing algorithms (in a similar fashion to that described by Demant et al. [9]). The dislocation value is proportional to the area fraction of the dislocations in the wafers.

Between the sample sets, a wide spread of dislocation area fractions can be observed (see Fig. 2). Brick B1 is found to have the most dislocations and the lowest lifetimes. This negative correlation between lifetime and dislocation area fraction is also observed in B2 and B3. Remarkably, a negligible dislocation area fraction is found throughout most of brick B3, which shows significant dislocations only in the top 20%.

Fig. 3 shows the height dependence of the profiles for bulk lifetime from PL measurements on bricks, the dislocation area fractions from wafer PL measurements, and the cell efficiencies (normalized to maximum efficiency). Similar trends for bulk lifetime, with a peak near the centre of the brick, are observed for all samples. The shapes of these profiles are a result of the dynamics of segregation and precipitation of transition metals, and the incorporation of light elements (O, C, N) and their silicides into the crystal [25,26] during solidification of the brick.

The dislocation profiles for bricks B2 and B3 show the typical trend, with increasing area fractions towards the top of the brick, reflecting the increasing stress release during crystal growth. Brick B1, however, reveals a different dislocation profile, with a minimum at the centre of the brick; the reasons for this unusual observation are unknown to the authors. It is noted that the availability of a large sample set mainly from the

bottom half of brick B3, which is virtually free of dislocations, provides a good set of data for the fitting of the model, with the intention of exploring the correlations between bulk lifetime and cell efficiencies, free of the potentially coupled variable that is represented by dislocations.

Cells produced from this experiment achieved maximum efficiencies well above 19%. The peak cell efficiencies are found in the bottom to middle height position of the bricks for B2 and B3, while B1 exhibits only small changes throughout the height profile, except at the very bottom and top. The efficiencies of B1 are determined to be approximately 3% lower than for both B2 and B3. Mean and peak efficiencies are similar for B2 and B3, despite the differences in as-grown lifetimes and dislocation area fractions.

Since there is a clear qualitative correlation between bulk lifetime and cell efficiency in Fig. 3, the cell efficiencies have been plotted as a function of bulk lifetime and are shown in Fig. 4. A linear fit was applied to the entire dataset (bricks 1–3) and a separate linear fit to only the dislocation-free wafers from brick 3. Both fits have a positive gradient with a similar slope, indicating that areas with increased bulk lifetime in the bricks lead to higher cell efficiencies, as expected. The residuals have a significant spread around the fitted line, which indicates that predictions may not be very accurate at the individual wafer level. The residuals along the fitted line are more evenly spread for the dislocation-free wafers, whereas more significant outliers exist at low lifetimes when fitting to the entire dataset. These outliers are in the heavily dislocated wafers of brick 1. These results suggest that a simple linear correlation between cell efficiency and bulk lifetime from brick measurements is sufficient, although the presence of dislocations may complicate the analysis, since dislocations may impact cell efficiency by a second

Figure 2. Dislocation structures for bricks 1–3, derived from PL imaging on as-cut wafers: typical raw PL images with defect overlay (blue) for the upper half (a) and the lower half (b) of each brick.
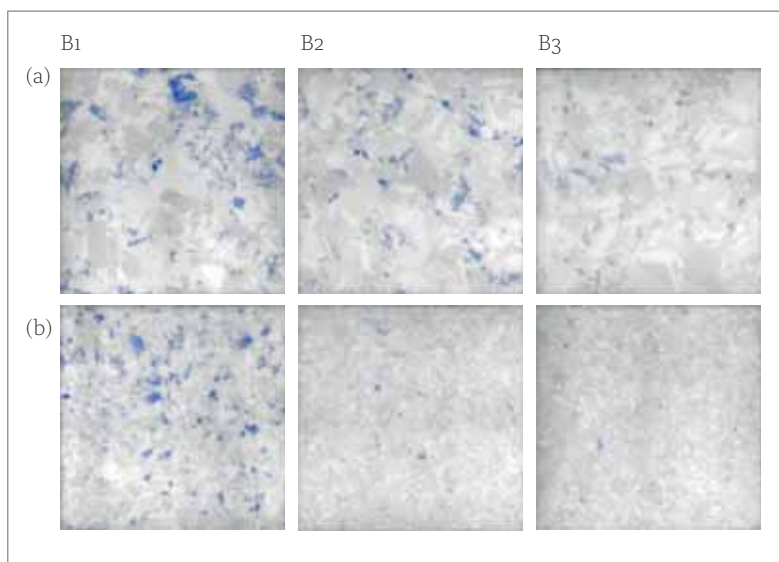
mechanism that is independent of the impact of dislocations on bulk lifetime.

The linear fit in Fig. 4 is in contrast to the simulated cell performance curves (i.e. cell bulk lifetime as a function of cell efficiency) for typical PERC solar cells, which are non-linear [27]. One important difference between Fig. 4 and typical simulated cell performance curves is the x axis, which is the as-grown bulk lifetime in Fig. 4, and cell bulk lifetime in the case of typical simulation curves. An improvement in the 'real' bulk lifetime is expected after cell processing because of the gettering effect of the diffusion process and the hydrogenation effect after firing with a silicon nitride layer; therefore, the as-grown bulk lifetime is not expected to follow the same correlation to cell efficiency as that for cell bulk lifetime. Respectable cell efficiencies are achieved even for very low-quality sections of the brick (see Fig. 4), as a result of substantial improvements in bulk lifetime during cell processing.

A deeper understanding through statistical modelling

To further investigate the relationship between the measured material-quality variables and the $I–V$ parameters of the fabricated PERC cells, a model was developed using the statistical analysis package R [21]. The cell's 1-sun $I_{sc} \times V_{oc}$ product was selected as the designated *response variable*, since it was desired to focus the analysis on lifetime and dislocation predictors, and to avoid the strong dependence of efficiency on the *FF*, which in turn is highly dependent on the base resistivity and the metallization. A similar line of argument can be applied to other $I–V$ parameters (e.g. V_{oc}) [9,12]. Using the $I_{sc} \times V_{oc}$ product also significantly reduces the impact of processing-related variations, e.g. series resistance and shunt resistance.

A linear mixed model [22,23] is used to fit the relationship between the response variable $I_{sc} \times V_{oc}$ and the measured metrology data, with a normal distribution assumption, using the package 'nlme' in R [24]. This approach is used instead of an ordinary least-squares multiple linear-regression approach, since the response data, i.e. the solar cell's $I_{sc} \times V_{oc}$ products, are clustered within bricks, and additionally a non-uniform within-brick correlation structure is expected. Hence these values cannot be regarded as independent of each other, especially if the wafers originate from an approximately similar location within the same brick.

Three models for various types of relationship (lifetime only, dislocation metric from wafer measurements only, and a combination of the two) were used to fit the data. Each model included a

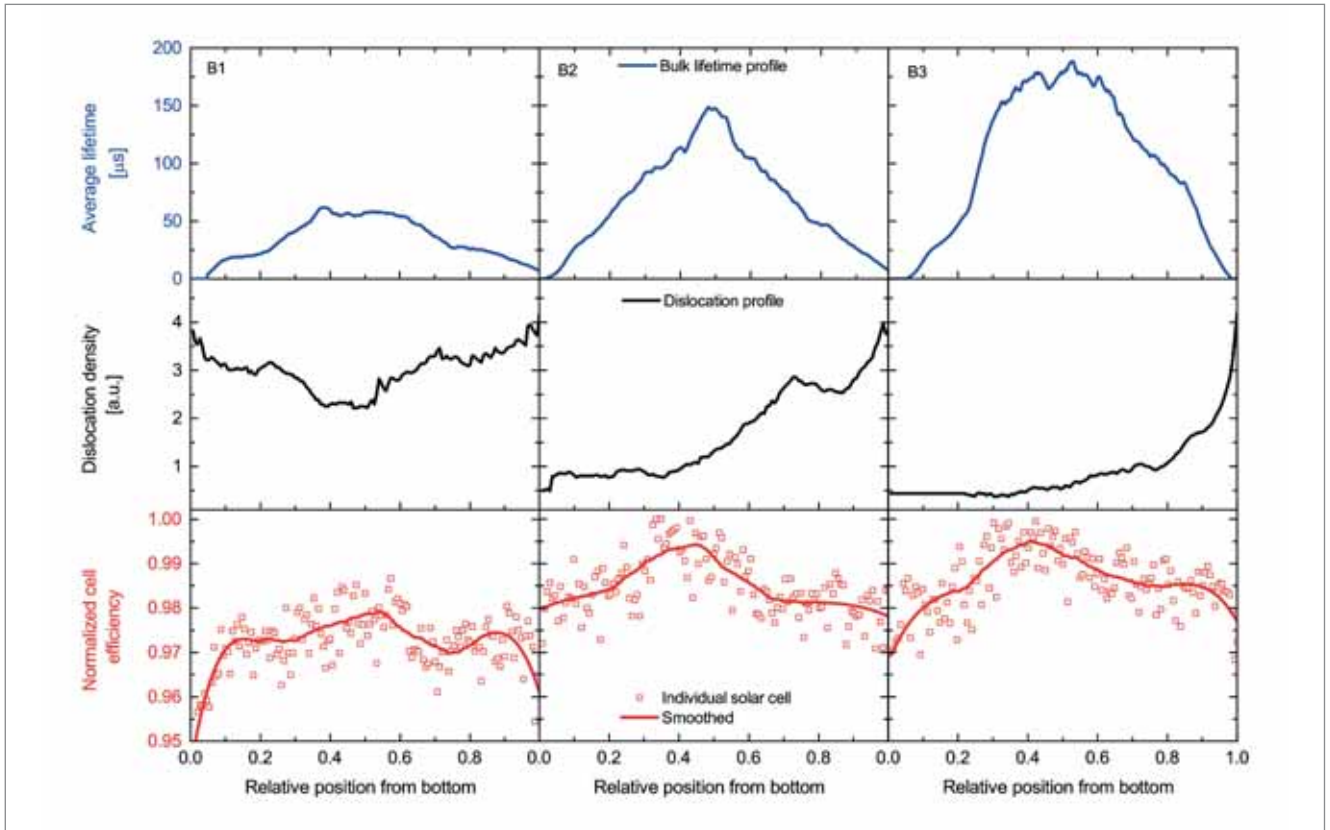Figure 3. As-grown bulk lifetime from brick measurements, dislocation area fractions from wafer measurements, and PERC cell efficiencies along the height profile for bricks B1, B2 and B3. Lifetime data is represented by the harmonic mean from all pixels at a given height using Equation 1, at an injection level of $1-8\times10^{13}cm^{-3}$, depending on the lifetime. The efficiency data is globally normalized to allow for comparisons between the three bricks, and a smoothed (polynomial fit?) curve is shown in the graphs. The spread of the data around the smoothed curve indicates the influence of the variability in cell processing and I–V measurements on the results.

'random effect' term for the bricks in order to allow the adjustment of the response 'baseline' for each brick. The combined model, for example, includes the bulk lifetime value and the wafer dislocation values, each with a single fitting parameter. A correlated random error term is included to account for the correlation between neighbouring wafers due to their physically sequential arrangement within the bricks. The model equation is:

$$y_{i\,j} = \beta_0 + \beta_1\tau_{i,j} + \beta_2\delta_{i,j} + b_i + e_{i,j} \qquad (1)$$

where

$y_{i,j}$ = observed value of the response variable for observation j in brick i (i = 1, 2, 3);

$\tau_{i,j}$ = harmonic mean of the observed bulk lifetime value;

$\delta_{i,j}$ = dislocation value;

b_i = random effect for brick i, assumed to be normally distributed with zero mean and variance σ_b^2;

$e_{i,j}$ = random error, assumed to be normally distributed with zero mean and variance σ_e^2;

β_o = overall intercept;

β_1, β_2 = the fitted parameters.

Before using the linear mixed models, each data point was normalized by subtracting the global
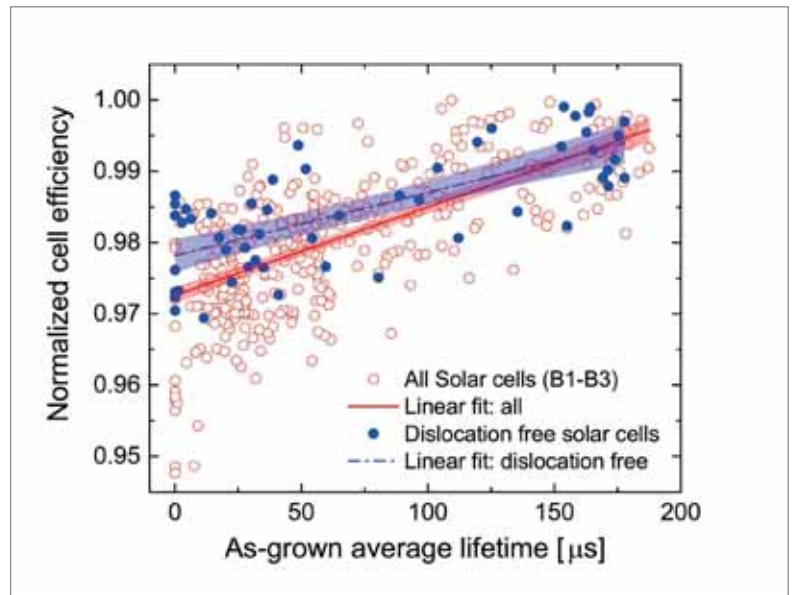
Figure 4. Correlation of cell efficiency, normalized to the highest-efficiency cell, and the harmonically averaged as-grown bulk lifetimes across the full sample set (red empty circles) and across the dislocation-free bottom half of brick B3 (blue filled circles). The shaded area is the standard error of the regression. Note that the bulk lifetime for the cell after processing is not known.

arithmetic mean and dividing by the global standard deviation for each of the data streams: τ, δ and $I_{sc} \times V_{oc}$. The resulting units of the data points used in the fitting can be thought of as the number of standard deviations from the mean, where the mean

©IEEE
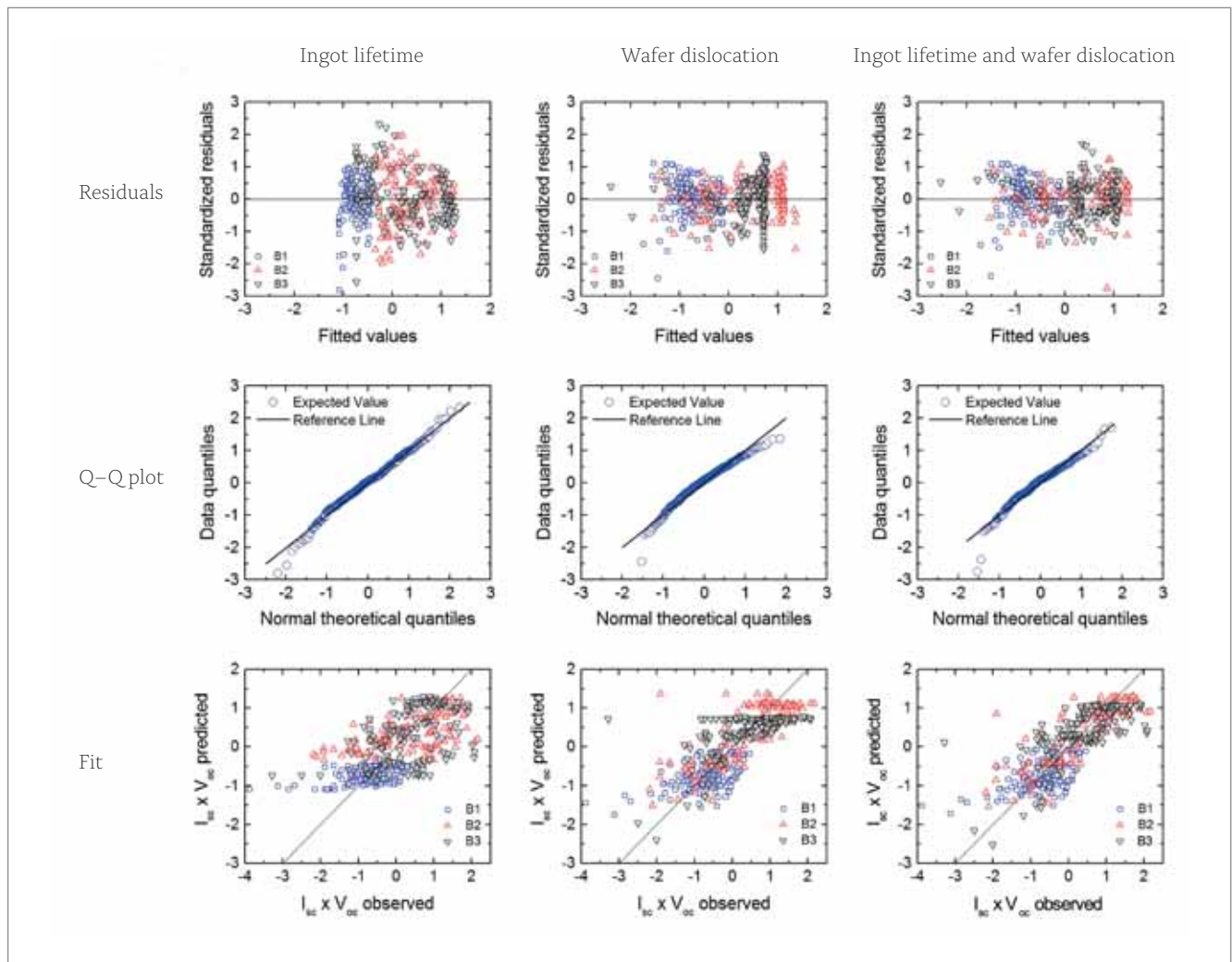
Figure 5. Residuals, Q–Q plots and fitted vs. observed values for three models: lifetime only (left), wafer dislocation only (centre), and lifetime with wafer dislocation (right). All values are standardized, i.e. the axis values show unitless multiples of standard deviation above or below the respective mean values.

> "Respectable cell efficiencies are achieved even for very low-quality sections of the brick, as a result of substantial improvements in bulk lifetime during cell processing."

is zero. This practice allows a fair comparison to be made between model equations and information, as presented graphically.

Three separate models are used here to investigate the influence of various measured variables on the measured response variable $I_{sc} \times V_{oc}$ (see Equation 1); the specific variables are the lifetimes measured on the bricks, and the dislocation area fractions measured on the wafers.

First, the influence of lifetime alone is investigated, followed by the influence of the dislocation area fraction, as measured on the wafers. Finally, the models are compared using the two variables in additive combination. The model is a linear mixed-effects model, with a normal distribution assumption, fitted with the restricted maximum likelihood (REML) algorithm. Because of the spatially sequential

arrangement of wafers in each brick, an appropriate correlation structure has been fitted to the model errors $e_{i,j}$. The correlation structure with the best fit (judged by likelihood ratio tests) is one which decays exponentially with the distance between the wafers. The same correlation structure is incorporated into all three models. Note that a standard linear model which neglects the correlation within the bricks and the random effect term resulted in similar best fits.

Graphs useful for assessing the assumptions in the models and for gauging the predictive ability of the fitted models are shown for each of the three models in Fig. 5. The plots of actual values vs. fitted curves allow the assumption of homoscedasticity (homogeneity of variance) to be assessed. This requirement appears to be satisfied for all three models. This is supported by Fig. 3, which shows that significant process-induced variance is observed, but appears uniformly spread across the data. The quantile–quantile (Q–Q) plots in Fig. 5 demonstrate the degree to which a normal distribution assumption holds; this appears to be satisfied by all three fitted datasets, which inspires confidence in drawing conclusions from these fitted datasets.

Variables	Ingot lifetime	Wafer dislocations	Ingot lifetime and wafer dislocations
Model number	1	2	3
AIC	813	773	752
P-value (fixed effects)	<0.001	<0.001	<0.001 (both)
Model 1 vs. Model 3			<0.001
Model 2 vs. Model 3			<0.001
RMSE	0.80	0.66	0.61

Table 1. Akaike information criterion, p-values and root mean square error for the set of three models. Note that the RMSE value contains significant process-induced variance.

From Table 1, the combined model (Model 3) is the preferred model, because it has the lowest Akaike information criterion (AIC) value compared with each of the single-predictor models. The AIC value measures the relative quality of each model for comparison purposes.

In Fig. 5 the data is gathered more tightly around the fitted line for Model 3 throughout the whole range. The results show that the correlation between lifetime and solar cell output parameter $I_{sc} \times V_{oc}$ is statistically significant. However, for the model with lifetime only (Model 1) there is a 'tail' of sample values that are not well fitted by the model: these samples originate largely from the very bottom of the bricks.

It was found that the model that uses solely the variation of dislocation area fraction as measured on wafers provides a better fit than the model that relies on lifetime alone for this sample set. The model using dislocation as the only variable has smaller AIC and RMSE values than in the case of the model based on brick lifetime (see Table 1). However, in the bottom section of bricks B2 and B3, where the wafers are virtually dislocation free, the dislocation metric cannot be used to fit changes in $I_{sc} \times V_{oc}$. In this section of the brick, lifetime is the dominant metric. Unsurprisingly, the combined parameter model also proves to be a better model than both the models that rely on a single variable. This modelling demonstrates that lifetime has a significant influence on efficiency when used together with the dislocation information from the wafer measurements. With increasing improvements in wafer quality in terms of dislocation densities, and with increasing cell efficiencies, it is expected that, practically speaking, bulk lifetime will play an increasingly significant role in determining cell performance.

The modelling results indicate that lifetime and dislocation are partially correlated with each other, since Model 3 still has a lower AIC value than either Model 1 or Model 2.

Conclusions and final remarks

As-grown bulk lifetimes derived from sPLIR measurements on mc-Si bricks have been found to have a statistically significant correlation with the performance, i.e. the $I_{sc} \times V_{oc}$ product

"sPLIR can be used to select the best high-bulk-lifetime and low-dislocation silicon for high-efficiency lines."

or the efficiency, in mc-Si PERC solar cells. For dislocation-free material, a good fit to a linear correlation between the as-grown bulk lifetime and the $I_{sc} \times V_{oc}$ product is found.

Models based on fitting the dislocation metrics derived from PL images measured on as-cut wafers remain more statistically significant across the sample set studied here. However, with further reductions in the variability of dislocation area fractions of mc-Si, as-grown bulk lifetime will become more relevant; this is a global industry trend and is demonstrated in bricks 2 and 3 in this study. Quantitative brick inspection, in particular the bulk lifetime analysis based on sPLIR, will therefore play an important role for routine quality-control inspection in production, and for faster and more efficient process feedback in R&D.

In the short term, sPLIR can be used to select the best high-bulk-lifetime and low-dislocation silicon for high-efficiency lines. The unselected material can be sent to Al-BSF cell lines with very little negative impact on these lines, since this older cell process is less sensitive, especially to bulk lifetime. For manufacturers the cost of adding sPLIR for brick inspection would probably be more than offset by the gains in cell efficiencies in high-efficiency PERC lines. Additionally, the spatially resolved sPLIR results yield direct and detailed feedback for optimizing ingot growth parameters over solidification time. And as more-advanced mc-Si solidification processes become more widespread, the situation may arise where dislocations are so controlled that bulk lifetime, as measured on bricks, will be the only measurable material-related metric that impacts cell efficiency, and hence will be the primary metric for quality control and efficiency sorting. Importantly, the relevant lifetime range, with bulk lifetimes exceeding 100μs or even in the millisecond range, is not measurable using microwave-detected photoconductance decay (PCD)-based tools, which report effective lifetimes only.

....

References
[1] ITRPV 2017, "International technology
roadmap for photovoltaic (ITRPV): 2016 results",
8th edn (Mar.) [http://www.itrpv.net/Reports/
Downloads/].
[2] Schmidt, J. & Bothe, K. 2004, "Structure and
transformation of the metastable boron- and
oxygen-related defect center in crystalline silicon",
Phys. Rev. B, Vol. 69, No. 2, p. 24107.
[3] Vargas, C. et al. 2017, "Recombination
parameters of lifetime-limiting carrier-induced
defects in multicrystalline silicon for solar cells",
Appl. Phys. Lett., Vol. 110, No. 9, p. 92106.

[4] Herguth, A. et al. 2008, "Investigations on the
long time behavior of the metastable boron–
oxygen complex in crystalline silicon", *Prog.
Photovol: Res. Appl.,* Vol. 16, No. 2, pp. 135–140.
[5] Hallam, B.J. et al. 2014, "Advanced bulk defect
passivation for silicon solar cells", *IEEE J. Photovolt.,*
Vol. 4, No. 1, pp. 88–95.
[6] Dullweber, T. & Schmidt, J. 2016, "Industrial
silicon solar cells applying the passivated emitter
and rear cell (PERC) concept – A review", *IEEE J.
Photovolt.,* Vol. 6, No. 5, pp. 1366–1381.
[7] Min, B. et al. 2017, "A roadmap toward 24%
efficient PERC solar cells in industrial mass
production", *IEEE J. Photovolt.,* Vol. 7, No. 6, pp. 1–10.
[8] Steinkemper, H., Hermle, M. & Glunz, S.W. 2016,
"Comprehensive simulation study of industrially
relevant silicon solar cell architectures for an
optimal material parameter choice", *Prog. Photovolt:
Res. Appl.,* Vol. 24, No. 10, pp. 1319–1331.
[9] Demant, M. et al. 2016, "Inline quality
rating of multi-crystalline wafers based on
photoluminescence images", *Prog. Photovolt: Res.
Appl.,* Vol. 24, No. 12, pp. 1533–1546.
[10] Haunschild, J. et al. 2010, "Quality control
of as-cut multicrystalline silicon wafers using
photoluminescence imaging for solar cell
production", *Sol. Energy Mater. Sol. Cells,* Vol. 94, No.

12, pp. 6–11.

[11] Deng, W. et al. 2016, "20.8% efficient PERC solar cell on 156 mm×156 mm p-type multi-crystalline silicon substrate", *IEEE J. Photovolt.,* Vol. 6, No. 1, pp. 3–9.

[12] Wasmer, S. et al. 2017, "Impact of material and process variations on the distribution of multicrystalline silicon PERC cell efficiencies", *IEEE J. Photovolt.,* Vol. 7, No. 1, pp. 118–128.

[13] Bothe, K. et al. 2010, "Determination of the bulk lifetime of bare multicrystalline silicon wafers", *Prog. Photovolt: Res. Appl.,* Vol. 18, No. 3, pp. 204–208.

[14] Mitchell, B. et al. 2011, "Bulk minority carrier lifetimes and doping of silicon bricks from photoluminescence intensity ratios", *J. Appl. Phys.,* Vol. 109, No. 8, pp. 83111-1–83111-12.

[15] Geerligs, L.J. 2003, "Impact of defect distribution and impurities on multicrystalline silicon cell efficiency", *Proc. 3rd WCPEC,* Osaka, Japan.

[16] Gibaja, F. et al. 2013, "Silicon ingot quality and resulting solar cell performance", *Energy Procedia,* Vol. 38, pp. 551–560.

[17] Mitchell, B., Chung, D. & Teal, A. 2016, "Photoluminescence imaging using silicon line-scanning cameras", *IEEE J. Photovolt.,* Vol. 6, No. 4, pp. 967–975.

[18] Mitchell, B. et al. 2016, "Metrology at the ingot level : Addressing the growing importance of bulk material quality", *Photovoltaics International,* 33rd edn, pp. 34–40.

[19] Mitchell, B. et al. 2017, "PERC solar cell performance predictions from multicrystalline silicon ingot metrology data", *IEEE J. Photovolt.,* Vol. 7, No. 6, pp. 1619–1626.

[20] BT Imaging 2017, "LIS-B3: Production tool for silicon ingot and brick inspection" [http://bit.ly/2gKFLZz].

[21] R Core Team 2016, "R: A language and environment for statistical computing", R Foundation for Statistical Computing, Vienna, Austria [http://www.R-project.org/].

[22] McLean, R., Sanders, W. & Stroup, W. 1991, "A unified approach to mixed linear models", *Am. Stat.,* Vol. 43, No. 1, pp. 54–64.

[23] Oberg A.L. & Mahoney, D.W. 2007, "Linear mixed effects models", *Methods Mol. Biol. Top. Biostat.,* Vol. 404, pp. 213–234.

[24] Pinheiro, J. et al. 2016, "nlme: Linear and nonlinear mixed effects models", R package [https://CRAN.R-project.org/package=nlme].

[25] Mitchell, B. et al. 2014, "Imaging as-grown interstitial iron concentration on boron-doped silicon bricks via spectral photoluminescence", *IEEE J. Photovolt.,* Vol. 4, No. 5, pp. 1185–1196.

[26] Schubert, M.C. et al. 2013, "Impact of impurities from crucible and coating on mc-silicon quality – The example of iron and cobalt", *IEEE J. Photovolt.,* Vol. 3, No. 4, pp. 1250–1258.

[27] Wagner, H. et al. 2015, "Device architecture and lifetime requirements for high efficiency multicrystalline silicon solar cells", *Energy Procedia,* Vol. 77, pp. 225–230.

About the Authors

Bernhard Mitchell is a semiconductor physicist with more than 10 years' experience in the PV sector, in both silicon and III-V technologies. He has worked at many leading PV research institutes around the world, including the University of Konstanz, UC Berkeley and Fraunhofer ISE, and has spent many years at UNSW Australia. He has developed a special expertise in metrology for silicon PV, and is now an R&D engineer with Wavelabs Solar Metrology Systems GmbH in Germany.

Daniel Chung is a Ph.D. student at the Australian Centre for Advanced Photovoltaics at UNSW Australia. His research focuses on the development of photoluminescence characterization of silicon ingots and applications in solar cell manufacturing.

Zhen Xiong is the chief engineer of ingot and wafer technology at Trina Solar. After graduating from the Chinese Academy of Sciences, he received his Ph.D. in 2010 and joined Trina Solar, where he focuses on research into silicon crystalline growth as well as the related characterization techniques.

Pietro P. Altermatt is the principal scientist at the State Key Laboratory for PV Science and Technology (SKL) at Trina Solar. In the 1990s he contributed to achieving the world-record PERL cell efficiencies at UNSW with numerical device modelling. He now equally successfully models mass-fabricated PERC cells, which are very similar in design to PERL cells.

Peter Geelan-Small is a biometrician with a background mainly in the area of natural resource management. He is currently a statistical consultant at UNSW, working in a broad range of areas, including projects from various engineering fields.

Thorsten Trupke is a semiconductor physicist with more than 15 years' experience in R&D in the PV sector, and with an emphasis on the development of novel characterization methods. He is a professor at the Australian Centre for Advanced Photovoltaics at UNSW, and also a co-founder and the CTO of BT Imaging, a start-up company that commercializes PL imaging inspection systems.

....

Enquiries
Bernhard Mitchell
Wavelabs Solar Metrology Systems GmbH
Germany

Email: b.mitchell@wavelabs.de

News

LONGi Solar plans 22% record PERC cell in production at end of 2017

Leading monocrystalline manufacturer LONGi Green Energy Technology has said its subsidiary, LONGi Solar, will ramp volume production of its Passivated Emitter Rear Cell (PERC) technology by the end of 2017.

LONGi Solar reported a world record conversion efficiency for a p-type monocrystalline PERC solar cell which was initially certified by CPVT in China at 22.17% in April and then, with further developments at Fraunhofer ISE CalLab in Germany, a new record efficiency of 22.71%.

Credit: LONGi Green Energy Technology.

LONGi is putting its record-breaking mono PERC cell into production almost immediately.

However, unlike many world record efficiency claims, LONGi Solar said it expected to take the 22% plus cell from its 100MW pilot cell line and start volume production only a few months later.

Dr. Li Hua, VP of cell R&D of LONGi Solar said: "Based on large-area, p-type monocrystalline silicon wafer, we are able to employ mass production compatible cell process technology and able to realize a conversion efficiency of 22.71%. This greatly enhances the entire industry's confidence in p-type monocrystalline cell. With continued R&D optimization, we believe the monocrystalline PERC cell can reach a conversion efficiency of greater than 23.0% in the near future."

TOOLING

Amtech bags follow-on order for next generation solar ALD systems for PERC line

A subsidiary of PV equipment supplier Amtech Systems has received a follow-on order for three next generation solar Atomic Layer Deposition (ALD) systems.

SoLayTec B.V. expects to ship the equipment and install it in this fiscal year. SoLayTec has booked a total of 25 ALD system orders since its inception, of which 15 will be used in mass production. The orders SoLayTec has received from this particular customer represent a total of 1GW of PERC production capacity.

Fokko Pentinga, CEO and president of Amtech, commented: "This follow-on order brings the total ALD tools ordered by this specific customer to seven. Four systems have been put in production of PERC solar cells in the second half of fiscal 2017.

"There is a high level of enthusiasm in the PV marketplace for PERC solutions and this manufacturing platform supports our customers' goals to improve the total cost of ownership by increasing cell efficiency."

Amtech Systems continued to benefit from major solar order conversion to revenue in its fiscal fourth quarter of 2017.

3D-Micromac supplies laser tools for PERC migration at Hanwha Q CELLS China cell plant

Laser micromachining specialist 3D-Micromac has said it is supplying Hanwha Q CELLS' solar cell plant in Qidong, Jiangsu-province, China, with its microCELL OTF laser system for its recently announced transition from aluminium back surface field (Al-BSF) to passivated emitter rear cell (PERC) technology.

PV Tech first reported that Hanwha Q CELLS had started to migrate to some of its cell capacity to PERC, which equated to 1.4GW, while retaining around 1.2GW of BSF production. The SMSL has kept capital expenditures very low in 2017 to support financial efforts to return to profitability.

3D-Micromac said that it had installed three of its microCELL OTF laser systems at the Qidong solar cell plant and had received a follow-on order for a fourth laser system.

The microCELL OTF laser system is used for contact opening of the rear side passivation layer, which reduces electrical losses in the cell, boosting conversion efficiencies.

Intevac hit by delays in shipping major 'ENERGi' solar ion implant tool order

Specialist semiconductor and PV equipment supplier Intevac has reported delays in supplying a 12-unit order for its 'ENERGi' solar ion implant tool to a customer in China planning to ramp n-type mono interdigitated back contact (IBC) solar cells and modules.

In reporting third quarter 2017 financial results, Intevac's management noted in the earnings call that only three ENERGi tools had been shipped to the customer during the quarter.

The US$23 million order, booked in March 2017, was to support 1GW of new high-efficiency n-type mono IBC cell production with cells also being bifacial. The company had previously said all 12 tools would be delivered in 2017 and recognised in revenue in 2018 after receiving the first customer
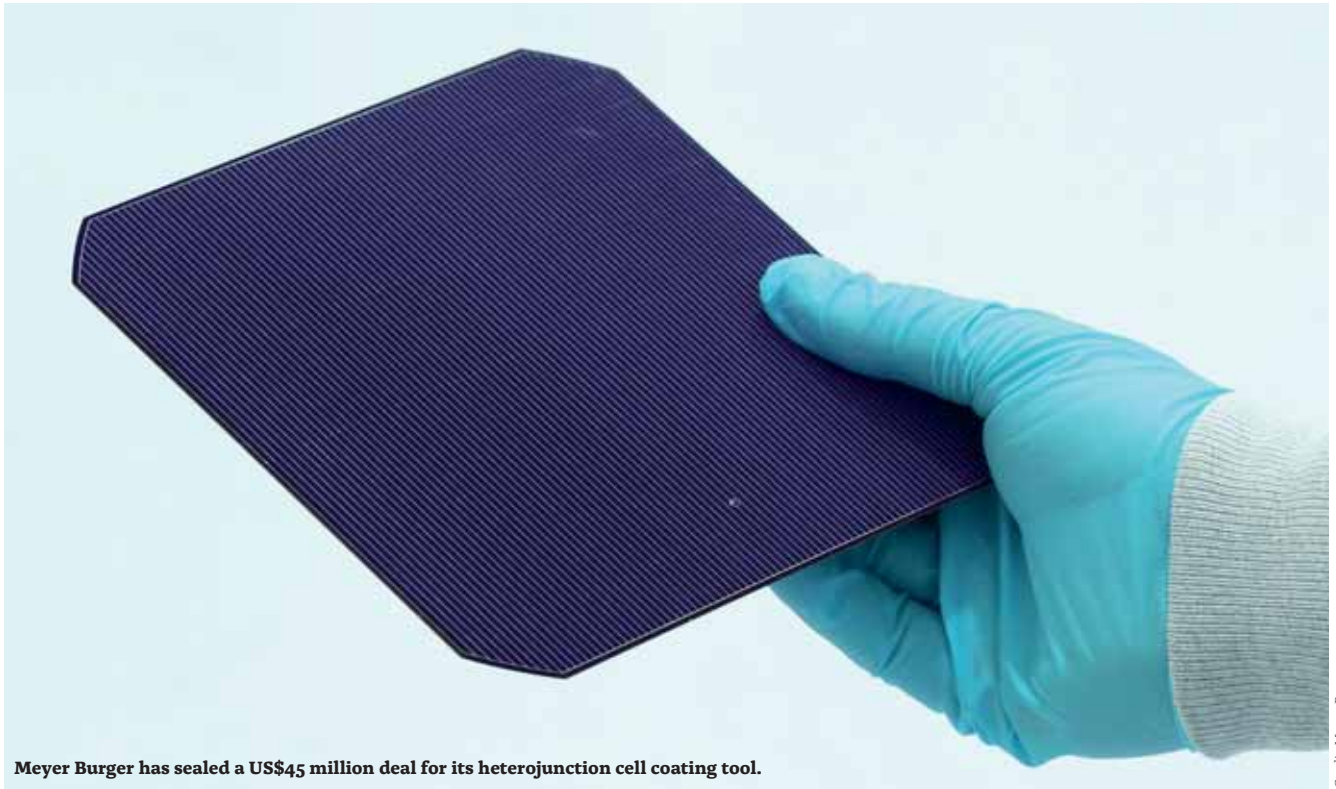
Credit: Meyer Burger

Meyer Burger has sealed a US$45 million deal for its heterojunction cell coating tool.

tool acceptances.

However, Wendell Blonigan, president and chief executive officer of Intevac said in the latest earnings call: "Our purchase contract calls for our customer to take delivery of all 12 tools before year end, but delays in their factory build has resulted in them delaying the delivery schedule for the systems. We shipped the first three in the third quarter with the scheduling of the remaining tools still being determined."

Blonigan added that "the first three tools should revenue in the first half [of 2018] with the revenue timing for the next nine tools dependent on the revised shipment schedule".

Intervac noted that the next four ion implant tools were near completion at its assembly facility but the first three tools had yet to be installed and therefore qualification of the tools had not started.

Meyer Burger confirms heterojunction deal worth over US$45 million

PV manufacturing equipment supplier Meyer Burger has confirmed a major order with an Italian PV manufacturer to supply heterojunction (HJ) solar cell coating technology as part of previously announced plans.

Meyer Burger said that the CHF45 million (US$45.6 million) deal included installation, on-site training and service of its HELiA platform for the production of high-efficiency bifacial HJ solar cells as well as a full interlink automation of the manufacturing facility, intended to provide capacity of 200MW of cells per annum.

The equipment supplier will also collaborate in a joint development partnership with the PV

manufacturer to drive average HJ cell efficiencies beyond 23%. This is expected to lead to the customer adopting Meyer Burger's SWCT module technology. Initial production is expected to use conventional busbars.

Delivery of the equipment to the customers existing facility in Catania, Italy was said to start by mid-2018, with full production expected to begin in 2019.

Singulus supplying SILEX II systems to China and US

Specialist PV manufacturing equipment supplier Singulus Technologies has secured new tool orders from China and the US for its 'SILEX II' wet cleaning batch system, primarily used for high-efficiency heterojunction (HJ) solar cells.

Singulus said it had received new orders for a total of four SILEX II processing systems for manufacturing of high-efficiency solar cells, while further deals for its vacuum coating technology as complementary to its wet processing system were being negotiated.

Stefan Rinck, CEO of Singulus, said: "We have now already sold over 30 SILEX II and supplied the systems to customers in the USA, China and Europe. In our SILEX II, we offer the solar market a machine with high modularity, enabling us to respond flexibly to a range of process requirements specifically in the production of high-performance solar cells. This system has secured us a leading market position that we have consistently extended."

HJ cell performance in fabrication is more susceptible to contamination than conventional

backside field) and PERC (technologies, requiring greater attention to cleanroom and processing induced contamination and wafer cleaning.

EFFICIENCY MILESTONES

New efficiency record of GCL-SI paves the way for black-silicon cells

'Silicon Module Super League' (SMSL) member GCL System Integration Technology (GCL-SI) has again improved the efficiency of its multicrystalline PERC cells with 'black-silicon' texture.

Wei Wang, senior manager for cell research and development at GCL-SI, presented a new peak efficiency of 20.78%, up from 20.6% announced in June, at the EU PVSEC conference in Amsterdam in September.

The company uses multicrystalline wafers sawn by diamond wire. As the standard acidic etching solution for texturing does not properly work on such wafers due to the smooth surface, GCL-SI has tested three alternatives for a so-called 'black-silicon' texture: reactive ion etching (RIE), metal-catalyzed chemical etching (MCCE) and an acidic etching solution with additives.

38,189 cells manufactured from RIE-treated wafers achieved an average efficiency of 20.43% in GCL-SI's production line; 69,320 cells made of MCCE-processed wafers yielded an average of 20.14%, and a smaller batch of 4,694 cells from wafers that went through an acidic solution with additives ended up with an average of 19.65%.

Fraunhofer ISE reaches record 22.3% multicrystalline cell efficiency in lab

Fraunhofer Institute for Solar Energy Systems ISE has achieved a record conversion efficiency for lab-sized multicrystalline solar cells of 22.3%.

Fraunhofer ISE said that its researchers had succeeded in decreasing the efficiency gap with monocrystalline solar cells, pushing beyond the magical threshold of 22%, confirming greater prospects of multicrystalline materials and solar cells reaching their maximum potential.

As a starting material, the researchers used hyperpure polysilicon from Wacker Chemie with an optimized plasma texture dubbed, 'Tunnel Oxide Passivated Contact Technology (TOPCon),' developed at Fraunhofer ISE for back side contacting. The TOPCon technology is known for applying electrical contacts over the entire rear surface of the cell without patterning, which reduces charge-carrier losses and leads to higher electrical efficiencies.

Fraunhofer ISE also noted that the whole process from multicrystallization and wafering through to the cell structure and processing had been optimized to achieve the results.

Jinko beats its own mono PERC efficiency record

JinkoSolar has beaten its own monocrystalline passivated emitter rear cell (PERC) cell efficiency record notching up a conversion rate of 23.45%.

The achievement has been verified by the Chinese Academy of Sciences' Photovoltaic and Wind Power System Quality Test Centre. It comes just a few weeks after the company registered a milestone of 22.78%.

Jinko claims it is now its fifth such record in the space of a year, which it credits in large part to the integration of a number of manufacturing innovations including data collection, yield traceability, smart diagnostics and self-reporting enabling improved workflow efficiencies at its fabs.

"With the assistance of intelligent manufacturing, we can translate these world record learnings into mass production, which will undoubtedly make a big splash in the market," claimed Kangping Chen, CEO, JinkoSolar.

Fraunhofer ISE has achieved a 22.3% conversion efficiency with a multicrystalline cell.

Credit Fraunhofer ISE

Industrial implementation of bifacial PERC+ solar cells and modules: Present status and future opportunities

Thorsten Dullweber, Henning Schulte-Huxel, Susanne Blankemeyer, Helge Hannebauer, Sabrina Schimanke, Ulrike Baumann, Robert Witteck, Robby Peibst, Marc Köntges & Rolf Brendel, Institute for Solar Energy Research Hamelin (ISFH), Emmerthal, Germany, & Yu Yao, Meyer Burger Technology AG, Gwatt (Thun), Switzerland

Abstract

Since its first publication in 2015, the PERC+ cell concept, which is based on a passivated emitter and rear cell (PERC) design with a screen-printed Al finger grid on the rear, has been rapidly adopted by several solar cell manufacturers worldwide. The rapid industrial implementation of bifacial PERC+ cells is facilitated by the very similar process technology to that of mainstream monofacial PERC cells. Conversion efficiencies of industrial PERC+ solar cells of up to 22.1% (ISFH) with front-side illumination, and of 17.3% (LONGi) with rear-side illumination, have been reported. Meanwhile, four companies offer commercial bifacial PERC+ modules with a maximum rated power of around 300Wp when illuminated from the front side only. These modules incorporate 60 PERC+ cells with four or five busbars, which are interconnected by conventional stringing and tabbing technology. The first small-scale outdoor installations have confirmed an increase in energy yield relative to monofacial PERC modules of between 13 and 22%. Two large-scale outdoor installations with peak capacities of 2MWp and 20MWp are currently under construction in Taiwan and China respectively. A novel bifacial PERC+ prototype module that uses Smart Wire Connection Technology (SWCT) is reported in this paper: a set of 18 halved PERC+ solar cells are interconnected by soldering 18 wires directly to the Ag front and Al rear fingers. The resulting prototype module exhibits independently confirmed front- and rear-side efficiencies of 19.8% and 16.4% respectively. Additionally, Meyer Burger has certified a full-size PERC+ SWCT module in accordance with the IEC 61215 norm, thereby demonstrating the long-term reliability of this novel module technology.

Introduction

The PV industry is currently undergoing a conversion of its production capacity from silicon solar cells with a full-area aluminium rear contact to passivated emitter and rear cells (PERCs) [1,2]. Accordingly, the PV technology roadmap ITRPV [3] forecasts an increased market share of PERC solar cells from the current 15% to 60% by 2027. These industrial PERC cells employ p-type wafers and a full-area screen-printed aluminium (Al) rear layer which only locally contacts the silicon wafer in areas where the rear passivation has been removed by laser contact opening (LCO) [2]. The full-area aluminium layer prevents any transmission of sunlight from the rear side into the silicon wafer and hence precludes any bifacial applications of these industrial PERC cells. This is unfortunate because there is a growing interest in bifacial solar cell concepts for several applications, such as in PV power plants, where the produced electricity can be increased by up to 20% using bifacial solar modules instead of monofacial ones [4,5]. Accordingly, the PV technology roadmap ITRPV predicts a market share of bifacial solar modules of 30% by 2026 [3].

At the moment, industrial bifacial solar cell concepts mainly utilize n-type wafers, such as passivated emitter and rear totally diffused (PERT) solar cells [6–9]. However, a challenge for these bifacial PERT cells is that they typically require screen-printed silver (Ag) finger grids on both sides of the wafer, and hence consume a significant amount of expensive Ag paste. Moreover, the n-PERT cells use single-sided boron and phosphorus doping, which requires additional or alternative process steps compared with those involved in p-type PERC cell processing; as a result, manufacturing costs may be higher.

In 2015 ISFH, in parallel with SolarWorld, introduced a bifacial PERC solar cell called *PERC+* [10], which employs a screen-printed Al finger grid on the rear side, enabling front-side efficiencies of up to 21.5% and rear-side efficiencies of up to 16.7% [11]. Depending on the specific installation conditions at a PV power plant, PERC+ cells can increase energy yield by up to 25% because of their bifacial nature when integrated in glass–glass modules [10,12]. Another potential application is building-integrated PV, where bifacial PERC+ cells could provide a more aesthetically pleasing appearance than solar cells with a full-area Al layer [13]. SolarWorld has pioneered the mass production of bifacial PERC+ cells [14]. Meanwhile, several other solar cell manufacturers have introduced bifacial PERC+ into large-volume production and are now offering commercial bifacial glass–glass modules incorporating PERC+ solar cells.

> "PERC+ cells can increase energy yield by up to 25% because of their bifacial nature when integrated in glass–glass modules."
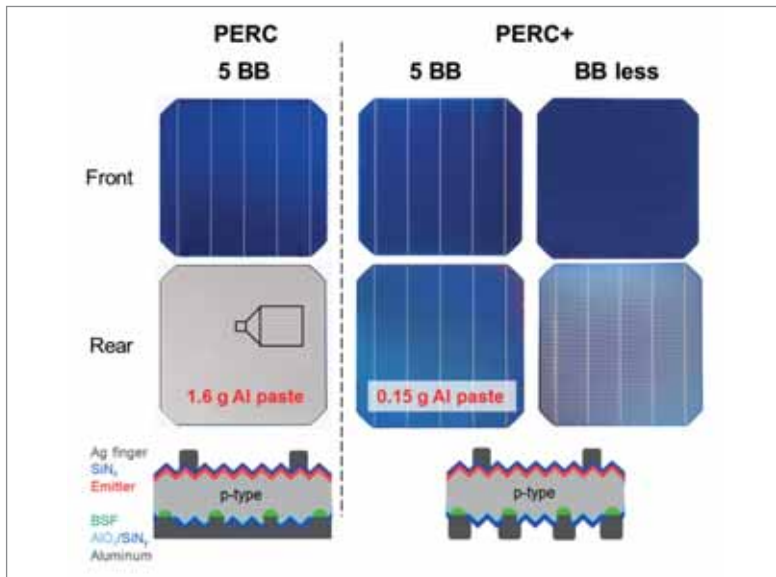
Figure 1. Photographs of the front and rear sides, as well as schematic cross-section drawings, of industrial PERC and PERC+ solar cells. PERC+ cells enable bifacial application and reduce the Al paste consumption, while using the same processing sequence as industrial PERC solar cells.

This paper provides an overview of the status of the implementation of the PERC+ solar cell concept in industrial solar cell and bifacial module production. The first section explains the process technology of PERC+ solar cells, summarizes the published front- and rear-side efficiencies of industrial PERC+ solar cells, and highlights the implications of the Al finger print for the Al-Si alloying process and Al contact formation.

The next section, on commercial PERC+ modules and field installations, outlines the status of commercial bifacial PERC+ glass–glass modules applying conventional tabbing and stringing interconnection technology, which have just recently been made available by several solar cell manufacturers. In addition, that section presents examples of the first outdoor field installations of bifacial PERC+ modules on rooftops or in PV power plants, along with their bifacial gains compared with monofacial PERC reference modules.

In the final section, a novel prototype module is demonstrated. Here, the Smart Wire Connection Technology (SWCT) [15] from Meyer Burger AG is applied to busbarless PERC+ solar cells by soldering 18 wires directly to the front Ag fingers and rear Al fingers, without the use of Ag pads. As a consequence, the Ag paste consumption is reduced to 55mg per PERC+ cell in the printing of the front-side Ag fingers [16]. The resulting PERC+ SWCT prototype module exhibits independently confirmed conversion efficiencies of 19.8% and 16.7% when illuminated from the front and the rear respectively [16].

Industrial PERC+ solar cells

ISFH and SolarWorld, initially independently and

Year	Efficiency [%] front/rear	Organization	Source	Comments
2015	21.5/16.7	ISFH	[11]	Industrial process flow. No rear Ag pads
2015	20.3/n.p.	Trina Solar	[13]	Optimized for optical appearance in BIPV
2016	20.7/13.9	Big Sun Energy Technology Inc	[17]	
2017	21.5/16.1	JinkoSolar	Pers. comm.	
2017	21.4/n.p.	Neo Solar Power	[18]	
2017	21.6/17.3	LONGi Solar	H. Li, pers. comm.	
2017	21.6*/n.p.	ISFH	[16]	Rear side optimized for monofacial applications
2017	22.1*/n.p.	ISFH	**	Busbarless Ag front-grid design

*Independently confirmed; ** This paper.

Table 1. Published efficiencies of industrial PERC+ solar cells when illuminated from the front or rear side. Several leading solar cell manufacturers, such as SolarWorld and Trina Solar, are currently producing bifacial PERC+ cells and modules (see Table 2), but have not reported any, or recent, PERC+ cell efficiencies. (n.p. = not published.)

later jointly, embarked upon the development of a bifacial PERC solar cell design in 2015, by applying a screen-printed rear Al finger grid instead of the conventional full-area aluminium (Al) rear layer (see Fig. 1). This venture was accomplished by the use of the same PERC manufacturing sequence, with only minimal recipe modifications for rear passivation, LCO and Al screen printing [10]. Hence, it was possible for a monofacial PERC cell production line to be switched to producing bifacial PERC solar cells, without requiring any investment in new or different production tools.

The novel cell concept has been named *PERC+*, several advantages of which have been demonstrated in initial publications [10,11]. In particular, the Al finger grid has enabled bifacial application of PERC+ cells, with front-side efficiencies of up to 21.2%, and rear-side efficiencies of up to 16.7%, measured with a black chuck [11]. The corresponding bifaciality (the ratio of rear and front conversion efficiencies) was around 80.0%. When measured with a reflective brass chuck, PERC+ cells demonstrated front-side efficiencies of up to 21.5%, compared with 21.1% efficiencies achieved by conventional PERC cells [11]. The Al paste consumption of the PERC+ cells was drastically reduced to 0.15g instead of 1.6g for conventional PERC cells [10]. PERC+ solar cells are therefore attractive for both bifacial and monofacial module applications [10], which is why the naming convention *PERC+* has been chosen, rather than (for example) biPERC or bifiPERC.

In 2015 two additional publications addressed the concept of bifacial PERC+ cells. Trina Solar reported bifacial glass–glass modules that incorporated bifacial PERC+ solar cells designed for aesthetic optical appearance in building-integrated PV applications [13]. In contrast, Fraunhofer ISE assessed the concept of bifacial PERC+ cells mainly by numerical simulations of the potential front and rear conversion efficiencies and corresponding bifacial gains [12]. Several solar cell manufacturers have since introduced PERC+ solar cells into pilot production or mass production.

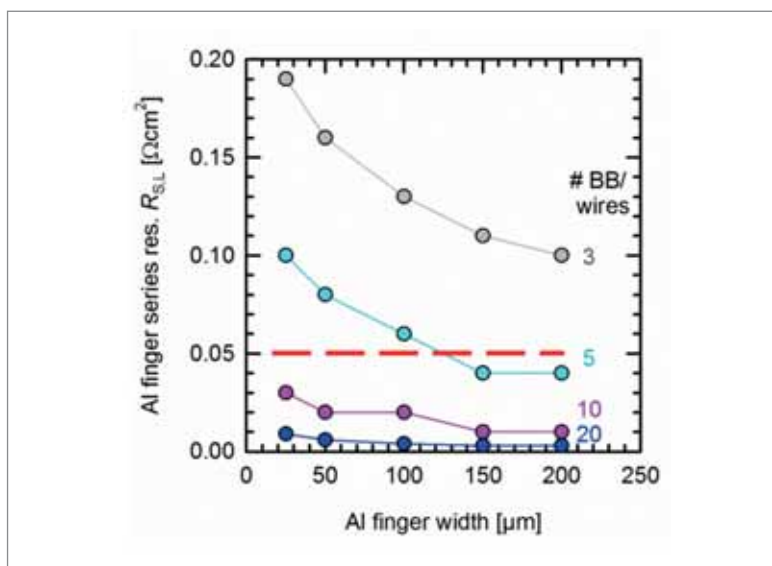Table 1 summarizes the published conversion efficiencies of PERC+ cells when illuminated

Figure 2. Calculated series resistance contribution $R_{s,L}$ of the Al finger grid as a function of the number of busbars/wires and the Al finger width.

from the front or rear side. Whereas ISFH set the benchmark in 2015 for high PERC+ front- and rear-side efficiencies as outlined above, the first published PERC+ conversion efficiencies achieved by solar cell manufacturers were 20.3% [13] in 2015 and 20.7% [17] in 2016; these values have continually improved, to 21.6% in 2017, as reported by LONGi Solar (H. Li, pers. comm.) and by ISFH [16]. The 21.6% efficiency obtained by ISFH has been independently confirmed by ISFH CalTeC.

In addition, a busbarless PERC+ solar cell has recently been developed at ISFH by screen printing just the Ag fingers on the front side, without printing the Ag busbars. As shown in Fig. 1, the Al rear grid still in fact employs a five-busbar layout, since the specific Al finger layout was designed with a five-busbar configuration. However, it is expected that the same efficiency will be obtained with a busbarless Al finger grid.

The busbarless PERC+ cell was measured by Fraunhofer ISE CalLab by contacting the front side with 30 wires and the rear side with a full-area brass chuck. As shown in the last line of Table 1, the

"A key issue with the development of bifacial PERC+ cells is the very high specific resistivity of 20μΩcm."

busbarless PERC+ cell exhibits an independently confirmed conversion efficiency of 22.1% when illuminated from the front side. The other solar cell parameters are: open-circuit voltage V_{oc} = 669mV, short-circuit current density J_{sc} = 40.4mA/cm^2 and fill factor FF = 81.5%. The V_{oc} and FF values correspond very well to the five-busbar reference PERC+ solar cell. The high J_{sc} value of the busbarless PERC+ cell is explained by the absence of busbar shadowing, which increases the J_{sc} by 0.7mA/cm^2 compared with the five-busbar PERC+ cell.

Benefiting from continuous improvements to industrial PERC solar cells, with a current record efficiency of 22.6% [19], it is very likely that even higher PERC+ front-side efficiencies will soon be demonstrated. At the same time, the conversion efficiency of PERC+ cells with rear-side illumination and produced by cell manufacturers has improved from 13.9% [17] in 2016 to 17.3% (pers. comm. H. Li, LONGi Solar) in 2017. For the 21.6%- and 22.1%-efficiency PERC+ cells fabricated by ISFH in 2017, the rear-side efficiency was not measured, as the rear Al finger grid had been optimized for monofacial applications rather than for high bifaciality. Unfortunately, several leading solar cell manufacturers, such as SolarWorld and Trina Solar, who are producing bifacial PERC+ cells and modules (see Table 2) have not published recent (or any) PERC+ cell efficiencies, and hence are absent from Table 1 or only appear there with preliminary results.

If we look at the rapid development and implementation of bifacial PERC+ cells, as demonstrated in Table 1, the question remains as to why it has taken almost 10 years of industrial monofacial PERC cell R&D for the concept of bifacial PERC+ cells to be proved and published. A key issue with the development of bifacial PERC+ cells is the very high specific resistivity of 20μΩcm [10] of screen-printed Al fingers, which is approximately six times higher than that of screen-printed Ag fingers. In consequence, the rear Al finger grid has to be designed in such a way that series resistance losses caused by the Al finger lines are minimized.

The series resistance contribution $R_{s,L}$ of the Al finger grid is calculated as a function of the number of busbars/wires and the Al finger width, as shown in Fig. 2. In order not to significantly reduce the front-side efficiency when switching from PERC to PERC+, as a rule of thumb the series resistance increase caused by the Al finger grid should remain below 0.05Ωcm^2. As this is not possible with a three-busbar configuration because of the large Al finger length between the busbars, the five-busbar design can be regarded as an enabling technology of bifacial PERC+ cells when wide Al fingers of around 150μm are used. When moving to narrow Al fingers below

100μm width, smart wire module interconnection technologies with, for example, 20 wires per PERC+ cell drastically minimize resistive losses of the Al fingers to under 0.01Ωcm². It is challenging, however, to print very narrow Al fingers because of the spreading nature of Al pastes during screen printing.

When research on PERC+ began at ISFH at the end of 2014, the initial Al finger print tests with a 100μm screen-opening width and conventional full-area PERC Al pastes resulted in around 200μm-wide Al fingers. Since then, paste vendors have optimized PERC Al pastes for line-print capability, which now results in the achievement of Al fingers of widths approximately 100–150μm when utilizing a 100μm screen opening. In order to further increase the rear-side efficiency and bifaciality of PERC+ cells in the future, further development of Al pastes with even better fine-line printing capabilities is necessary.

Another challenge with PERC+ is the precise alignment of the Al finger print on top of the LCOs. In the case of extreme misalignment, when the Al finger does not overlap the LCO area, the open silicon surface of the LCO area leads to very high surface recombination of minority-charge carriers, and hence to significantly reduced open-circuit voltages. Accordingly, the alignment tolerances between Al finger print and LCO are in the range ±30μm depending on the detailed Al finger and LCO geometries. This requires high-precision laser processes and Al screens, as well as camera-based alignment schemes between LCO and Al screen print.

An interesting effect is that the limited Al volume of the Al fingers changes the alloying process with the silicon wafer during furnace firing, resulting in deeper Al-BSFs [10,22] compared with PERC cells with a full-area Al layer. The limited Al volume of the Al fingers leads to a higher silicon concentration in the screen-printed aluminium during furnace firing, which causes thicker Al-BSFs during the epitaxial regrowth in the cool-down phase [20]. This effect becomes more pronounced for narrow LCO widths of around 50μm, which are preferred, from a commercial perspective, in order to increase the throughput of the LCO tool.

Whereas with PERC cells a considerable number of voided contacts can be found, especially for narrow LCOs, in the case of PERC+ cells no fully voided contacts are present. Further analysis reveals that voids occur in particular for Al contacts where the Al-Si eutectic extends to a depth of more than 20μm into the Si wafer [21]. To explain this finding, an analytical model has been proposed, which calculates the surface energies of the liquid Al-Si melt, the Si wafer surface and the screen-printed Al particle surface [21]. According to this model, voids form for deep contacts, since in this situation during furnace firing a sufficient amount of Al-Si melt is available in order to wet the large surface area of Al particles, rather than the small surface area of the Si wafer. The Al fingers reduce the Al contact depth by about 7μm, which is the reason why PERC+ cells do not exhibit voids [21]. The increased Al-BSF thickness and the

Figure 3. Photographs of the front and rear sides of a commercial Bisun module from SolarWorld, incorporating PERC+ solar cells (image taken from Dullweber et al. [10]). Whereas this photograph still shows a three-busbar design, the more recent Bisun modules, as well as other bifacial PERC+ modules, use a four- or five-busbar design, as summarized in Table 2.

reduced number of voids of PERC+ cells compared with conventional PERC cells result in up to 3mV higher open-circuit voltages, because of reduced rear-contact recombination [10,21]. This is one reason why PERC+ cells are attractive for both monofacial and bifacial applications.

Commercial PERC+ modules and field installations

SolarWorld pioneered the mass production of bifacial PERC+ solar cells and the fabrication of novel PERC+ glass–glass bifacial modules named Bisun, which were launched at the Intersolar 2015 conference [14,22] (see Fig. 3). Since then, Neo Solar Power, Trina Solar and LONGi Solar have followed this technology route and are now also offering commercial bifacial glass–glass modules incorporating PERC+ solar cells [23–25], as summarized in Table 2. All the manufacturers concerned implement four- or five-busbar designs and obtain maximum power ratings of between 290Wp and 305Wp with 60 PERC+ cells per module [22–25]. These power ratings are stated for front-side illumination only. When additional rear-side illumination is employed, the output power increases accordingly: for example, with 10% additional rear-side illumination, the output power will increase by approximately 8%, to a total output power of close to 330Wp.

A larger number of busbars, such as four or five, is preferred for PERC+ modules, since the specific resistivity of Al fingers is six times higher than that of Ag front fingers [10]. The use of more busbars allows shorter Al finger lengths, thereby lowering the Al finger line resistance and the related resistive power losses. Since the first publication of a PERC

Company/Product	Maximum power rating [Wp]	Busbars/Cells	Source
SolarWorld/Bisun	290	5/60	[22]
Neo Solar Power/Glory BiFi	300	4/60	[23]
Trina Solar/DUOMAX	300	5/60	[24]
LONGi Solar/LR6 -60PD	305	4/60	[25]

Table 2. Commercially available bifacial modules incorporating PERC+ solar cells. The maximum power rating is stated for front-side illumination under standard test conditions (STC: AM1.5, 25°C) and with no rear-side illumination.

Company	Installation	Increased energy yield	Source
SolarWorld, ISFH, ISE	Theoretical calculation	Up to 25% (80% albedo, 0.5m mounting height)	[10]
SolarWorld	3.2kW, Bisun modules, roof installation, Germany	13% measured, 13.3% calculated (74% albedo, 0.28m mounting height)	[27]
SolarWorld	13kW, Bisun modules, single-axis tracker, Germany	22% measured (17% albedo, 0.9m mounting height)	[27]
Trina Solar	20MWp, DUOMAX modules, solar power plant, China	Under construction on sandy ground with high diffuse reflection	[28]
Neo Solar Power	2MWp, Glory BiFi modules, roof installation, Taiwan	Under construction on a Taiwan government building	[29]

Table 3. Examples of field installations of bifacial modules incorporating PERC+ solar cells. When available, simulated and measured outdoor performance values have been provided. The increase in energy yield refers to the additional energy yield generated by bifacial PERC+ modules relative to monofacial reference PERC modules.

Figure 4. Field installations of bifacial modules using PERC+ solar cells: (a) 13kWp Bisun modules from SolarWorld mounted on a single-axis tracker system [27]; (b) 2MWp rooftop installation currently under construction by Neo Solar Power, implementing their Glory BiFi modules [29].

cell using a five-busbar design [26], the PV industry has migrated from three busbars to four (or even five), which is beneficial to the industrial adoption of PERC+ cells as explained above. The interconnection of PERC+ cells in strings is accomplished using conventional tabbing–stringing technology, whereby the Cu ribbons are soldered to the Ag front busbars and to Ag pads on the PERC+ rear side.

In the application of bifacial PERC+ modules to outdoor field installations, the albedo of the ground and the mounting height of the module are particularly important parameters for maximizing the additional diffuse illumination of the module rear side, and hence for maximizing the additional energy yield of a bifacial PERC+ module compared with a monofacial PERC module. Numerical simulations predict that the energy yield of PERC+ modules could increase by up to 25% when mounted at a height of 0.5m above ground that has an albedo of 80% [10].

SolarWorld has made efforts to measure the energy yield of Bisun modules at two different small-scale outdoor test installations, as summarized in Table 3. A 3.2kWp installation on top of a flat roof with a high albedo of 74% as a result of white ballast stones demonstrated an increased energy yield of 13% compared with a monofacial PERC reference module; this compared well with the calculated energy yield of 13.3% [27]. When mounted on a single-axis tracker system, the Bisun modules produced 22% additional energy yield, despite the relatively low albedo of 17% of the sandy ground (Fig. 4(a)) [27].

At present, two large-scale bifacial PERC+ field installations are under construction, as listed in Table 3. Trina Solar is supplying its bifacial DUOMAX modules to a 20MWp power plant in China installed on sandy ground with a high albedo [28]. At the same time, Neo Solar Power is constructing a 2MWp rooftop installation on a Taiwanese government building, which uses its bifacial Glory BiFi modules (Fig. 4(b)) [29]. Both installations will be important for verifying the predicted energy yield increase of bifacial PERC+ modules in actual large-scale outdoor field installations.

Novel PERC+ prototype module employing SWCT

As shown in Fig. 2, one step further in terms of reducing resistive losses caused by PERC+ rear Al

fingers is to move from four- or five-busbar designs to PERC+ solar cells without any busbars. In this case, the module interconnection is accomplished by 18 wires which are soldered directly to the Ag front and Al rear fingers by implementing the SWCT developed by Meyer Burger [15]. This novel PERC+ SWCT module concept was presented at the EU PVSEC conference in 2017 [16].

The PERC+ cells of the PERC+ SWCT prototype module were fabricated at ISFH using a process sequence described in detail in Dullweber et al. [10]. In the reference split group 1, a five-busbar Ag front-grid design was employed. These conventional five-busbar PERC+ cells were used later to calibrate the $I{-}V$ tester which measures the busbarless PERC+ cells. The PERC+ cells of split group 2, which are later used for the SWCT module, are not furnished with Ag busbars on the front; instead, just the Ag fingers are printed, and hence the resulting PERC+ cells of split group 2 are busbarless, as shown in Fig. 1.

For the Al screen printing, the five-busbar reference PERC+ cells of group 1 are printed using an Al screen design with a five-busbar H-pattern, whereas the PERC+ cells of split group 2 are printed using a different screen without Al busbars, but which prints only the Al fingers. Both of these aluminium screens have a finger opening width of 100μm and a pitch p that is identical to the LCO pitch. The Al fingers are printed in alignment with the LCOs. Since the busbarless PERC cells receive only a Ag finger print and no Ag front busbars or Ag rear pads, the Ag paste consumption is reduced to 55mg per busbarless PERC+ cell.

The Ag front and Al rear contacts are fired in a conventional belt furnace, during which the Al paste locally alloys with the silicon wafer in areas where the rear passivation has been removed by laser ablation. A schematic drawing of the resulting bifacial PERC+ solar cell can be seen in Fig. 1. Finally, 18 busbarless PERC+ cells are laser cut into half cells, which are later used for the PERC+ SWCT module fabrication.

The $I{-}V$ characteristics of the five-busbar reference PERC+ cells are measured using a conventional $I{-}V$ tester, which contacts the rear-side full area with a brass chuck, and the front-side busbars with contact bars. The busbarless PERC+ cells are measured using a grid touch $I{-}V$ tester from PASAN, which contacts the front Ag fingers with 30 wires and the rear Al fingers with 20 wires. The PASAN $I{-}V$ tester is calibrated with a five-busbar reference PERC+ cell which has been measured using the conventional $I{-}V$ tester.

A set of 18 halved busbarless PERC+ solar cells are used to fabricate a bifacial prototype module; a Meyer Burger SWCT system installed at the ISFH SolarTeC technology centre is also employed in the module fabrication process. The foil-wire assembly (FWA) tool from Meyer Burger is used to embed 18 wires (with a diameter of 200μm coated with InSn as a low-temperature solder) in a transparent foil.
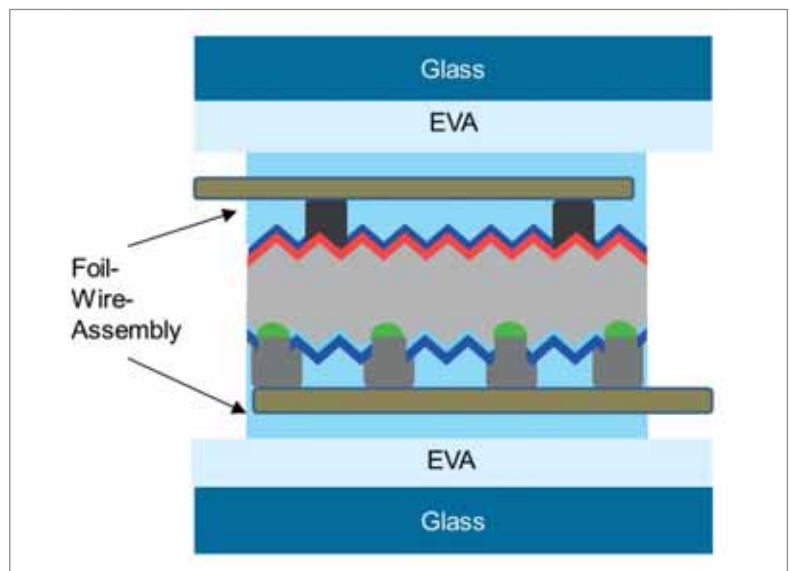

Figure 5. Schematic drawing of the interconnection of PERC+ cells by applying SWCT. During the lamination process, 18 InSn-coated wires are soldered directly to the Ag front and Al rear fingers.

Subsequently, the PERC+ SWCT prototype module is assembled as shown schematically in Fig. 5. The wires contact the Ag front and Al rear fingers directly, without the use of Ag busbars or Ag pads.

The PERC+ cells, including the FWA, are encapsulated by ethylene-vinyl acetate (EVA) foils with enhanced UV transmission [30] on both sides in a glass–glass module configuration. Both glasses are coated with an anti-reflection layer in order to reduce optical losses. Light-reflective films (LRF) produced by the company 3M are placed between neighbouring PERC+ cells; these films guide the incident light towards the cells, thereby increasing the light absorption in the module [31].

"One step further in terms of reducing resistive losses caused by PERC+ rear Al fingers is to move from four- or five-busbar designs to PERC+ solar cells without any busbars."

The module is laminated using a conventional lamination tool. During lamination, the InSn-coated wires are soldered to the Ag front fingers and Al rear fingers. Photographs of the front and rear sides of the resulting PERC+ SWCT prototype module are shown in Fig. 6(a) and (b) respectively. The $I{-}V$ parameters of the PERC+ SWCT prototype module were measured independently by TÜV Rheinland, Germany, for both front- and rear-side illumination conditions.

When illuminated from the front, the five-busbar reference PERC+ cells exhibit efficiencies η_{front} of up to 21.1% with a very narrow distribution, whereas the front-side efficiency of the busbarless PERC+ cells ranges from 20.0 to 20.8%. This reduced efficiency is caused by a decrease in FF from 80.8% for the five-busbar PERC+ cells to between 76 and 78% for the busbarless PERC+ cells. Part of this drop in FF is caused by Ag finger interruptions which occurred as

	V_{oc} [V]	I_{sc} [A]	FF [%]	η [%]
PERC+ SWCT module, front	11.8	4.80	78.7	19.8[a]
PERC+ SWCT module, back	11.8	3.94	78.8	16.4[a]
18 busbarless PERC+ cells, front	11.9[b]	4.91[c]	77.3[c]	20.5[c]

[a] *Independently confirmed by TÜV Rheinland;* [b] *Sum;* [c] *Average.*

Table 4. Measured I–V parameters of the PERC+ SWCT prototype module, as well as those measured independently by TÜV Rheinland, for both front- and rear-side illumination conditions. Additionally, for the 18 PERC+ cells that were used for the module fabrication the sum of the V_{oc} values, along with the average I_{sc}, FF and η values, are given.
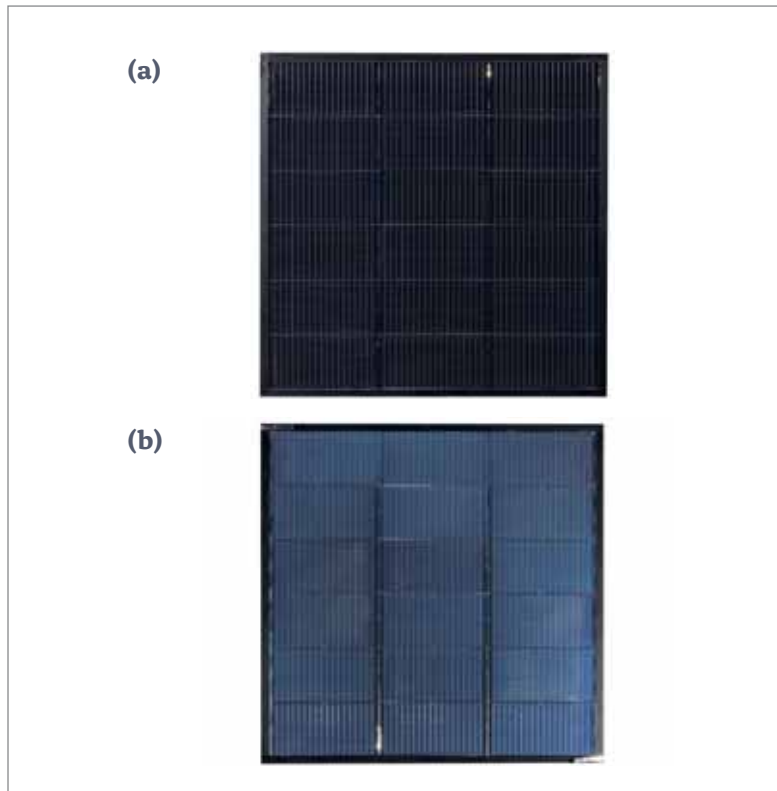
Figure 6. Photographs of the front (a) and rear (b) sides of the PERC+ SWCT prototype module, which incorporates 18 halved busbarless PERC+ cells.

a result of a non-optimized screen-printing process for the busbarless PERC+ cells.

With regard to V_{oc}, this ranges from 657 to 663mV for both five-busbar and busbarless PERC+ cells. The busbarless PERC+ cells yield the highest J_{sc} values of up to 40.4mA/cm² because of the absence of busbar shadowing, whereas the five-busbar PERC+ cells produce values of up to 39.7mA/cm². Whereas the busbarless PERC+ cells described above were used to process the PERC+ SWCT prototype module, in a later PERC+ cell batch the Ag screen-printing issue was fixed and the Al finger grid design was optimized for monofacial PERC+ applications; this then resulted in a 22.1%-efficient PERC+ solar cell, as shown in Fig. 1 and described earlier in the industrial PERC+ solar cells section.

"A full-size PERC+ SWCT module in compliance with the IEC 61215 norm has been certified by Meyer Burger, thereby demonstrating the long-term reliability of this novel module technology."

When illuminated from the rear, the busbarless PERC+ cells exhibit conversion efficiencies η_{rear} of between 15.8 and 16.5%. This relatively low rear-side efficiency is primarily due to a low J_{sc} of around 32mA/cm². As analysed and explained in detail in Dullweber et al. [10], the low J_{sc} values are caused by a high reflectance of the PERC+ rear side. The high reflectance is due to 1) the relatively wide Al fingers, accounting for approximately 10% of the metallized area; and 2) the non-ideal anti-reflection properties of the AlO_x/SiN_y rear passivation between the Al fingers. The bifaciality of the busbarless PERC+ cells is defined as η_{rear} divided by η_{front} and reaches values of up to 79%. As a figure of merit of bifaciality, the equivalent bifacial efficiency is defined as:

$$\eta_{eq,0.1} = \eta_{front} + 0.1 \times \eta_{rear} \tag{1}$$

The factor '0.1' describes the additional stray light intensity irradiating the rear of the PERC+ cells relative to the AM1.5g front-side illumination. In practice, this factor can vary between 0 and 0.25 depending on, for example, the albedo of the ground and the detailed mounting geometries of the bifacial modules [10]. Inserting the measured front- and rear-side efficiency values (see above) in Equation 1 reveals an equivalent bifacial efficiency $\eta_{eq,0.1}$ of up to 22.4% for the busbarless PERC+ cells.

The I–V parameters of the PERC+ SWCT prototype module were independently measured by TÜV Rheinland, Germany, and are summarized in Table 4. When illuminated from the front side, the module exhibits an aperture conversion efficiency η_{front} of 19.8%, a V_{oc} of 11.8V, a short-circuit current I_{sc} of 4.8A and a FF of 78.7%. The module V_{oc} corresponds well to the sum of the V_{oc} values (11.9V) of the 18 busbarless PERC+ solar cells, as indicated in line 3 of Table 4. Moreover, the average I_{sc} of 4.91A of the 18 PERC+ cells corresponds well to the module I_{sc} when account is taken of the optical losses due to, for example, the higher reflectance of the module glass compared with the PERC+ cell. However, the module FF is 1.4% higher than the average FF of the 18 PERC+ cells, which is an indication that the PASAN I–V tester might be underestimating the PERC+ cell FF, since the calibration procedure was not yet optimized.

When illuminated from the rear side, the module I_{sc} decreases to 3.94A, resulting in a rear-side module efficiency η_{rear} of 16.4%; this corresponds well to the respective PERC+ cell rear-side efficiencies (not shown in the table). Accordingly, the module bifaciality

$\eta_{\text{rear}}/\eta_{\text{front}}$ is 83%. Applying Equation 1 results in an equivalent bifacial efficiency $\eta_{\text{eq,0.1}}$ of 21.4% of the PERC+ SWCT prototype module. For comparison purposes, the highest monofacial PERC module efficiency reported so far is 20.2% [33], which demonstrates the additional energy yield to be expected from the novel bifacial PERC+ SWCT module when used in suitable outdoor field installations.

In addition to high conversion efficiencies, another important criterion for a new module technology is its reliability in terms of guaranteeing 20 or 25 years of module operation without significant degradation of the nominal output power. For the novel PERC+ SWCT module technology, the reliability of the interconnection between the Al fingers and the wires in particular has to be demonstrated, in addition to other reliability tests. To this end, Meyer Burger recently fabricated a PERC+ SWCT module utilizing 60 full-size PERC+ solar cells that were interconnected using SWCT module technology with 18 wires per PERC+ cell [32]. The wires had a diameter of 300µm and were coated with an In-free low-temperature solder material. The PERC+ SWCT module was externally certified [32] at Certisolis, France, in accordance with the IEC 61215 norm, which tests all reliability-relevant issues, such as module performance under temperature cycling and mechanical loading. In addition, the PERC+ SWCT module passed the IEC 61730 norm [32], which tests product safety, for example in terms of fire-protection standards.

Conclusions

Since its first publication by ISFH and SolarWorld in 2015, the PERC+ cell concept has been rapidly adopted by several solar cell manufacturers worldwide. The rapid industrial implementation of bifacial PERC+ cells is facilitated by the very similar process technology to that of monofacial PERC cells, which are becoming mainstream in the PV industry.

A novel bifacial PERC+ prototype module which implements SWCT technology has been presented. A batch of 18 halved PERC+ solar cells were interconnected by soldering 18 wires directly to the Ag front and Al rear fingers without the use of Ag busbars or Ag pads. The resulting prototype module exhibited independently confirmed front- and rear-side efficiencies of 19.8% and 16.4% respectively. These values correspond to an equivalent bifacial efficiency of 21.4%, which exceeds the world-record monofacial PERC module efficiency by more than $1\%_{\text{abs}}$. Additionally, a full-size PERC+ SWCT module in compliance with the IEC 61215 norm has been certified by Meyer Burger, thereby demonstrating the long-term reliability of this novel module technology.

Acknowledgements

....

References

[1] Blakers, A.W. et al. 1989, *Appl. Phys. Lett.,* Vol. 55, p. 1363.

[2] Dullweber, T. & Schmidt, J. 2016, *IEEE J. Photovolt.,* Vol. 6, No. 5, p. 1366.

[3] ITRPV 2017, "International technology roadmap for photovoltaic (ITRPV): 2016 results", 8th edn (Mar.) [http://www.itrpv.net/Reports/Downloads/].

[4] Comparotto, C. et al. 2014, *Proc. 29th EU PVSEC,* Amsterdam, The Netherlands, p. 3248.

[5] Janssen, G.J.M. et al. 2015, *Energy Procedia*, Vol. 77, p. 364.

[6] Romijn, I.G. et al. 2013, *Proc. 28th EU PVSEC*, Paris, France, p. 736.

[7] Song, D. et al. 2012, *Proc. 38th IEEE PVSC*, Austin, Texas, USA, p. 3004.

[8] Mihailetchi, V.D. et al. 2010, *Proc. 25th EU PVSEC*, Valencia, Spain, p. 1446.

[9] Dullweber, T. et al. 2016, *physica status solidi (a)*, Vol. 213, No. 11, p. 3046.

[10] Dullweber, T. et al. 2016, *Prog. Photovolt: Res. Appl.,* Vol. 24, p. 1487.

[11] Dullweber, T. et al. 2015, *Proc. 31st EU PVSEC,* Hamburg, Germany, p. 341.

[12] Krauß, K. et al. 2016, *physica status solidi (a)*, Vol. 213, p. 68.

[13] Liu, B. et al. 2015, *Proc. 31st EU PVSEC*, Hamburg, Germany, p. 659.

[14] SolarWorld 2015, Press release [http://www.pv-tech.org/news/intersolar_europe_solarworld_to_launch_glass_glass_bifacial_modules].

[15] Faes, A. et al. 2014, *Proc. 29th EU PVSEC,* Amsterdam, The Netherlands, p. 2555.

[16] Dullweber, T. et al. 2017, *Proc. 33rd EU PVSEC,* Amsterdam, The Netherlands [in press].

[17] Chen, S.-Y. et al. 2016, *Proc. 32nd EU PVSEC,* Munich, Germany, p. 772.

[18] NSP 2017 [https://www.nsp.com/nspsolarcells?lang=en].

[19] Deng, W.W. et al. 2017, *Proc. 44th IEEE PVSC,* Washington DC, USA [in press].

[20] Kranz, C. et al. 2016, *IEEE J. Photovolt.*, Vol. 6, No. 4, p. 830

[21] Kranz, C. et al. 2016, *Sol. Energy Mater. Sol. Cells*, Vol. 158, p. 11.

[22] SolarWorld 2017 [https://www.solarworld.de/en/products/sunmodule-bisun-protect/].

[23] NSP 2017 [https://www.nsp.com/nspsolarmodules?lang=en].

[24] Trinasolar 2017 [http://www.trinasolar.com/en-uk/product/duomax4060/duomax-twin-deg5c07ii].

[25] LONGi Solar 2016 [http://en.longi-solar.com/Home/Products/module/id/12_.html].

[26] Hannebauer, H. et al. 2014, *physica status solidi*

(RRL), Vol. 8, p. 675.

[27] Neuhaus, H. (SolarWorld) 2017, Presentation at PV CellTech Conf., Penang, Malaysia.

[28] Trina Solar 2017 [http://www.trinasolar.com/en-uk/resources/newsroom/mon-05012017-1500].

[29] PV-Tech 2017 [https://www.pv-tech.org/news/nsp-to-construct-first-commercial-rooftop-system-using-its-bifacial-solar-m].

[30] Vogt, M.R. et al. 2016, *Energy Procedia*, Vol. 92, p. 523.

[31] Schulte-Huxel, H. et al. 2016, *IEEE J. Photovolt.*, Vol. 7, No. 1, p. 25.

[32] Yao, Y. et al. 2017, Presentation at 11th SNEC Int. PV Power Gen. & Smart Energy Conf. & Exhib., Shanghai, China.

....

About the Authors

Dr. Thorsten Dullweber leads the industrial solar cells R&D group at ISFH. His research focuses on high-efficiency industrial-type PERC and PERC+ silicon solar cells and ultrafine-line screen-printed Ag front contacts. Before joining ISFH in 2009, he worked for nine years in the microelectronics industry as a project leader at Siemens AG and then at Infineon Technologies AG.

Henning Schulte-Huxel studied physics in Leipzig and Bucharest, and laser technology in Jena, Germany. Between 2009 and 2010 he worked on laser ablation of CuInSe2. In 2010 he joined ISFH, and received his Ph.D. in physics in 2015 from the Leibniz University of Hanover. His research focuses are novel concepts for module integration and the analysis and reduction of cell-to-module losses.

Susanne Blankemeyer trained as an optician at Krane-Optik in Rheda-Wiedenbrück, Germany, and worked there until 1986. Between 1999 and 2007 she was a laboratory assistant in the R&D department at Orbotech, a manufacturer of automated optical inspection systems, in Bad Pyrmont, Germany. In 2007 she joined the module and interconnection technology group at ISFH, where she is currently involved in the development of novel interconnection techniques and optimization of module concepts.

Dr. Helge Hannebauer studied technical physics at the Leibniz University of Hanover from 2005 till 2009. His diploma thesis at ISFH involved the optimization of screen-printed solar cells. In 2016 he completed his Ph.D. thesis, also at ISFH, on advanced screen printing and selective emitters.

Sabrina Schimanke joined ISFH in 2008 as a technical assistant. She is responsible for an industrial wet chemical polishing tool at ISFH, including the development of improved chemical polishing processes. She is also in charge of processing PERC and PERC+ solar cells for different R&D projects at ISFH.

Ulrike Baumann graduated in 2011 as a laboratory technical assistant in chemistry. She then joined the industrial solar cells R&D group at ISFH, where she is in charge of processing industrial PERC and PERC+ solar cells. In addition, she is responsible for the optimization and maintenance of a production-type wet-chemical batch-processing tool.

Dr. Robby Peibst received his diploma degree in technical physics in 2005. In 2010 he received his Ph.D. from the Leibniz University of Hanover, with a thesis on germanium-nanocrystal-based memory devices. He joined ISFH in 2010 and has been in charge of the emerging solar technologies group since 2013. His research focuses on the development of enabling techniques for producing high-efficiency silicon solar cells.

Dr. Marc Köntges received his Ph.D. in physics in 2002 from the University of Oldenburg, for his research into thin-film solar cells. From 2002 he was in charge of the thin-film technology group at ISFH, and then became head of the module and interconnection technology group in 2005. He currently develops characterization and production methods for PV modules.

Rolf Brendel is the scientific director of ISFH. He received his Ph.D. in materials science from the University of Erlangen, for which he researched infrared spectroscopy. In 2004 he joined the Institute of Solid State Physics at the Leibniz University of Hanover as a full professor. His main research focuses on the physics and technology of crystalline silicon solar cells.

....

Enquiries

Thorsten Dullweber
Industrial Solar Cells Group
Institute for Solar Energy Research Hamelin (ISFH)
Am Ohrberg 1, D-31860 Emmerthal, Germany

Yu Yao
Meyer Burger Technology AG
Schorenstrasse 39, CH-3645 Gwatt (Thun), Switzerland

Texture etching technologies for diamond-wire-sawn mc-Si solar cells

Jochen Rentsch, Bishal Kafle, Marc Hofmann, Katrin Krieg & Martin Zimmer, Fraunhofer Institute for Solar Energy Systems ISE, Freiburg, Germany

Abstract

Texturing approaches for diamond-wire-sawn multicrystalline silicon (mc-Si) wafers represent a very active and important R&D field in solar cell manufacturing. Diamond-wire sawing (DWS) of mc-Si wafers demands new approaches for the texturization, as this type of cutting leaves a relatively smooth surface, which poses a significant challenge for texturing using standard acidic texturing methods. Many equipment manufacturers have been working on solutions to prepare mc-Si for DWS by using different dry- and wet-chemical-based approaches. Some of these approaches create a nanotextured surface, often called *black silicon*, which necessitates further adaptations of subsequent processing steps, such as emitter diffusion, passivation and metallization. This paper describes the most common texturing methods, and lists the currently available commercial solutions from equipment suppliers.

Introduction

Optical confinement is essential in order to increase the amount of photogeneration in a crystalline silicon (c-Si) solar cell. Especially in conventionally textured multicrystalline silicon (mc-Si) solar cells, the highly reflecting surface is one of the major limiting factors causing reduced short-circuit current density (J_{sc}) of the solar cell. Additionally, the switch from standard multiwire

"DWS leaves a relatively smooth surface, which presents significant challenges with regard to texturing using standard acidic texturing approaches."

Figure 1. Total cost of ownership (TCO) comparison of MWSS and DWS approaches for cutting mc-Si wafers.

slurry sawing (MWSS) to diamond-wire sawing (DWS) for mc-Si wafers calls for new approaches for the texturization of the wafer surface during solar cell processing. DWS itself has the potential to almost halve the wafer-manufacturing cost for mc-Si wafers (Fig. 1).

The DWS process is faster than the slurry method and silicon kerf loss is lower; moreover, its operational costs are dramatically lower, because the fixed abrasive principle frees wafering fabs from expensive and complex slurry use and management. The DWS approach has nearly completely replaced the traditional slurry cutting for monocrystalline silicon wafers, whereas for mc-Si only about 5% of the manufacturers were using DWS as of 2016, according to the International Roadmap for Photovoltaics (ITRPV) [1]. The relatively slow introduction of DWS for mc-Si is due to the fact that DWS leaves a relatively smooth surface, which presents significant challenges with regard to texturing using standard acidic texturing approaches.

Many equipment manufacturers have been working on solutions to make mc-Si ready for DWS by using different dry- and wet-chemical-based approaches, the most prominent and commercially viable solutions being:

- Acidic texturing with additives
- Standard acidic texturing with pretreatment
- Metal-assisted etching (MAE) or metal catalyst chemical etching (MCCE)
- Reactive ion etching (RIE)
- Atmospheric dry etching (ADE)
- Laser texturing

Many of the currently developed texturing approaches claim to produce a 'black-silicon' surface, where *black silicon* refers to silicon surfaces covered by a layer of submicron structures. Black silicon helps to reduce reflectance in different ways, depending on the size and shape of its surface texture. First, there is a reduction in reflection because of a multitude of interactions of light with the textured surface. Second, when the size of the texture features is large compared with the wavelength of the solar spectrum, surface scattering is responsible for an elongated light path and enhanced absorption. Third, for sub-100nm nanostructured silicon, the surface feature
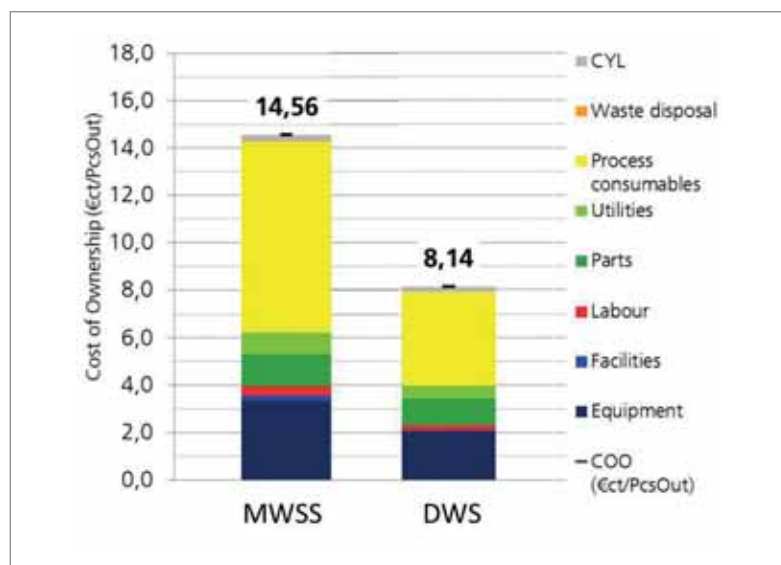
sizes are so small that the surface essentially acts as an effective index medium and is optically flat.

Because of the nature of black-silicon-textured surfaces, adaptations of the subsequent processing steps – such as emitter diffusion, passivation and metallization – become necessary.

Overview of commercial wet-texturing solutions

The wet texturing of mc-Si is a standard process in solar cell manufacturing, most commonly carried out within inline wet-chemical equipment. The traditional HF/HNO_3 texturing solutions, with either a HF-rich or a HNO_3-rich composition, use the saw damage from the slurry sawing to etch deep into surface defects initially, and then to widen the resulting holes. As previously mentioned, DWS wafers do not have such deep damage, and therefore the DWS wafers etched in $HF/HNO_3/H_2O$ remain smooth and the sawing grooves are still visible as lines.

Adapted standard acidic texturing solutions

The simplest approach to adapting existing HF/HNO_3 texturing solutions for DWS of wafers is the use of additives in the texturing solution. Cell manufacturers would easily be able to implement these solutions within their existing tool set-ups, without major additional investment.

The company RENA claims to have already sold a couple of GWs of its adapted metal-free chemistry based on standard HF/HNO_3 etching solutions. No specific information about this solution has been released so far [2]; however, the additive solution allows inline processing with footprints similar to those of conventional acidic texturing tools.

The LINEX inline system developed by Singulus incorporates a texturing process that removes the saw marks made by the diamond wire on the wafers when cut. The innovation is a two-step process using new additives and ozone for post-cleaning to create a homogeneous structure [3]. Singulus has also developed a new conveyor system within its LINEX inline processing tool; the company says that this innovation guarantees 'extra-gentle' handling of the multi wafers, thereby delivering a marked reduction in breakages. Unlike mono wafers, multi wafers can become fragile when sawn, leading to problems with texturing.

Another possibility for texturing smooth surfaces is a solution consisting of HF/HNO_3 and sulphuric acid (H_2SO_4) developed by Fraunhofer ISE. The favourable texturing behaviour of this solution as opposed to HF/HNO_3 might be due to the high viscosity of the sulphuric acid. For $HF/HNO_3/H_2SO_4$ mixtures, the process temperature plays an important role in controlling the etch depth and the reflection. At temperatures above 45°C, it is possible to achieve a texture with total reflection values of 22% at 600nm, a total etch depth of 15µm in 60s, and a structure height of 2µm (see Fig. 2). This result represents a promising starting point for finding an adequate additive for the mc-Si DWS texturing process (further results to be published soon).
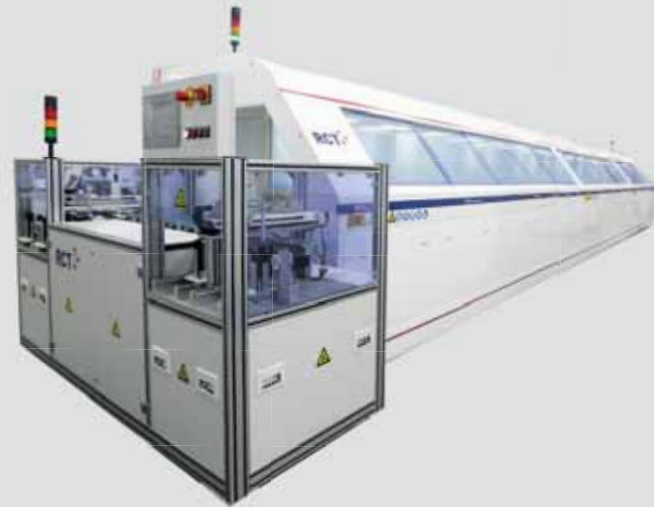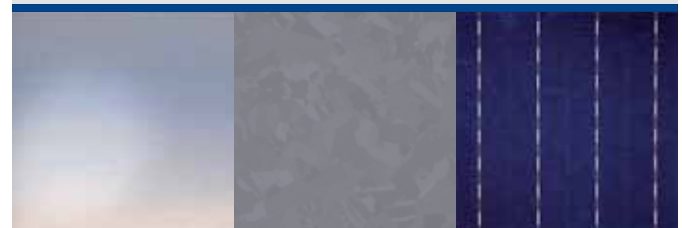
A slightly different approach has been developed by the company Schmid: instead of using additives for the actual HF/HNO$_3$-based texturing process, Schmid has implemented a pretreatment step with the aim of generating micro-defects at the silicon surface in order to enable subsequent conventional acidic texturization. The preconditioning procedure, called *DW PreTex*, is a simple one-step process implemented before multicrystalline wafers are textured [4].

Metal catalyst chemical etching (MCCE)

Silicon can be etched in the presence of HF and an oxidative agent, catalysed by noble metals, to form micro- or nanostructured surfaces with various morphologies [5]. In a typical etching process, the silicon substrate is partly covered by noble metal nanoparticles and immersed in a solution of HF and an oxidative agent [6–8]. For the noble metals, gold (Au) and silver (Ag) are the most popular candidates; upon attachment to the silicon substrate, noble metal ions acquire electrons from the silicon valence band and are reduced to form seed nuclei which develop into nanoparticles. Concurrently, these ions inject holes underneath the silicon, causing oxidation into SiO or SiO$_2$, which are then removed by HF (see Fig. 3) [6].

As a result of the continuous formation of silicon oxide underneath the metal particles and the corresponding removal action by the HF, the metal particles sink into the silicon and create porous structures. Once the desired surface structures have been created, the metal nanoparticles are removed by another etchant – such as HNO$_3$ – and a cleaning process then follows.

A generic process flow for metal catalyst chemical etching (MCCE) of a crystalline silicon wafer is given in Fig. 4 [9]; all the relevant steps necessary for processing a wafer from an as-cut state to readiness for emitter diffusions are included. The saw damage after wafering needs to be removed (about 3 to 5µm); this can be performed as a separate process step or during the MCCE. Since the MCCE is a process in which a metal is used as a catalyst in order to promote etching in the vicinity of the metal, the respective metal precipitates need to be deposited, e.g. Ag nanoparticles. Metal nanoparticle deposition is carried out by dipping the wafer into a wet-chemical solution containing metal ions, which is in most cases a solution of AgNO$_3$. Additionally, HF needs to be present to initiate the deposition.

After metal deposition, the texturing process begins, which requires an oxidant (e.g. H$_2$O$_2$ or HNO$_3$) and HF. Depending on the bath composition, a porous Si layer can be formed. The surface morphologies can also vary (Fig. 5): as an example, a pit-like structure can be obtained, with typical diameters in the range 50 to 200nm,
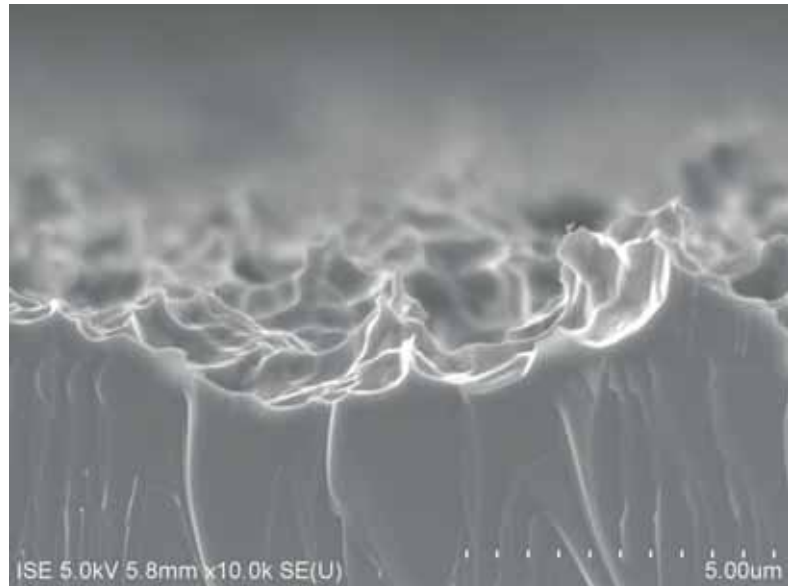

Figure 2. Scanning electron microscope (SEM) image of an mc-Si DWS wafer textured in HF, HNO$_3$ and H$_2$SO$_4$.
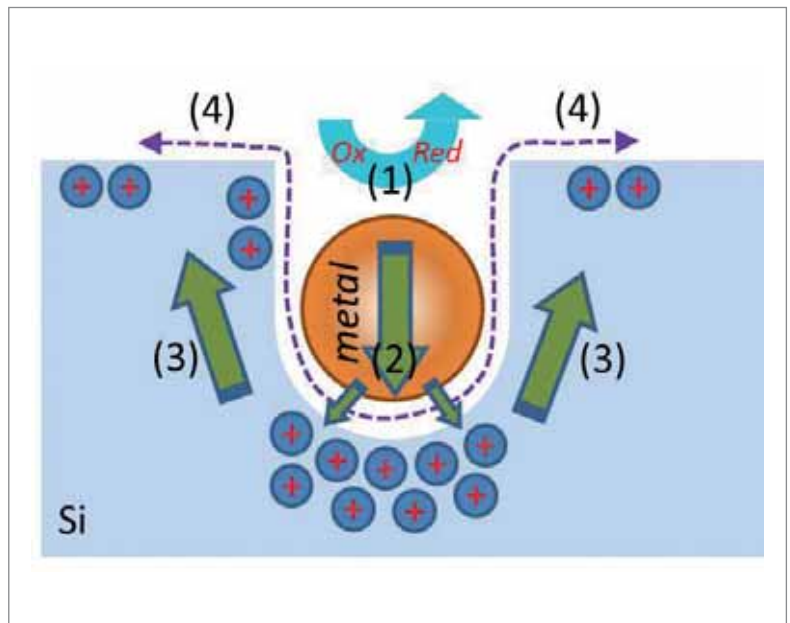

Figure 3. Illustration of the metal catalyst chemical etching process: (1) reduction of an oxidative agent (such as H$_2$O$_2$) catalysed by a noble metal particle; (2) injection of holes generated during the reduction reaction into the silicon substrate, with the highest hole concentration underneath the metal particle; (3) migration of holes to silicon sidewalls and surfaces; and (4) removal of oxidized silicon via HF [6].

with depths in a similar range. In addition, alternative structures, such as nanowires or pores, can be created. Such structures can lead to low reflectivity; however, their use in solar cells is not ideal (as they are deep and steep structures, with high surface enlargement and challenges for good surface passivation, including low J_{oe}). Therefore, post-treatments are optionally carried out (either alkaline or acidic) in order to determine an optimum structure for superior solar cell performance; this optimized structure is a trade-off between low reflectivity (necessary for high J_{sc}) and reduced surface enlargement (necessary for high V_{oc} and fill factor *FF*). In addition, the wafer

surface needs to be cleaned of any metal and contaminations prior to emitter diffusion.

In the field of MCCE, Advanced Silicon Group (ASG) uses a version of metal-enhanced etching of silicon, a process that can be run on modified standard wet benches. ASG has innovated changes to the standard MCCE process to make it more uniform and repeatable, and also to allow control over the nanotexture geometry. Furthermore, since a novel material requires a new device design to make use of the material's unique properties, ASG has made alterations to the device design to obtain improved performance and lower cost. The cost of the technology per wafer is comparable to that of standard mc-Si texturing, and ASG has so far seen efficiency gains between 0.5 and 1.5%$_{abs}$, depending on the starting process. With these efficiency gains, the price per watt is lower than that for standard texturing; this is in addition to the materials cost savings made possible by the use of diamond-wire-sawn wafers, which the process accommodates. ASG offers consulting to help companies optimize their cell process using black silicon, and then provides a licence to manufacture cells using the improved process.

Another supplier in the MCCE field is the company RCT solutions, who has called its product *i-BlackTex*. The tool on offer accomplishes the entire surface treatment – saw damage removal, texturization and cleaning – in a single inline system. As in the case of the other MCCE processes, RCT employs silver nitrate as the metal, but avoids the use of any additives or H_2O_2. The system employs standard chemicals that are typically used in the texturing process – HF, HNO_3, water and KOH for cleaning. Another important feature of the system is its length of 12m, which is the same as the well-known branded texturing wet benches, and therefore allows easy replacement. The process can be adjusted to obtain reflectivities between 12 and 20%. The lower reflectivity, however, entails additional attention within the solar cell process – especially for emitter formation and passivation (see below) – to harvest the full benefit. RCT affirms an efficiency gain of 0.2 to 0.4%$_{abs.}$ at the cell level over standard mc-Si cells.

MCCE represents a very attractive solution for the texturization of DWS mc-Si wafers; however, large-scale exploitation of MCCE texturing approaches in industrial manufacturing will also pose challenges, especially in terms of waste management. Large amounts of metal nanoparticles need to be filtered out of the waste water, which requires additional effort and investment in waste-water treatment plants. From the solar cell perspective, metal contamination is also a major concern with this technique, and thorough metal removal and cleaning processes are essential in order to address this problem.

Overview of commercial dry-texturing solutions

Plasma-based texturing has been widely investigated as a dry-texturing alternative for forming nanotextures in c-Si, achieving very low reflection values in both monocrystalline and multicrystalline wafers.

From the field of microelectronics, reactive-ion-etching (RIE) processes using oxygen-fluorine-containing etching gas mixtures to effectively pattern silicon surfaces have long been the accepted standard method [10–12]. In these processes, the directionality of the RIE plasma etching is exploited in order to realize precisely defined vertical etching structures. A so-called *black-silicon method* was developed by Jansen et al. [13], which was then applied by Schnell et al. [14] to solar cells on a laboratory scale; weighted reflectivities of less than 3% were achieved, but with (at that time) relatively poor homogeneity and reproducibility over large areas.

In the last 10 years many different research groups, as well as dry-etch equipment manufacturers, have investigated technical solutions for the large-scale application of plasma-based texturing. Not only have technical issues had to be taken into account, but also environmental

Figure 4. Generic process flow for black silicon based on metal catalyst chemical etching (MCCE) [9].
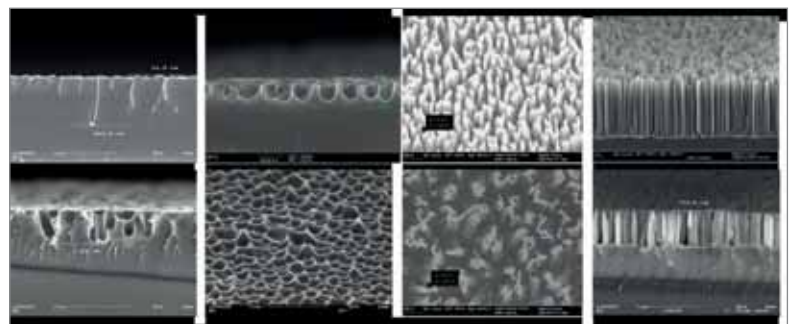

Figure 5. MCCE processes can produce a wide variety of nanotexture structures (SEM images provided by ASG).

aspects. Generally, gases with high global-warming potential (GWP) – such as SF_6, CF_4 and NF_3 – are used as a source of fluorine species in order to etch silicon [15]. This means that high-end in situ abatement systems are additionally needed in order to curb direct emissions from the etching process, which still cannot provide a 100% capture rate of the waste gases. In the industrial-scale production of solar cells, high amounts of F-containing gases need to be used, and this exacerbates the effect of these waste gases on the climate [16]. Developments in the direction of more environmentally friendly gases, such as F_2, are therefore needed to ensure the large-scale exploitation of this technology at acceptable costs, and to keep solar cell production a climate-friendly industry.

Reactive ion etching

The use of RIE to form grass-like black-silicon surfaces was first reported by Jansen et al. in 1995. This method employs SF_6 and O_2 gases to generate F* and O* radicals. F* is responsible for etching silicon, producing volatile products such as SiF_x. These products, particularly SiF_4, react with O* to form a passivation layer of SiO_xF_y on a cooled silicon substrate (Fig. 6). This passivation layer is partly removed by ion bombardment, and the exposed silicon is further etched by F*. The etching reaction is exothermic, and reduces the chance of producing a new passivation layer, since SiO_xF_y is prone to desorption upon heating.

In contrast, there is far less ion bombardment on the side walls of the formed silicon columns; thus, the passivation layer in those regions is largely preserved, preventing further etching. This etching/passivation competition mechanism leads to the formation of random silicon microstructures with very high aspect ratios in a self-masking fashion (Fig. 7).

The morphology of the black silicon fabricated in this manner can be adjusted by changing various RIE parameters, such as gas composition and flow rate, system temperature, substrate bias and RF power.

Another alternative reactive gas is Cl_2; although it offers a lower etching rate than SF_6/O_2, it is much easier to manage, owing to the formation of non-volatile by-products, and thus makes the control over the passivation layer deposition and silicon etching comparatively straightforward. Cl_2 can also be added into SF_6/O_2 to extend the gas composition working window.

Commercial solutions for RIE-based dry-texturing are offered by the Korean companies WONIK IPS and Jusung and the Japanese company ULVAC; however, no further details of the individual process set-ups have been released by these companies.

Atmospheric dry etching (ADE)

F_2 is known for its role in the isotropic etching of Si in a plasma-less process for bulk micromachining of Si for its application in microelectromechanical systems (MEMS). A very high reactivity to Si in atmospheric pressure conditions and a zero GWP make F_2 an interesting candidate for applications in photovoltaics. Atmospheric pressure texturing of Si is based on the principle of

spontaneous reaction of F_2 with Si to release SiF_x species; this reaction occurs with a very low energy barrier, and without any need for ion-induced excitation.

Fig. 8 shows the basic layout of the etching tool developed by NINES PV: diluted F_2 is used as the only etchant. The etching gas is preheated to a certain temperature before it is delivered to the Si wafer in order to facilitate partial dissociation of F_2 molecules into individual atoms. The heated wafer is transported continuously through the reactor at a set velocity. A series of gas curtains contains the reactive gases inside the reactor, while allowing the continuous feeding of wafers. The temperature of the wafer governs the surface kinetics of the reaction. Elevated temperatures to supply more energy to the F_2-Si reaction system are possible. The F_2 can be diluted by mixing it with N_2, and the F_2/N_2 gas mixture is delivered uniformly to the wafer.

The wafer is etched at a constant speed while passing through the reaction zone. The etching process is single sided, which means that only the side facing the etching gases is textured. The dynamic etch rate is a function of F_2 concentration, total gas flux, temperature of the heated gas, temperature of the wafer, and velocity of the transport band. The process parameters can be optimized to form nanotextures of different aspect ratios: for example, nanotextures with a depth of up to 1µm and an estimated weighted reflection (R_w) of < 2% for <100> Si and < 5% for mc-Si.

Challenges of implementing black silicon in solar cell processing

The creation of black-silicon surface structures on the front side of a solar cell dramatically lowers its final surface reflection. Especially in case of mc-Si surfaces, the final surface reflection achieved by this method is much lower than in the case of the traditionally used acidic texturing. However, the incorporation of these black-silicon structures in a solar cell is not straightforward because of the notable difference in feature sizes compared with the structures formed by standard texturing techniques.

"MCCE represents a very attractive solution for the texturization of DWS mc-Si wafers."
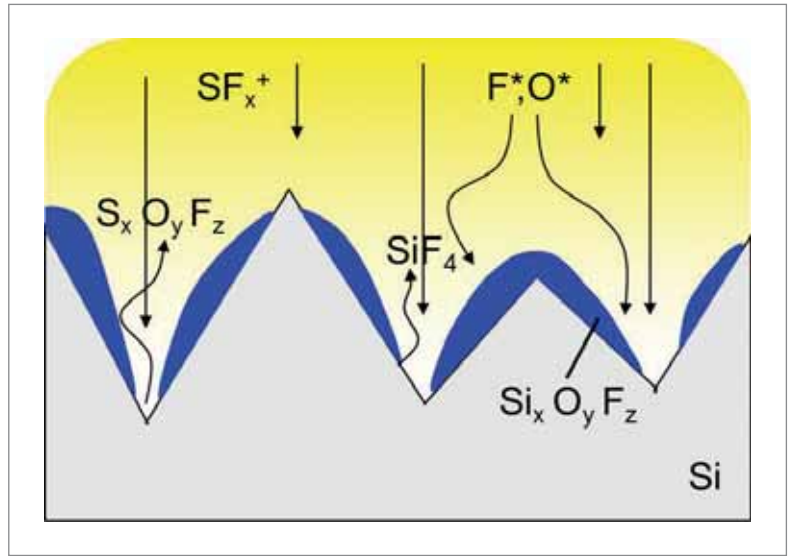

Figure 6. Etching mechanisms for plasma-based dry etching of silicon surfaces.
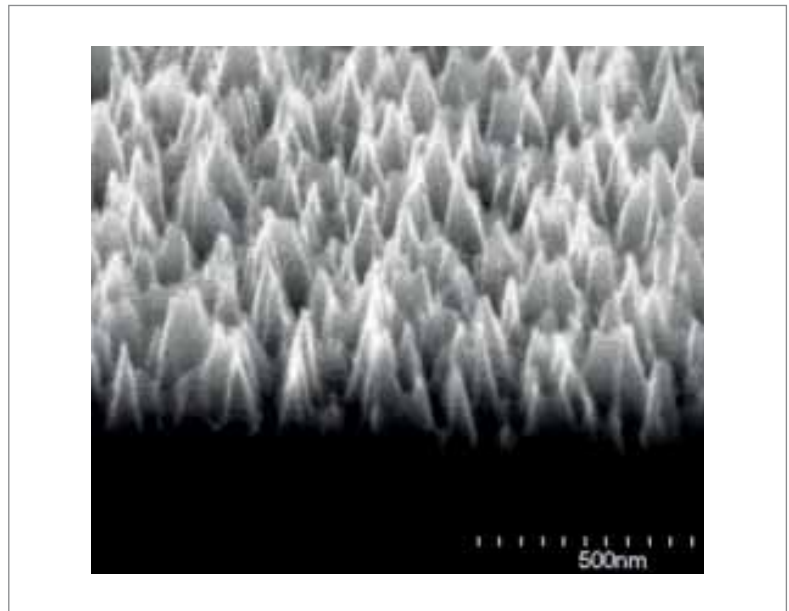

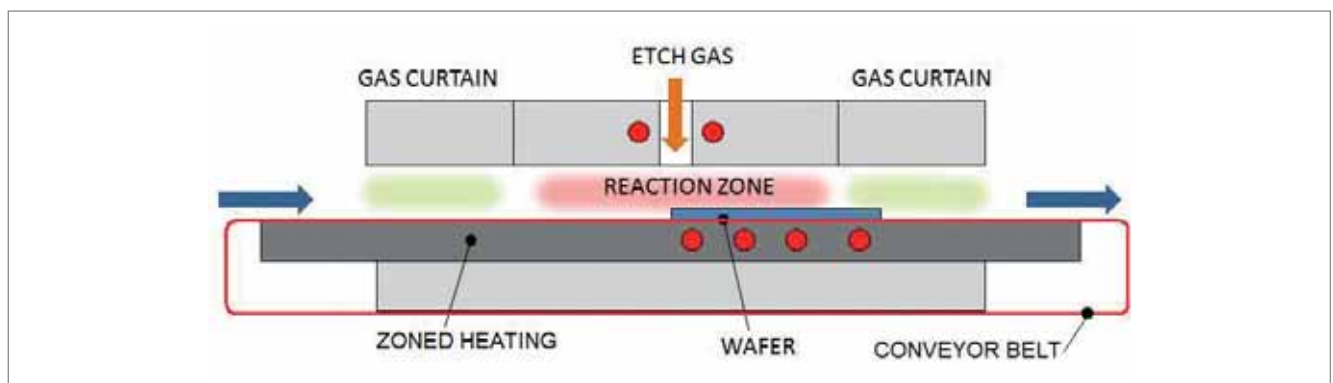Figure 7. SEM image of a typical black-silicon structure fabricated by RIE.

Figure 8. Schematic showing the chemical etching process of Si by thermally activated F_2 gas at atmospheric pressure conditions. The mixture of inert gas (N_2) and process gas (F_2) is led through a heated zone to facilitate a partial dissociation of F_2 atoms or to form radicals.
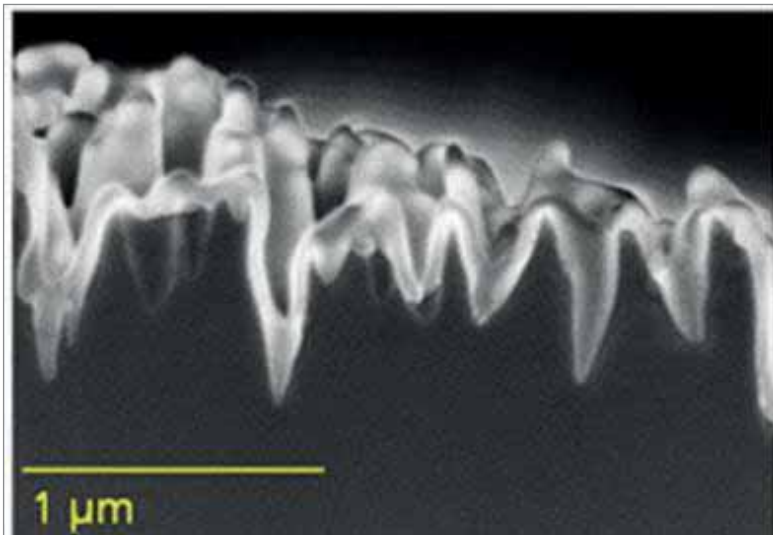
Figure 9. SEM image showing conformal deposition of phosphosilicate glass (PSG) layers on a nanotexture during the emitter diffusion process [34].
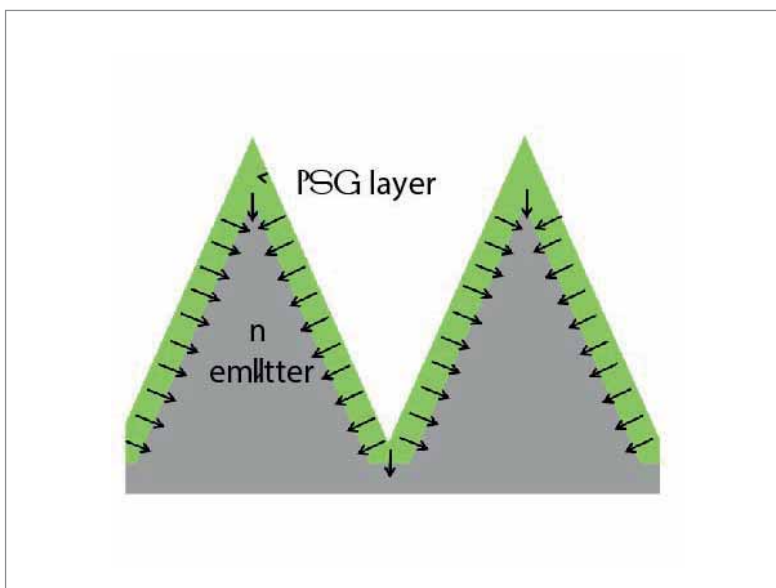

Figure 10. Sketch of heavy diffusion of phosphorus from the deposited PSG layers in a nanotexture [34].

"The surface passivation of nanotextured surfaces has been found to be one of the major challenges in fabricating high-efficiency solar cells."

Since the surface texturing of a Si wafer is one of the first steps in solar cell fabrication, each of the subsequent processes is significantly influenced by the introduction of a nanotexture with unique surface features; therefore, an adaptation of these process steps is necessary in order to fabricate efficient solar cells on nanotextured surfaces. Furthermore, the selection of process tools and technologies in a solar cell production line is currently made with the aim of optimizing the efficiency, production and yield of standard solar cells. If conventional texturing is replaced by a novel process, the adoption of additional novel technologies could be essential in order to realize the full potential.

Nevertheless, these technological developments should also be feasible for rapid upscaling from the laboratory to industry in order to provide economic competitiveness. The introduction of nanotextures therefore presents new challenges that need to be addressed to ensure that the higher power gain promised by their excellent light-trapping abilities is eventually realized in the industrial production lines in an economically competitive way.

Surface passivation

The passivation of nanotextured surfaces has been found to be one of the major challenges in fabricating high-efficiency solar cells. The black-silicon structures are reported to be difficult to passivate by the typically used plasma-enhanced chemical vapour deposition (PECVD) SiN_x layer [17–19], whereas a variable level of passivation is achieved after applying a thermal SiO_x layer [20,21]. The major reasons behind the insufficiency of the passivation are: 1) greater surface area; 2) potentially more surface defects because of texturing damage; 3) higher level of crystal-orientation-dependent recombination; and 4) conformality issue of the deposited layer.

Meanwhile, the rapid development of the atomic layer deposition (ALD) technique has made it possible to form conformal AlO_x layers on nanostructured surfaces and to achieve surface recombination velocities that are comparable to those of the reference texture [22–25]. Several studies have subsequently focused on the issue of surface passivation on nanotextured surfaces, and a good understanding has been developed, especially in respect of the application of ALD AlO_x layers.

Another strategy to improve the conformality of the deposited layer is a modification of the surface topography; this method has been simultaneously developed by many groups in recent years [26–33]. The individual results have not been reviewed here, but can be consulted in the listed references.

Emitter diffusion

Another challenge for nanotextured surfaces relates to the formation of the pn junction. Typically, the application of a standard emitter diffusion process to nanotextured surfaces has resulted in poor electrical performance. This downside is attributed to a lower level of surface passivation and a high active doping in the emitter region; in particular, the Auger recombination mechanism is reported to dominate other recombination channels in nanostructures. These accounts have been supported by both experimental observations and device simulations (see Figs. 9 and 10).

On the basis of carrier-lifetime measurements on diffused nanotextured surfaces, Oh et al.
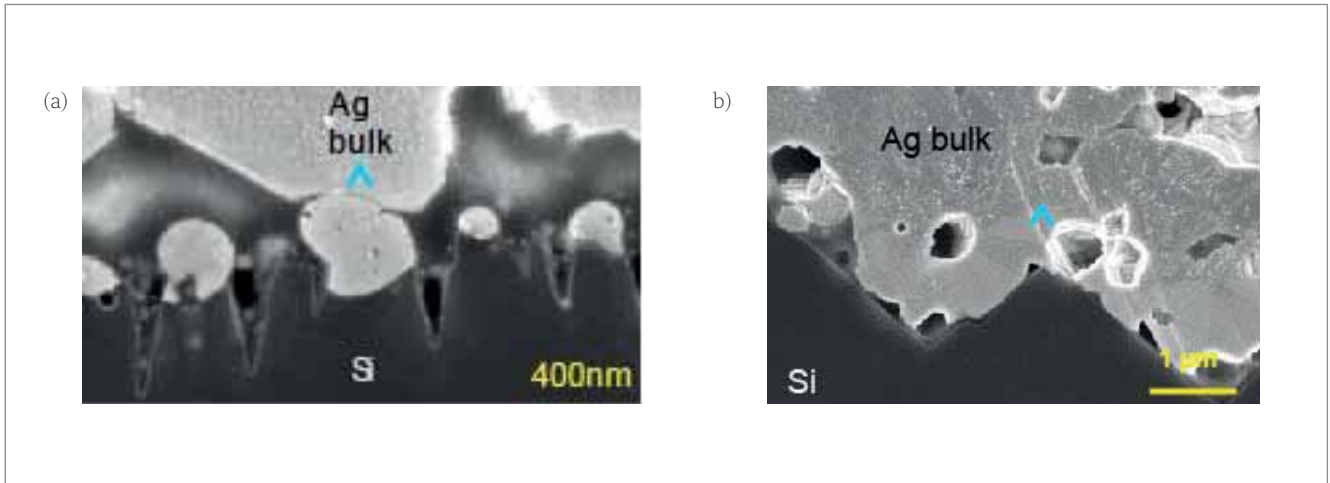
[26] showed that Auger recombination is more dominant in comparison to surface recombination in the case of high to medium doping of the emitter. A higher emitter sheet resistance (R_{sh}) is associated with a lower Auger recombination, and is reported in many studies to improve the quantum efficiency of the nanotextured solar cell in the short to medium wavelengths [17,26–27]. Furthermore, several authors have reported a reduction in emitter recombination either by tailoring the size of the nanotexture [17,26,27,31,35,36] or by increasing the R_{sh} [37]. Similar conclusions have been reached by simulating diffused nanostructures using PC1D, and regarding them as a planar surface with a highly doped region (dead layer) that does not account for current generation [27,36]. Hence, a broad agreement in this field of research is that reducing the Auger recombination is the key to increasing the performance of p-type nanotextured solar cells.

Metallization

Apart from the composition of the silver paste, the firing process and the thickness of the dielectric coating, the emitter properties and the surface topography are assumed to play an important role in the contact formation process [38,39]. A low specific contact resistivity (ρ_c) value for both pyramid- and acidic-textured samples has previously been attributed to the better wetting behaviour of the glass layer [39,40], which leaves the tips of these structures virtually free and promotes direct contacting [39,41]. Further investigations performed by varying the size of the pyramids have shown that when the size of pyramid is larger than the thickness of the glass layer, then the ρ_c values do not change abruptly [39]. On the basis of microscopic investigations of contact areas, it is maintained that the direct local interconnection of Ag crystallites to the Ag bulk and/or the formation of direct macroscopic contact between the Ag bulk and the emitter surface offer the major contribution to the current transport mechanism in all nanotextured surfaces (see Fig. 11).

To the authors' knowledge, no dedicated study with the goal of understanding the contact formation on nanotextured surfaces (which have significantly smaller feature sizes than conventional textures) has so far been carried out. In the literature relating to nanotextures, there have been several conflicting reports about the possible impact of nanotexture dimensions on the series resistance (R_s) and fill factor (FF) values of solar cells. Hsu et al. [20] reported that the increasing depths of the nanorods are detrimental to the series resistance for screen-printed contacts. In another study, Repo et. al. [42] explained their lower FF value on a black-silicon solar cell as an inability of evaporated metal to reach the valleys of the texture. In the meantime, high FF values on similar surfaces have been achieved by several other authors [28,29,31,35,43]; however, the difference in emitter and/or lack of detailed information about the contacting procedure make it difficult to correlate the contact behaviour with the nanotexture dimensions.

Summary

Several promising wet- and dry-etching-based technologies for the texturing of diamond-wire-sawn mc-Si are currently available for high-throughput industrial application in solar cell manufacturing. Up to now, none of these technologies has made its way to representing the current standard in the industry; however, simple approaches, mainly using the same tool set-up of existing production lines (acidic texturing process), offer some advantages. These approaches basically offer only the means of homogeneously texturing DWS silicon wafers; they do not offer the possibility of creating a superior texturing alternative with significant lower surface reflectance. For that, technologies (such as MCCE, RIE or ADE texturing) that are able to create black-silicon-like surface

"To fully exploit the potential of more advanced texturization processes, additional efforts and adaptations of the subsequent processing steps during solar cell manufacturing are necessary."

structures are necessary. To fully exploit the potential of these more advanced texturization processes, additional efforts and adaptations of the subsequent processing steps during solar cell manufacturing are necessary. From a cost of ownership perspective, the overall efficiency gain resulting from black-silicon textures needs to be weighed against the cost of these potential adaptations (additional CAPEX) in the later processing chain, up to module fabrication.

....

References

[1] ITRPV 2017, "International technology roadmap for photovoltaic (ITRPV): 2016 results", 8th edn (Mar.) [http://www.itrpv.net/Reports/Downloads/].

[2] RENA 2017, Press release (Mar.).

[3] Singulus 2017, Press release, (Dec.).

[4] Marketing Information provided by Schmid.

[5] Li, X. et al. 2000, *Appl. Phys. Lett.,* Vol. 77, pp. 2572–2574.

[6] Huang, Z. et al. 2011, *Adv. Mater.*, Vol. 23, pp. 285–308.

[7] Nishioka, K. et al. 2008, *Sol. Energy Mater. Sol. Cells,* Vol. 92, pp. 919–922.

[8] Yae, S. et al. 2003, *Electrochem. Commun.*, Vol. 5, pp. 632–636.

[9] Joos, W. et al. 2017, "Development and optimization of a novel inline black silicon texturing process for increased solar cell performance", *Proc. 33rd EU PVSEC*, Amsterdam, The Netherlands.

[10] Jansen, H. et al. 1969, "A survey on the reactive ion etching of silicon in microtechnology", *J. Micromech. Microeng.*, Vol. 6, pp. 14–28.

[11] Sze, S.M. 1985, *Semiconductor Devices, Physics and Technology.* New York: John Wiley & Sons.

[12] Economou, D.-J. 2000, "Modeling and simulation of plasma etching reactors for microelectronics", *Thin Solid Films*, Vol. 365, pp. 348–67.

[13] Jansen, H. et al. 1995, "The black silicon method: A universal method for determining parameter settings of a fluorine-based reactive ion etcher in deep silicon trench etching with profile control", *J. Micromech. Microeng.*, Vol. 5 (1995) 115–120.

[14] Schnell, M., Lüdemann, R. & Schaefer, S. 2000, "Plasma surface texturization for multicrystalline silicon solar cells", *Proc. 28th IEEE PVSC*, Anchorage, Alaska, USA, pp. 367–370.

[15] Rentsch, J. et al. 2005, "Economical and ecological aspects of plasma processing for industrial solar cell fabrication", *Proc. 31st IEEE PVSC*, Lake Buena Vista, Florida, USA.

[16] de Wild-Scholten, M. et al. 2007, "Fluorinated greenhouse gases in photovoltaic module manufacturing: Potential emissions and abatement strategies", *Proc. 22nd EU PVSEC*, Milan, Italy.

[17] Liu, Y. et al. 2012, Nanostructure formation and passivation of large-area black silicon for solar cell applications", *Small*, Vol. 8, No. 9, pp. 1392–1397.

[18] Liu, B. et al. 2012, "Silicon nitride film by inline PECVD for black silicon solar cells", *Int. J. Photoenergy* 2012, pp. 1–5.

[19] Kafle, B. et al. 2013, "Industrial screen-printed solar cells with novel atmospheric pressure dry texturing process", *Proc. 28th EU PVSEC*, Paris, France, pp. 1344–1350.

[20] Hsu, W.C. et al. 2012, "High-efficiency 6" multicrystalline black solar cells based on metal-nanoparticle-assisted chemical etching", *Int. J. Photoenergy 2012,* pp. 1–7.

[21] Dimitrov, D.Z. et al. 2011, "Nanotextured crystalline silicon solar cells", *physica status solidi (a)*, Vol. 208, No. 12, pp. 2926–2933.

[22] von Gastrow, G. et al. 2015, "Analysis of the atomic layer deposited Al_2O_3 field-effect passivation in black silicon", *Sol. Energy Mater. Sol. Cells,* Vol. 142, pp. 29–33.

[23] Otto, M. et al. 2012, "Extremely low surface recombination velocities in black silicon passivated by atomic layer deposition", *Appl. Phys. Lett.*, Vol. 100, No. 19, p. 191603.

[24] Repo, P. et al. 2013, "Effective passivation of black silicon surfaces by atomic layer deposition", *IEEE J. Photovolt.*, Vol. 3, No. 1, pp. 90–94.

[25] Song, J.-W. et al. 2015, "Hydroxyl functionalization improves the surface passivation of nanostructured silicon solar cells degraded by epitaxial regrowth", *RSC Adv.*, Vol. 5, No. 49, pp. 39177–39181.

[26] Oh, J., Yuan, H.-C. & Branz, H.M. 2012, "An 18.2%-efficient black-silicon solar cell achieved through control of carrier recombination in nanostructures", *Nat. Nano.*, Vol. 7, No. 11, pp. 743–748.

[27] Lin, X.X. et al. 2015, "Realization of improved efficiency on nanostructured multicrystalline silicon solar cells for mass production", *Nanotech.*, Vol. 26, No. 12, pp. 125401.

[28] Yue, Z. et al. 2014, "Large-scale black multi-crystalline silicon solar cell with conversion efficiency over 18 %", *Appl. Phys. A: Mater. Sci. Process.,* Vol. 116, No. 2, pp. 683–688.

[29] Cao, F. et al. 2015, "Next-generation multi-crystalline silicon solar cells: Diamond-wire sawing, nano-texture and high efficiency", *Sol. Energy Mater. Sol. Cells*, Vol. 141, pp. 132–138.

[30] Dimitrov, D.Z. et al. 2011, "Nanotextured crystalline silicon solar cells", *physica status solidi (a)*, Vol. 208, No. 12, pp. 2926–2933.

[31] Ye, X. et al. 2014, "18.45%-efficient multi-crystalline silicon solar cells with novel nanoscale pseudo-pyramid texture", *Adv. Funct. Mater.*, Vol. 24, No. 42, pp. 6708–6716.

[32] Kafle, B. et al. 2015, "Nanotextured multicrystalline Al-BSF solar cells reaching 18% conversion efficiency using industrially viable solar cell processes", *physica status solidi (RRL)*, Vol. 9, No. 8, pp. 448–452.

[33] Kafle, B. et al. 2016, "Plasma-free dry-chemical texturing process for high-efficiency multicrystalline silicon solar cells", *Energy Procedia*, Vol. 92, pp. 359–368.

[34] Kafle, B. 2017, Mask-less dry texturing of crystalline silicon solar cells in atmospheric pressure conditions", University of Freiburg, Germany.

[35] Xiao, G. et al. 2014, "The study of defect removal etching of black silicon for solar cells", *Mater. Sci. Semicon. Proc.*, Vol. 22, pp. 64–68.

[36] Zhuang, Y.F. et al. 2016, "Versatile strategies for improving the performance of diamond wire sawn mc-Si solar cells", *Sol. Energy Mater. Sol. Cells*, Vol. 153, pp. 18–24.

[37] Liu, S. et al. 2014, "Improvement of conversion efficiency of multicrystalline silicon solar cells by incorporating reactive ion etching texturing", *Sol. Energy Mater. Sol. Cell*s, Vol. 127, pp. 21–26.

[38] Kontermann, S. 2009, "Characterization and modeling of contacting crystalline silicon solar cells", Dissertation, University of Konstanz, Germany.

[39] Cabrera, E. et al. 2013, "Influence of surface topography on the glass coverage in the contact formation of silver screen-printed Si solar cells", *IEEE J. Photovolt.*, Vol. 3, No. 1, pp. 102–107.

[40] de Wijs, G.A., de Vita, A. & Selloni, A. 1997, "Mechanism for SiC l2 formation and desorption and the growth of pits in the etching of Si(100) with chlorine", *Phys. Rev. Lett.*, Vol. 78, No. 25, pp. 4877–4880.

[41] Cabrera, E. et al. 2011, "Experimental evidence of direct contact formation for the current transport in silver thick film metallized silicon emitters", *J. Appl. Phys.*, Vol. 110, No. 11, p. 114511.

[42] Repo, P. et al. 2013, "N-type black silicon solar cells", *Energy Procedia*, Vol. 38, pp. 866–871.

[43] Yoo, J. et al. 2013, "Random reactive ion etching texturing techniques for application of multicrystalline silicon solar cells", *Thin Solid Films*, Vol. 546, pp. 275–278.

About the authors

Jochen Rentsch is the head of the Production Technologies – Surfaces and Interfaces department at Fraunhofer ISE. He studied physics at the Technical University of Braunschweig, obtaining his diploma degree in 2002. He then received his Ph.D. in physics in 2005 from the Albert Ludwig University of Freiburg, Germany. His research at Fraunhofer ISE focuses on the development of rear-passivated solar cells, new wet- and dry-chemical processing technologies, and the coordination of cell technology transfer projects.

Bishal Kafle was awarded his M.S. and Ph.D. in microsystems engineering by the Albert Ludwig University of Freiburg, Germany, in 2011 and 2017 respectively. For his Ph.D. he developed a novel texture for mono- and multicrystalline Si wafers and integrated them into the subsequent solar cell processing steps. His current research at Fraunhofer ISE focuses on the integration of novel textures at the cell and module levels, and on the optimization of the processing steps for rear-passivated solar cells.

Marc Hofmann is head of the Plasma Technology group at Fraunhofer ISE. He received his diploma degree in electrical engineering from the University of Applied Sciences Koblenz, Germany, in 2003, and his Ph.D. in physics from the University of Konstanz, Germany, in 2008. His research focuses on thin film and etching processes for high-efficiency crystalline silicon solar cells.

Katrin Krieg studied geoecology and process engineering at TU Bergakademie Freiberg. She worked at Fraunhofer ISE on her diploma thesis in the field of alkaline texturing and its analytics. She currently focuses on wet-chemical process development in the department of Wet Chemical and Plasma Technologies at ISE.

Martin Zimmer is head of the Wet Chemical Process Technology group at Fraunhofer ISE. After finishing his studies in chemistry in Heidelberg, he received his Ph.D. from the Albert Ludwig University of Freiburg in cooperation with Fraunhofer ISE, where he investigated industrial texturization processes. His current research focuses on wet-chemical approaches for the texturization of new wafer materials.

Enquiries

Dr. Jochen Rentsch
Head of Department of Production Technology:
Surfaces and Interfaces
Photovoltaics Division
Fraunhofer Institute for Solar Energy Systems ISE
Heidenhofstrasse 2
79110 Freiburg, Germany

Tel: +49 (0) 761 4588 5199
Email: jochen.rentsch@ise.fraunhofer.de
Website: http://www.ise.fraunhofer.de

Industrialized high-efficiency mono PERC cells

Guanlun Zhang, Lan Wang, Junmin Wu, Qing Chang, Tao Yan, Yaohui Xie, Lei Yang, Bushuang Hong, Yuanqiu Zhang, Peng Zhang & Bingwei Yin, TongWei Solar (Chengdu) Co. Ltd., P. R. China

Abstract

Passivated emitter and rear cell (PERC) technology can significantly increase the absolute efficiency of PV cells by over 1.2%. Since PERC processing is also compatible with current cell processing, and does not incur overly high manufacturing costs, many PV manufacturers are focusing on developing the industrialization technologies for PERC cells. This paper describes industrial p-type mono five-busbar (5BB) PERC cells with an average efficiency of 21.6%. Compared with standard aluminium back-surface field (Al-BSF) cells, the absolute efficiency has increased by 1.3%, and the open-circuit voltage (V_{oc}) has increased by 25mV, demonstrating that an aluminium oxide passivation film by atomic layer deposition (ALD) has excellent rear-side passivation performance. Furthermore, PERC cells have more concentrated efficiency distributions, which means they are able to achieve more than 300W module power in 60-cell standard modules. TongWei has set a target of achieving the mass production of PERC cells with an efficiency of over 22%. This paper also presents a loss analysis for current TongWei PERC cells, along with a roadmap of future efficiency development.

Introduction

The deployment of renewable energy, especially solar, is becoming ever more popular. It is estimated that with every 1% increase in PV cell efficiency, electricity costs would decrease by 7%; therefore, improving solar cell efficiency is very important for reducing the average electricity-generating cost of solar and driving it towards grid parity. While wafer products are becoming higher quality, and progress is being made on the development of cell processes, equipment and materials, the efficiency of standard mono Al-BSF solar cells is approaching its limit.

Process improvements for conventional Al-BSF cells are mostly performed on the front side of the cells. Studies have shown that the rate of rear-side recombination is still quite high in the case of Al-BSF cell structures, and only 60–70% of the IR radiated light that reaches the Al-BSF could be reflected. These are the two intrinsic factors that prevent further increases in Al-BSF cell efficiency; however, solar cells based on the passivated emitter and rear cell (PERC) concept could effectively solve these two problems. Studies have also shown that if the BSF metal electrodes of conventional Al-BSF cells are replaced by passivation layers or stacked layers along with many small local busbar electrodes, the rear-side recombination rate could be dramatically reduced to below 200cm/s, while at the same time the long-wavelength spectral response in the over-800nm waveband would be improved, resulting in a density increase in short-circuit current (I_{sc}).

Because of the excellent passivation performance on the rear side, V_{oc} rises substantially. PERC cells could therefore significantly improve the solar cell conversion efficiency [1].

The PERC concept was introduced by Blakers and Wang [2], with a reported laboratory conversion efficiency of 22.8%; in 1999 Zhao et al. [3] pushed this up to 24.7% – a world-record laboratory conversion efficiency. The lab preparation for PERC cells deploys several technologies, including photoetching, evaporation, thermal oxidation passivation and electroplating. All these technologies could result in higher PERC cell performance, but inevitably in higher costs as well.

Since the initial advances, the industrialization of PERC cells has experienced slow progress, and it was not until 2010 that significant headway was made. The success of the industrialization of PERC cells is due to a variety of different elements, including the rear-side passivation process. The processing requirements for PERC cells are met by the aluminium oxide deposition, the laser grooving, the conductive aluminium pastes for rear-side passivation, and the development of front-side Ag pastes for conductive contacts on PERC cells.

PERC cells are increasingly favoured by many cell manufacturers because of their high conversion efficiency, their developed technology, and their good compatibility with conventional cell production processes. Almost all Tier-1 PV companies have plans for PERC mass production. In fact, in the next one to three years it is estimated that PERC will become the standard technology configuration for c-si cell manufacturers. Many major cell manufacturers – such as Q CELLS, SolarWorld and Trina Solar – have already begun mass production of PERC solar cells. In addition, more PV manufacturers are migrating their conventional Al-BSF lines to PERC cell lines. The ITRPV roadmap [4] estimates that PERC capacity will reach 25GW by the end of 2017.

TongWei Solar is a dedicated cell manufacturer with 6GW mono- and poly c-si cell production capacity. With the use of advanced cell manufacturing equipment and technologies, over 20.3% conversion efficiency has been achieved for conventional mono c-si cells, and over 18.6% for poly c-si cells. The company's S2 plant in Chengdu was the first to implement smart manufacturing, with expectations of achieving 12GW mono and poly c-si
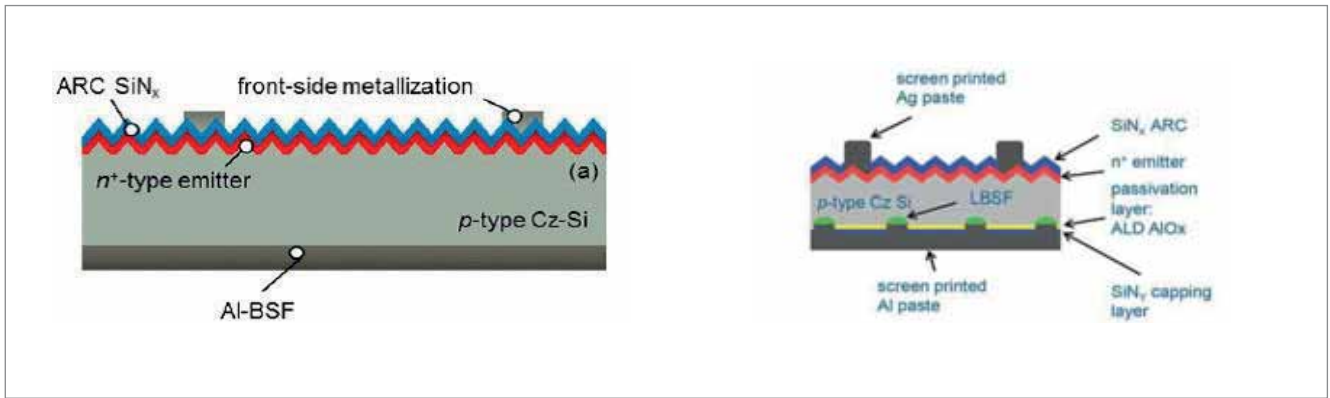
Figure 1. Comparison of the structures of conventional Al-BSF cells and PERC cells.

cell production capacity by the end of 2018. This paper describes the progress of the industrialization of TongWei Solar PERC cells, along with efficiency loss analyses of these cells. Future developments in order to achieve 22% conversion efficiency are also discussed.

Mono PERC cell manufacture

Conventional Al-BSF cells require processes that include texturing, diffusion, etching, plasma-enhanced chemical vapour deposition (PECVD), screen printing and firing tests. The PERC cell front-side processes are the same as those for an Al-BSF cell, while on the rear side an aluminium oxide passivation film is used to form a passivation layer; by using local metal contacts, the rear-surface recombination rate is greatly reduced. With a polishing process on the rear surface of the wafers, and a second deposition of SiN film on the aluminium oxide passivation film, the reflection of the incident light on the rear surface can also be improved, thus increasing V_{oc} and I_{sc} and resulting in an enhanced cell conversion efficiency.

TongWei Solar's PERC cells utilize aluminium oxide ALD for the rear-side passivation. Al_2O_3 is chosen as the passivation film, mainly because of its high density of fixed negative charge, which has excellent stabilizing properties for both field effect and chemical passivation performance. Low-cost nanosecond laser grooving and subsequent Al paste screen printing and firing are all used to form the PERC structure. Fig. 1 shows a comparison of the structures of conventional Al-BSF cells and PERC cells. From this figure, it can be seen that upgrading from conventional Al-BSF cells to PERC cells requires only the addition of aluminium oxide coating equipment for the rear sides and laser grooving equipment, as well as some fine-tuning of each process to suit the PERC cells.

Fig. 2 shows TongWei Solar's 5BB PERC cell, featuring:
- Uniformed pyramid texture by alkaline texturing on the front and polished mirror structure on the rear.
- Negative pressure diffusion to form uniform emitters with high sheet resistances.

- Optimized SiN coating on the front side and additional thin oxidization process, resulting in an improved potential-induced degradation (PID) performance and better consistency in appearance of the cells.
- Aluminium oxide passivation film realized by NCD's atomic layer deposition (NCD-ALD) on the rear side, and PECVD deposition of the SiN protective film.
- DR Laser's nanosecond laser grooving on the rear passivation film.
- Printing on the rear side using Al paste, to form an aluminium local back-surface field (LBSF) structure.
- Printing using high-quality low-temperature Ag paste, for better electrode adhesion and current collecting.
- Light-induced regeneration (LIR) with fast online light injection, to ensure that light-induced degradation (LID) is <1.5% on PERC cells.

"Al_2O_3 is chosen as the passivation film, mainly because of its high density of fixed negative charge, which has excellent stabilizing properties for both field effect and chemical passivation performance"

A 6-inch (156.75mm × 156.75mm) CZ solar-grade boron-doped monocrystalline wafer, with a resistance of 1–3Ω·cm and a thickness of 180–190μm, was selected to undergo the manufacturing processes shown in Fig. 3. The $I–V$ testing for the electrical properties of the wafer was carried out on a HALM machine, in compliance with the Fraunhofer ISE third-party cell-testing standards.

Fig. 4 shows the PERC cell efficiency distribution profile of a single mass-production line, with an average mass-production efficiency of 21.61% and an optimum single-cell efficiency of >21.9%. The narrow Gaussian distribution of the cell efficiencies proved that the current PERC processes have excellent stability properties. Compared with the performance of cells from the control group (i.e. Al-BSF cells processed using the same single production line), the PERC cells fabricated with the current processes

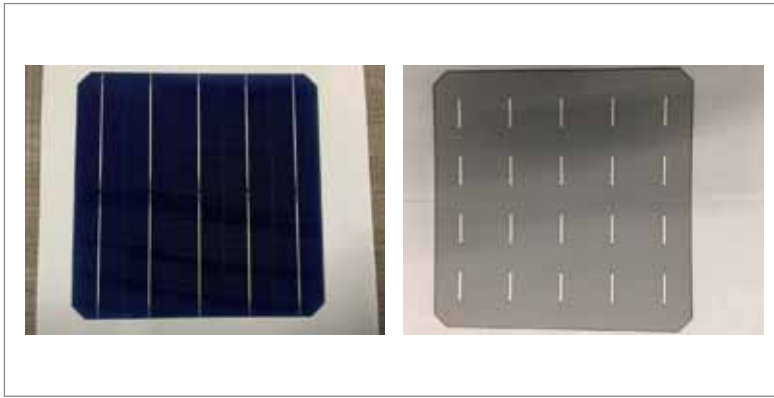**Figure 2. TongWei Solar's 5BB PERC cell.**
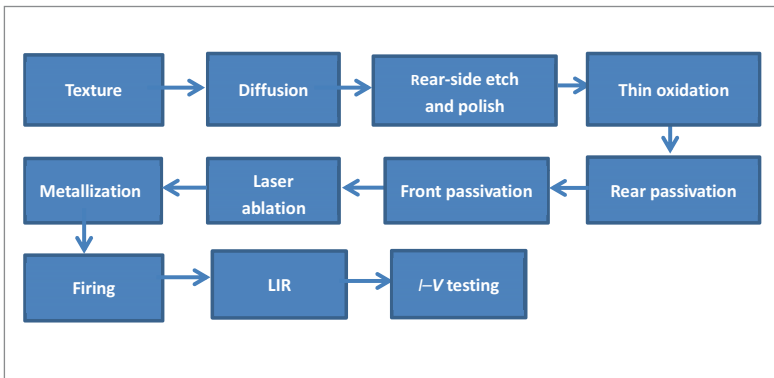
Figure 3. Manufacturing processes for PERC cells.
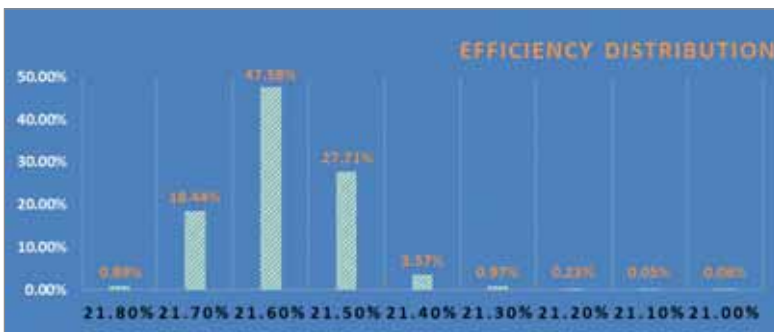
Figure 4. Efficiency distribution of PERC cells.

ΔV_{oc} [mV]	ΔI_{sc} [mA]	ΔFF [%]	ΔEff [%]
25	300	−0.5	1.3

Table 1. Absolute differences of the parameters for the PERC cell compared with the Al-BSF group based on the same wafers.

achieve 1.3% additional conversion efficiency and an extra 25mV in V_{oc} (see Table 1), indicating that the performance of the aluminium oxide passivation process on the rear-side passivation is excellent. In addition, the rear-side polishing and the deposited SiN anti-reflection film contribute to the internal reflection of the incident light, resulting in an increase of 300mA in I_{sc}. However, the fill factor (*FF*) of the PERC cells is 0.5% lower than that of the

"The narrow Gaussian distribution of the cell efficiencies proved that the current PERC processes have excellent stability properties"

conventional Al-BSF cells, mainly because of the change of the conduction path of aluminium LBSF contacts; this results in a series resistance (R_s) that is higher for PERC cells than for conventional Al-BSF cells, and thus a lower *FF* (Table 1).

Reliability controls for product performance have been introduced within the cell processing line at TongWei Solar; these controls utilize 100% EL detection, 100% LID pre-regeneration and inline welding tension monitoring, in order to ensure the stability of the PERC cell processes and high reliability. With the distributed printing process used in PERC cells, pastes with high adhesion could be chosen for the front-side busbars to improve cell performance while maintaining the weld quality, and hence to guarantee the long-term reliability of PERC modules. Fig. 5(a) shows the electrode adhesion test results for the PERC cells: the peel strength was >2.5N/shift for the front-side busbar, and >4.9N/shift for the rear-side busbar.

Fig. 5(b) shows the LID attenuation results for the PERC cells. Six cells within each shift were measured at random time points, and the measured attenuation values for each batch were below 1.5%, meeting the current mainstream cell product specifications. PERC solar cells in TongWei's main efficiency band were used in the standard 60-cell modules, resulting in over 300W per module on average.

P-type mono PERC cells efficiency roadmap
SolarWorld and Trina Solar have both reported cell conversion efficiencies above 22% [5] for their industrialized screen-printed PERC solar cells. From efficiency simulations, it is expected that a conversion efficiency of greater than 24% on PERC technology could be realized by further reducing electrical and optical losses, as claimed by some studies [6].

TongWei has set a short-term goal of achieving an efficiency of more than 22% for mass-produced PERC cells. Table 2 shows the values for the relevant electrical parameters required in order to reach this target.

The ideal fill factor FF_0 is close to 84% for cells with 21.6% efficiency, without taking into account the series resistance, parallel resistance and recombination losses. However, if the ideality factor $n = 1$, on the assumption of the current levels of series and parallel resistance the theoretical *FF* for R_s could reach 81.4%, but the actual *FF* for R_s is only about 80.68%, according to Table 1. Therefore, some of the loss in *FF* arises from the ideality factor. Fig. 6(a) shows the decrease in *FF* as the ideality factor n increases: a higher value of n indicates a higher emitter recombination loss, which needs to be further optimized.

Fig. 6(b) shows the correlation between the *FF* and R_s for PERC cells: a strong negative correlation can be observed. To further increase the *FF* in the efficiency-improving processes for future PERC cells requires a further reduction in losses brought about by R_s and n.
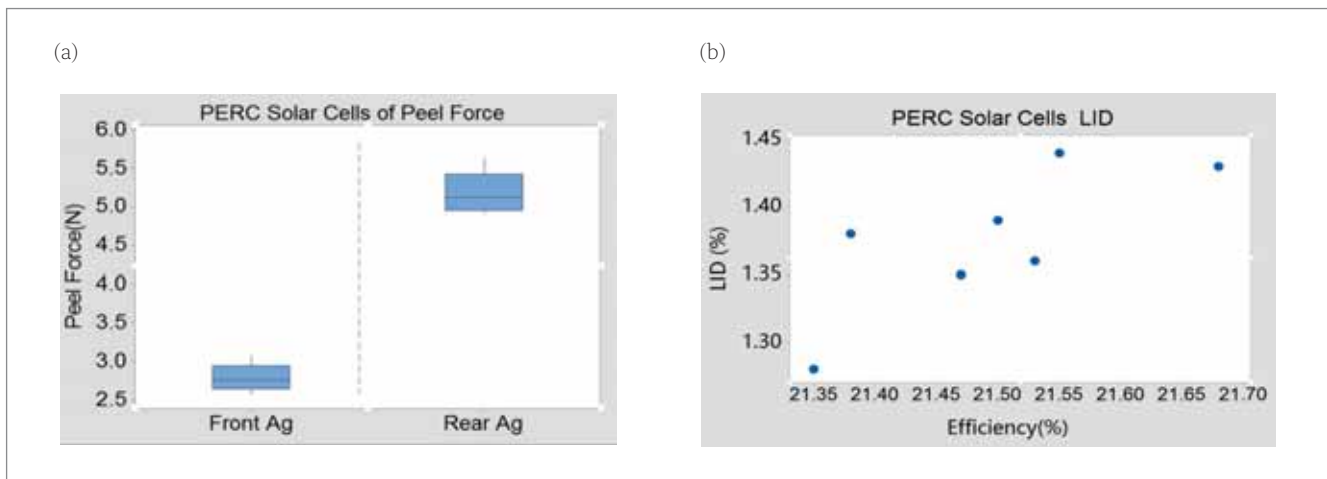
In order to push the V_{oc} of cells up to 680mV,

Figure 5. (a) The electrode peel strength testing conditions are: the angle used is reversed 180 degree, peeling speed is 300mm/min, ribbon width is 1.0mm, welding process temperature is 360°C, welding worktop temperature is 50°C, and the result is calculated by the average value of 5 busbars' pulling force; (b) LID test results for PERC cells.
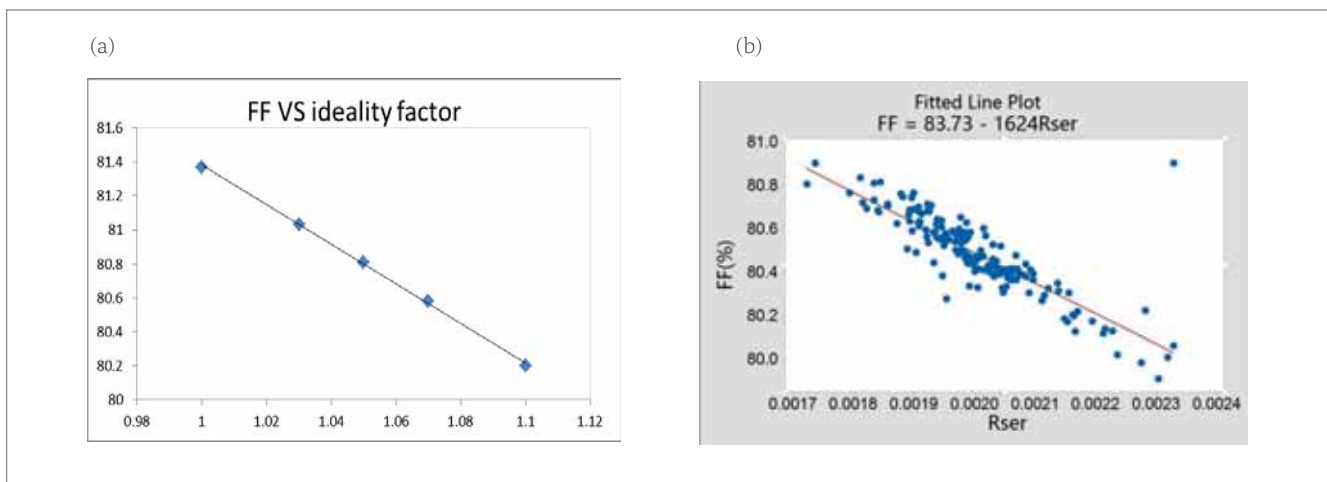

Figure 6. (a) Relationship between FF and ideality factor n; (b) correlation between FF and R_s.

	I_{sc} [A]	V_{oc} [V]	FF [%]	$\Delta\eta$ [%]
Baseline	9.767	0.670	80.68	21.61
Target	9.820	0.676	81.40	22.11

Table 2. I–V parameters for current PERC cells and for simulated target cells.

it is necessary to further reduce the value of J_o. Studies have shown that the existing J_o that affects PERC cells efficiency mainly lies in the emitter recombination and Ag-Si contact recombination [7–8]. The key to further increasing the V_{oc} of PERC cells therefore relies on a combination of various methods: emitter structure doping with low recombination rates, enhancing the surface contact characteristics, and improving wafer quality. Provided the contact resistances are sufficiently maintained, I_{sc} could be increased by reducing shading and conductive resistance through a better aspect ratio of the printed busbars, and by further optimizing the texture process, polishing process on the rear side and matching up, as well as the coating process of the front and rear sides.

On the basis of the above analysis, Fig. 7 shows the paths of improvement for PERC cell efficiencies for each operational process, to achieve >22% mass-production efficiency through further optimization

of processes, such as emitter doping, front and back conductive path design and passivation process improvements. At the same time, further reductions in the LID of PERC cells will also be the main focus in the future.

Conclusion

A mass-production efficiency of 21.60% for PERC p-type mono cells has been achieved at TongWei Solar; cell efficiency has a narrow distribution band in mass production, demonstrating excellent process stability and quality reliability. ALD aluminium oxide technology yields outstanding

"To achieve 22%+ efficiency for PERC solar cells in mass production, it is noted that further investigation regarding passivation and emitter doping processes is required"
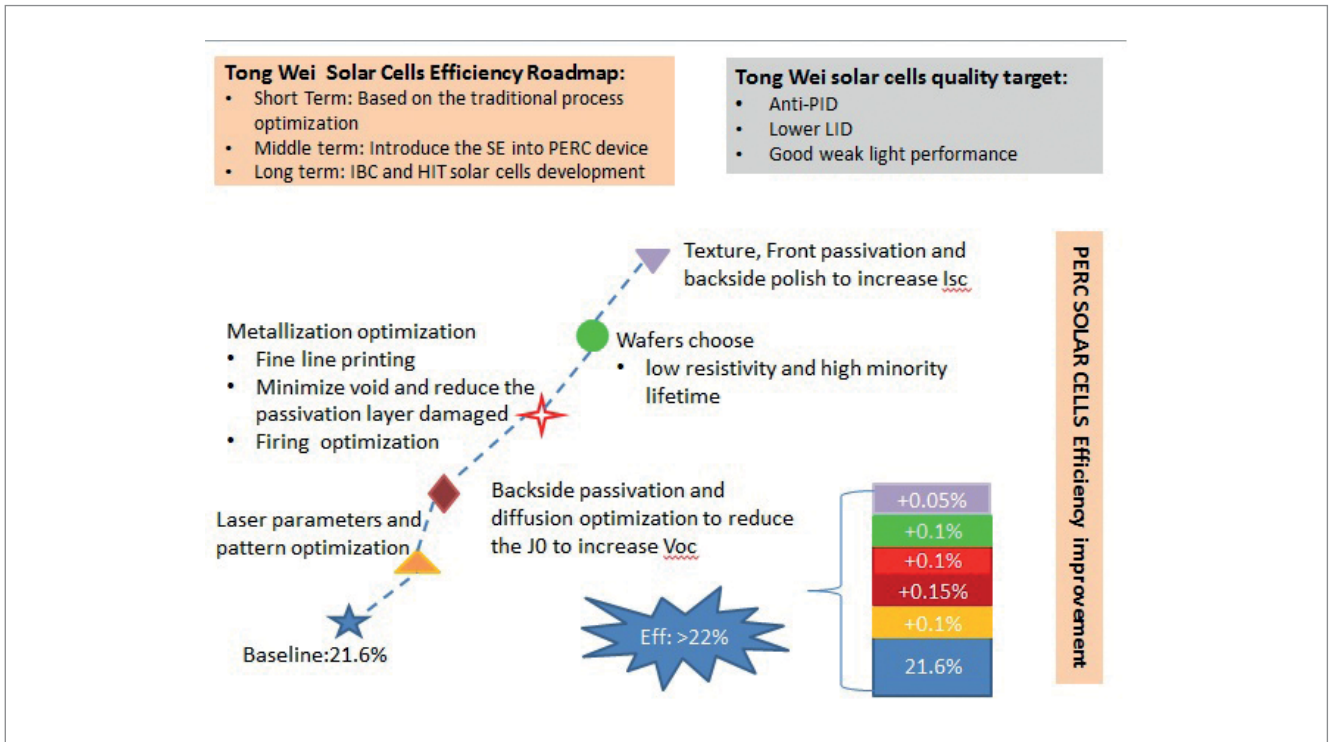
Figure 7. TongWei PERC cells efficiency roadmap.

passivation properties, increasing V_{oc} by 25mV. However, in order to achieve 22%+ efficiency for PERC solar cells in mass production, it is noted that further investigation regarding passivation and emitter doping processes is required, and that the metallization process needs to be optimized and high-quality wafers are necessary.

References
[1] Ye, F. et al. 2016, "22.13% efficient industrial p-type mono PERC solar cell", *Proc. 43rd IEEE PVSC*, Portland, Oregon, USA, pp. 3360–3365.
[2] Blakers, A.W. & Wang, A. 1989, *Appl. Phys. Lett.*, Vol. 55, No. 13, pp. 1363.
[3] Zhao, J. Wang, A. & Green, M.A. 1993, *Prog. Photovolt: Res. Appl.,* Vol. 1, pp. 133–143.
[4] ITRPV 2017, "International technology roadmap for photovoltaic (ITRPV): 2016 results", 8th edn (Mar.) [http://www.itrpv.net/Reports/Downloads/].
[5] [http://www.pv-tech.org/news/solarworld-reaches-22-efficiency-in-p-type-perc-cell].
[6] Min, B. et al. 2015, "Incremental efficiency improvements of mass-produced PERC cells up to 24%, predicted solely with continuous development of existing technologies and

wafer materials", *Proc. 31st EU PVSEC*, Hamburg, Germany, pp. 473–476.
[7] Weber, T. et al. 2013, "High volume pilot production of high efficiency PERC solar cells – Analysis based on device simulation", *Energy Procedia*, Vol. 38, pp. 474–481.
[8] Gatz, S. et al. 2012, "Analysis and optimization of the bulk and rear recombination of screen printed PERC solar cells", *Energy Procedia*, Vol. 27, p. 024107.

About the authors
Lead author Dr. Zhang Guanlun worked at TSMC as an R&D manager, and then joined Motech in 2011, where he led several technical research activities, including increasing the efficiencies of conventional mono cells as well as of Motech PERC mono cells. In 2015 he also developed methods to significantly reduce the LID of mono cells and PERC cells to ~1%. He is currently the R&D vice president at TongWei and heads the team working on PERC processing technologies for further increasing c-si cell efficiencies.

Enquiries
Zhang Guanlun
TongWei Solar (Chengdu) Co. Ltd.
No. 999, Huangjiashuangxing Road
Shuangliu County
Chengdu, Sichuan
P. R. China

Email: zhanggl02@tongwei.com

News

Solliance improves perovskite roll-to-roll processing with record efficiencies

The thin-film photovoltaics research initiative Solliance, which is focused on the commercialisation of perovskite thin-film technology, has fabricated small cells with industrially applicable, roll-to-roll (R2R) production processes, setting a number of new conversion efficiency records.

Solliance, which includes commercial partners Panasonic, GreatCell (formerly Dyesol) and Solartek said that the perovskite material was successfully processed at temperatures below 120°C and selected two foil zones of each about 10 metres in length with a visual good perovskite quality. The perovskite foils then went through a range of processing settings to produce 20 individual 0.1cm2 solar cells in each designated foil zone.

For each zone six 2 x 2cm2 (or 4cm2) aperture modules, four 3.5 x 3.5cm2 (or 10.5cm2) aperture modules and one 13 x 12.3cm2 (or 160cm2) aperture module were produced by laser scribing with 100% yield over all 22 fabricated modules.

CREDIT Solliance

Solliance said after processing the R2R cells that in one zone the maximum stabilized efficiency reached 13.5%.
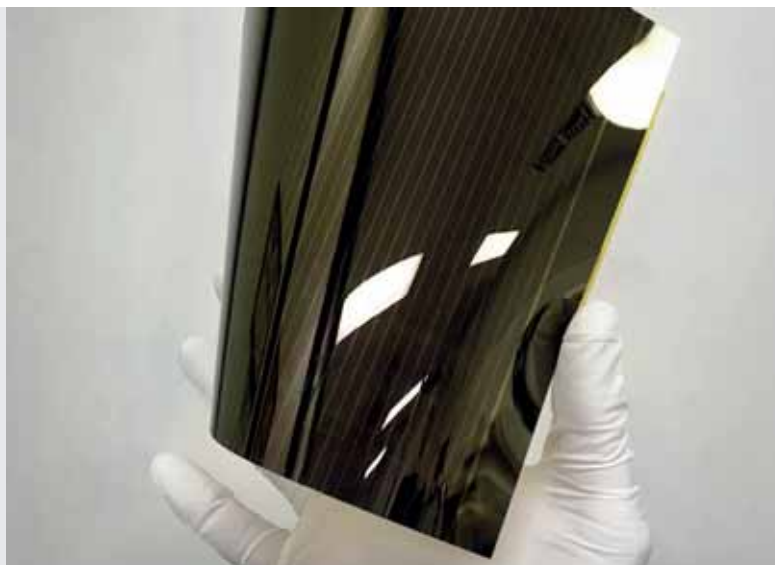
The Solliance partners noted after processing the R2R cells that in one zone the maximum stabilized efficiency reached 13.5% (measured under maximum power point tracking conditions over 5 minutes) and in the second zone a maximum of 12.5% was reached. The average stabilized cell efficiency in the best performing zone was about 1% higher than the previously reported run in March 2017.

For the modules prepared from the best performing zone, the smaller modules of 4cm2 showed a maximum aperture stabilized efficiency of 12.1%, with an average of 11.1% across the six modules.

The larger modules of 10.5cm2 achieved a maximum aperture stabilized efficiency of 12.2% with an average of 11.0% across the four modules.

However, the largest module of 160cm2 was said to have achieved an aperture stabilized efficiency of 10.1%, which highlights the progress made to ultimately achieve high-volume production of perovskite solar cells.

"These results show that the developed R2R process is very reproducible over different runs in time, which is very important for future reliable manufacturability," said Pim Groen, Professor of SMART materials at the Technical University of Delft and programme, manager at Holst Centre/Solliance.

RECORD EFFICIENCY
Solar Frontier breaks thin-film efficiency record with lab-scale cell

PV manufacturer Solar Frontier has set a new thin-film cell efficiency record of 22.9%.

The result, on a 1cm2 cell, was achieved in partnership with Japan's National Research and Development Agency's New Energy and Industrial Technology Development Organization (NEDO).

The record was verified by the National Institute of Advanced Industrial Science and Technology (AIST) and is 0.3% higher than the previous record set by Germany's ZSW.

The cell uses Solar Frontier's Copper, Indium and Selenium (CIS) architecture with enhancements via "absorber engineering and enhanced surface treatment of the absorber layer".

The company claimed it was further evidence of the ongoing potential CIS technology improvements.

FIRST SOLAR
First Solar executives 'losing hair' over first 'Series 6' panel produced

Leading thin-film manufacturer First Solar highlighted at its 2017 Analyst Day event that it had recently fabricated the first functional CdTe Series 6 thin-film panel at its Perrysburg, Ohio plant, which is spearheading the transition to the larger
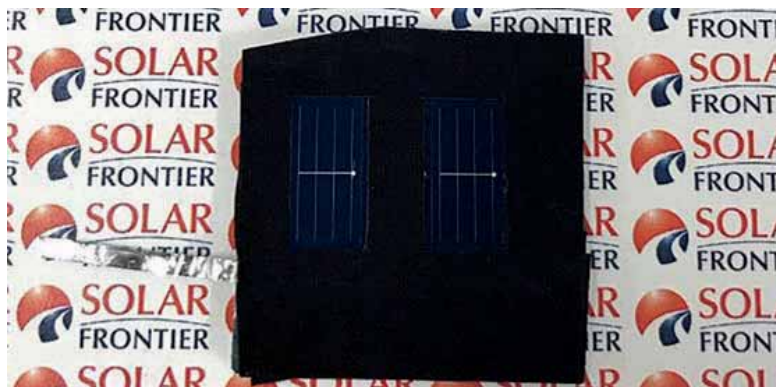
Credit: Solar Frontier

format at all of the company's manufacturing plants based in Malaysia and Vietnam.

First Solar said that the major milestone in a factory retooling that had started just under one year ago included approximately US$177 million in capital investment and a bet with the site engineers and employees that should the first panel be produced before the beginning of December then two of its executives would have their heads shaved.

The executives having shaved heads the day after the analyst event are CTO, Raffi Garabedian and COO, Tymen deJong. PVI can confirm that locks were lopped but no photographic evidence will be placed in the public domain.

The new production line at the Perrysburg plant for Series 6 panels was said to have an initial 600MW capacity.

"This is an extraordinary accomplishment, by any measure," said First Solar CEO Mark Widmar. "Last November, we were in full Series 4 production mode. Since our decision at the end of 2016 to rapidly transition to Series 6, we've hit every incremental target with precision. We are absolutely delighted to be on track for delivery of commercial product early next year."

First Solar building second 1.2GW production plant in Vietnam

First Solar said at its 2017 Analyst Day event that it was already building its second CdTe module plant in Vietnam to support the transition to its Series 6 large format panel.

The second fab is adjacent to its existing plant, which is undergoing readiness for the initial ramp of Series 6 panels. Both facilities have an initial nameplate capacity of 1.2GW each.

Fab 2 is expected to be built and ready fro tool install in the third quarter of 2018. The company also highlighted that first module production was expected in the first quarter of 2019.

As a result of the capacity expansion, First Solar is expecting to reach a total global manufacturing capacity of 5.4GW in 2020 with capex of US$1.4 billion through 2020.

TOOLS

Manz reliant on major CIGS thin-film order execution to meet 2017 guidance

PV and electronics equipment manufacturing and automation specialist Manz AG needs to book revenue of around €157 million in the fourth quarter of 2017 to meet guided expectations of full-year revenue of at least €350 million in 2017.

Much of the sales required rely on being paid on initial execution phases of a major CIGS thin-film turnkey order from Chinese JV partners Shanghai Electric Group and Shenhua Group.

According to Manz in reporting third quarter financial results the CIGS solar orders are being "handled within the projected schedule," noting

that it expected to recognise the majority of "solar segment revenues planned for 2017 over the fourth quarter."

Solar segment sales have been only a small part of quarterly revenue for Manz so far in 2017. Solar segment sales in the first quarter were only €1.5 million. However, second and third quarter solar segment sales increased to €14.9 million and €14.3 million, respectively.

Manz reported third quarter 2017 revenue of €73.4 million and first nine months revenue of €193 million. Earnings before interest, taxes, depreciation, and amortization (EBITDA) were €8.5 million, compared to a negative EBITDA of €25.7 million in the prior year period.

Manz is dependent on the CIGS revenue recognition to meet guidance of €350 million and a return to profitability.

Singulus receives order for CIGS wet-chemical coating tools from China

Specialist PV manufacturing equipment supplier Singulus Technologies has secured another order from a customer in China for its TENUIS II wet-chemical coating process tools.

Singulus said that the multiple tool order was in the higher single-digit million range.

Stefan Rinck, CEO of Singulus Technologies said: "This additional order for CIGS production systems confirms our leading role in the field. Our company offers solutions for all important steps in the manufacture of CIGS solar modules."

Previously in October, the company had secured new tool orders from China and US for its 'SILEX II' wet cleaning batch system, primarily used for high-efficiency heterojunction (HJ) solar cells.

The company has a joint venture with 'Silicon Module Super League (SMSL) member GCL in China for HJ solar cells.

Credit: First Solar

PID issues in thin-film PV plants

Thomas Weber, Steven Xuereb, Cyril Hinz, Mathias Leers & Lars Podlowski,
PI Photovoltaik-Institut Berlin AG (PI Berlin), Germany

Abstract

Thin-film plants which were installed within the past 10 years have been known to suffer from quality issues such as underperformance and poor module quality. Potential-induced degradation could be identified as one of the major defect types, which sometimes results in an underperformance far beyond the warranty terms. Affected projects end up in legal confrontations and quite often require technical experts to evaluate the situation and to determine and validate the failure. Finally, in many cases the modules must be replaced. In recent years, results of PID-affected PV plants have been collected by the authors showing underperformance. Results of three investigated plants are presented in which the performance of the technologies CIGS, CdTe and µc-Si was studied. Investigation and characterization in the field and in the laboratory, including PID tests, were performed. The CdTe modules during field investigations show a clear degradation towards the negative string end. The PID test proved their sensitivity to the phenomenon and revealed TCO-corrosion. For µc-Si TF modules a PID sensitivity could also be proven but here the power evaluation and failure distinguishing to the "white spot" phenomenon was challenging. The CIGS modules under investigation showed also a very clear PID degradation towards the negative string end which could be proven by PID tests and electroluminescence on complete strings in the laboratory.

Introduction

Nowadays, there is a worldwide production capacity of about 5GW of thin-film module technology. In total, an estimated cumulative installed capacity of 15 to 24GW exists (5-8% of 300GW installed worldwide in 2016). Thin-film plants which were installed within the past 10 years have been known to suffer from quality issues like underperformance and poor module quality. PID could be identified as one of the major defect types, sometimes resulting in an underperformance far beyond the warranty terms. Affected projects end up in legal confrontations and quite often require technical experts to evaluate the situation and to determine and validate the failure. Finally, in many cases the modules must be replaced.

This work does not focus on the development of a thin-film test standard [1,2] or the mechanisms behind PID in thin-film modules [3-6]. When results of TF PID were presented in the past, they almost always focused on results gained in the laboratory. In this work, the authors present real data gathered from the field compared with results from the same test specimen generated in the lab. This approach gives the opportunity to validate the outdoor results and to deepen the investigation of supposed findings.

First, a definition of the terms and methods related to PID for thin film is essential. "Voltage potential that exists between the active circuit and the grounded module surfaces can lead to module degradation by multiple mechanisms including ionic transport in the encapsulant, superstrate or substrate; hot carriers in the cell; redistribution of charges that degrade the active layer of the cell or its surfaces; failure of adhesion at interfaces, and corrosion of module components. These degradation mechanisms in thin-film modules caused by voltage stress and promoted by high temperature and humidity have been labelled potential-induced degradation, polarization, electrolytic corrosion, bar-graphing [, TCO-corrosion,] and electrochemical corrosion. They are most active in wet or damp environments and in environments prone to soiling of modules with conductive, acidic, caustic, or ionic species that lead to increased conduction on the module surfaces. In the field, modules have been observed to degrade in positive as well as negative polarity strings depending on the cell construction, module materials, and design [2]." The cited paragraph is out of the technical specification for TF PID testing (IEC TS 62804-2). This specification describes the test methods to determine module PID susceptibility under positive and negative bias directions. Correlating stress levels from tests to PID durability in a natural environment is important but a completely different topic [4,7].

In recent years, the results of PID-affected PV plants were gathered by the authors showing underperformance. Results of three investigated plants are presented in which the performance of the technologies CIGS, CdTe and µc-Si was studied. Investigation and characterization in the field and in the laboratory as well as PID tests were performed.

Methodology

Once in operation, PV plants have to be regularly inspected and tested to ensure reliable and safe operation and that the investment is providing the expected revenue and is operating in a safe and reliable manner. The operation and maintenance (O&M) teams and the installed monitoring systems are able to provide the first indications of performance ratio (PR) losses. In-depth analysis is necessary to address the origin of the failures. For this purpose, usually external experts are commissioned to work in the field for troubleshooting and to advise the plant owners. The objective is to develop the best approach to solve the issues. The variety of services inter alia range from monitoring data and PR analysis, data monitoring, documentation check, on-site inspections and module selection for laboratory testing. For the PV plants considered in this work, all of these

	I	II	III	
Technology	CIGS	CdTe	µc-Si	
Plant age in years		4	6	2
Size in MW	21	2.3	2.0	
Nominal Module-Power in W		105 & 110	67.5	128
Grounding Instruction		None, APT (Anti PID Technology)	None, not specified	Neg.-pole grounding

approaches were used to get a complete overview. With the focus on PID-analysis on thin film within this work, only a selection of results gathered during on site inspections and laboratory testing at module level are presented. The results in this work are not representative for a general statement of the quality of a particular module type, manufacturer or technology.

To investigate the modules on-site, engineers conduct IV-curve tracing at module and string level, infrared thermal imaging and electroluminescence tests. Visual inspections also play an important role to evaluate the current status and workmanship of the plants. For the PV plants presented here, the following measurement equipment was used:

- Power measurements were performed with a calibrated HT I V400 peak power measuring device and IV-curve tracer with a measurement uncertainty of +/-5%), including calibrated irradiation and temperature sensors for corrections to STC conditions;
- By means of an electroluminescence (EL) camera EL pictures were taken to visualize module failures

like shunts and inactive areas. The modules were powered string-wise with the short circuit current. Further information can be found elsewhere [8,9].

In PI Berlin's accredited test laboratory (ISO 17025) tests are performed according to IEC 61646 Ed.2.0 (2008) and 61215-X Ed.1.0 (2016) [10,11] and beyond. The PID tests were conducted according to TS 62804-2 TF (simulating the original mounting construction and applying maximum system voltage in a climate chamber of 85°C and relative humidity of 85%). They were divided in the categories of sensitivity test (selection of non-affected modules), risk assessment (selection of medium-affected modules) and recovery tests (selecting strongly degraded modules with an application of reverse voltage). Before and after each exposure the IV curves have been recorded using a Class AAA flasher Pasan SSIIIb. The maximum power (Pmax) has been extracted from the IV curve under standard test conditions (STC). The measurement uncertainties are ±2.9% for single junction (CdTe and CIGS) and ±5% for double junction (µc-Si). Furthermore, visual and EL inspections were performed before and after

Table 1. Overview of the PV plants investigated.

Figure 1. Degradation of power output (compared to label) string-wise for the CIGS plant. Mean power deviations were determined for the marked sections and below for all tested modules.

String \ Mod-Pos.	1	2	3	4	5	6	7	8	9	10
1										
2										
3										
4										
5										
6										
7										
8								no data		
9										
⋮										
20										
Mean *	-56%	-48%	-35%	-23%	-7%	0%	1%	0%	-1%	-1%
	-18%									

ΔP in %

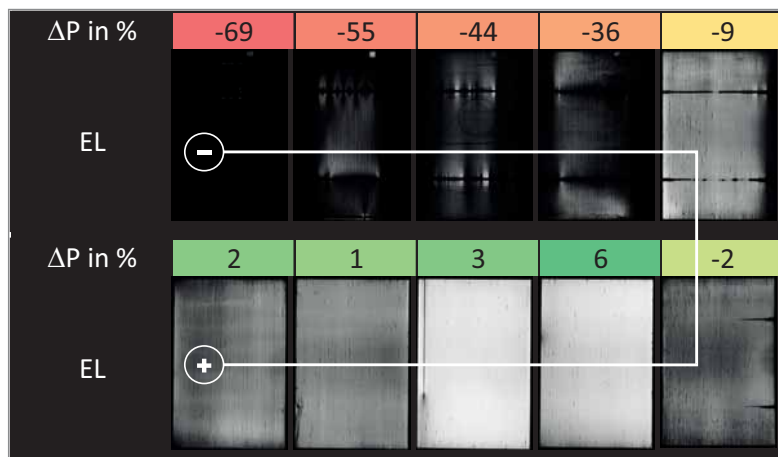-100   -60   -30   -10   +10
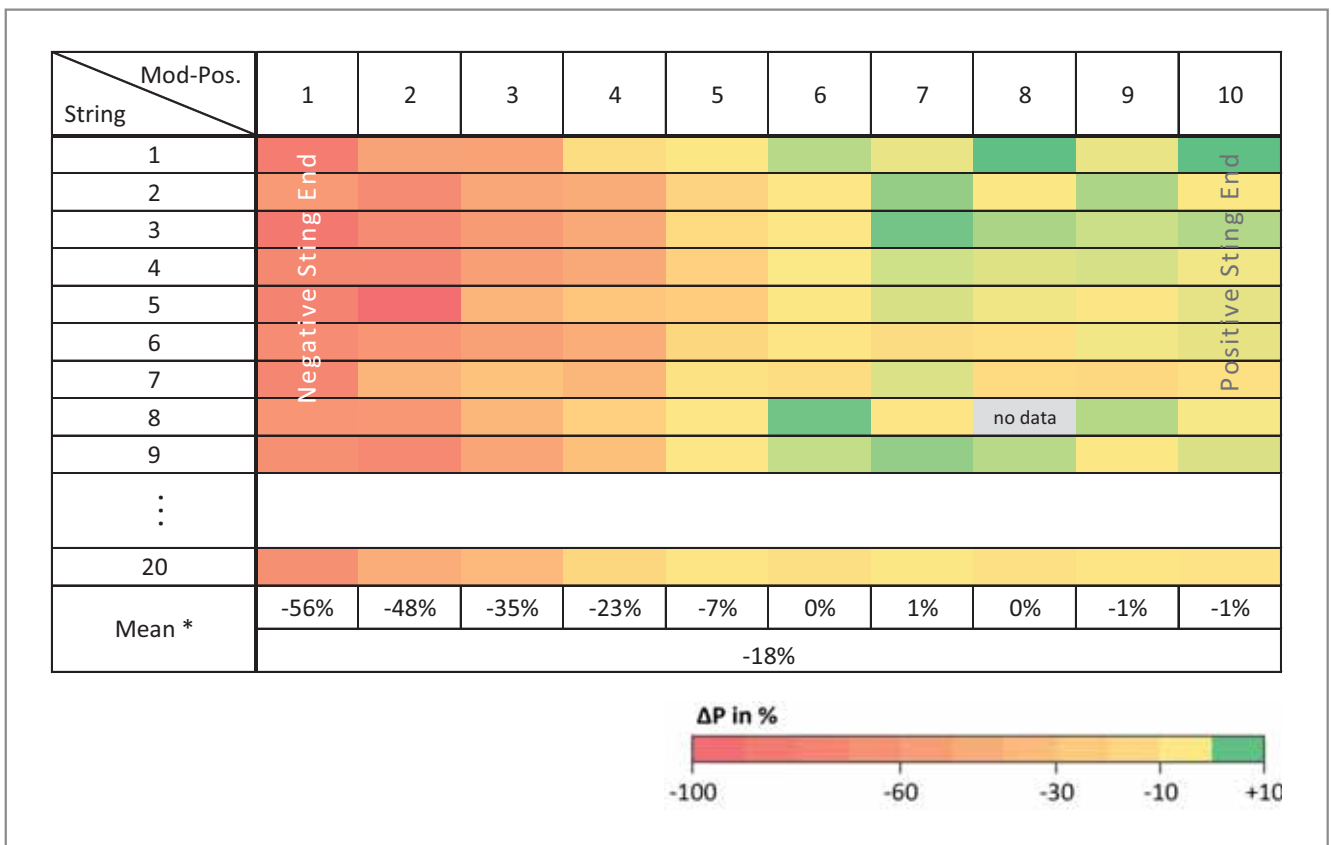
Figure 2. Module power output degradation and corresponding EL pictures for modules of one investigated string. Left top side negative end of the string and left bottom side positive end.
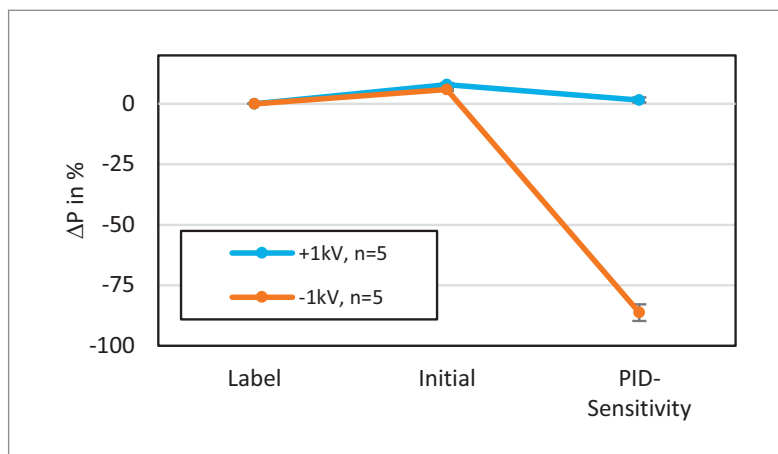

Figure 3. Module power evolution for PID-sensitivity tests. Blue +1kV and orange -1kV PID-Sensitivity tested for 96 hours.
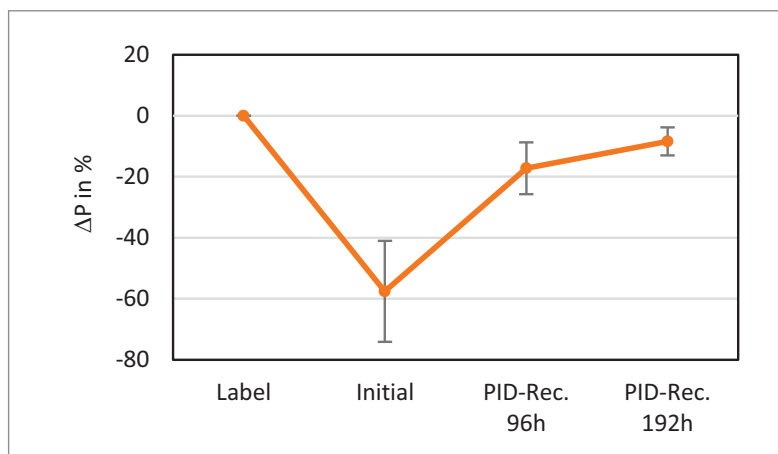

Figure 4: Module power output evolution during the PID-Recovery Tests determined as mean value of 15 modules.

the stress tests to evaluate the results [8]. A Nikon D800 camera, with removed IR-filter with a high-sensitivity 36 megapixel CCD-chip and a 50 mm f/1.4 high-precision IR-optimised optic from Zeiss, was used.

Three different TF PV plants with CIGS, CdTe and microcrystalline silicon tandem (µc-Si) module technologies were selected. For a short overview, basic parameters of each site can be found in Table 1. All plants are ground-mounted installations and located in central Europe.

Results and discussion
Plant I (CIGS)

For the laboratory investigation, 20 complete strings of 10 modules were selected randomly out of the power plant to ensure a representative result distribution. Figure 1 shows the power output measurement results string-wise of all modules. The deviations of the module performance were determined by a comparison of the measured results with the nominal value. In the result presentation of Figure 1, the colour code ranges from green, representing compliance of guaranteed performance values, over yellow and orange to red, which indicates the modules with the lowest residual power output. One can see that all strings show degradation in a few modules up to -40% to -90%. If one looks at the individual string and correlates the power loss to the module position in the string, it can be seen that modules at the negative string end degrade most (see Figure 2). The corresponding EL pictures confirm the results with increasing inactive cell areas by a darkening of the cells towards the negative string end. These evenly distributed results lead to the suspicion of a potential-induced degradation as the main reason for the power deviation.

To verify this suspicion, PID tests were performed to evaluate the modules in terms of general susceptibility, further risk during operation and regeneration potential. The sensitivity tests were each carried out with five modules per polarity. Only the least affected modules were selected for the 96 hour-long PID test. Figure 3 shows the results. The module's power output evolution is shown (including the standard deviations) for modules tested at positive bias (blue) and at negative bias (orange). The initial power measurements have revealed results with 7% higher power output compared to the nominal value for all modules. The group of modules connected to positive bias degraded slightly whereas the modules stressed at negative bias degraded about -86%.

A recovery test was also performed with 15 severely degraded modules by an exposure to the opposite polarity during the PID test. Figure 4 shows the average deviation to the nominal value received at the final measurements. Initially, the modules suffered from an average degradation of (58 ± 17)%. After 96 hours of PID recovery exposure, the modules recovered to an average power loss of (17 ± 9)%. An additional recovery cycle of 96 hours led to a further improvement, ending with an average negative power output deviation of (8 ± 5)%. In the case that the used module type possesses the property of recoverability, an adaption of the plant design by grounding the negative pole could be a feasible solution to stop the degradation and to induce the recovery process.

In this presented case study, a change of the plant design was not possible and the test

specimen suffered also from other types of ongoing degradation effects, partly induced by the PID recovery procedure. Figure 5 shows exemplarily such induced degradation mechanisms in the appearance of discoloration and bubbles in the edge sealing leading to a reduced insulation. Furthermore, worm-like delamination has occurred directly over the semiconductor. The backside of the module showed strong glass corrosion at the edges and in front of the rails of the mounting structure. A closer look at the distribution of power deviations within the strings reveals another degradation effect at the positive end (see Figure 2, visible in power loss and EL). The highest power output of an individual module in the string is around module position seven (counted from the negative string-end, left side – see Figure 1). Towards the positive string-end, a slight decrease is visible for the majority of strings.

The results of PV plant I can be summarized as

- PID with increasing severity towards negative string-end;
- PID-sensitivity tests validate this result;
- Regeneration at positive bias not possible due to superimposed degradation mechanisms induced during exposure leading to new module failures.

Finally, all modules in the plant were replaced by new modules.

Plant II (CdTe)

In PV plant II, 12 strings with 20 modules each

Figure 5: Visual degradations after PID-recovery test at +1kV 196h on module front (left) and back (right).

were investigated with IV-curve measurements and electroluminescence. Figure 6 shows the STC-corrected data for each module in its string position. The 67.5W CdTe modules were in the sixth year of operation, which results in a maximum allowed power output deviation of 12.6% to the nominal value according to the producer's guarantee conditions (90% guaranteed for the first 10 years). This value is also taking into consideration a

Figure 6. On-site power measurements of 12 strings, each with 20 modules. Some modules already show a total failure (grey) in the sixth year of operation. The power deviations for each module are presented according to the colour code. *Mean power deviations were determined for the marked sections and below for all tested modules.

String \ Mod-Pos.	1	2	3	4	5	6	7	8	9	10	11	12	13	14	15	16	17	18	19	20
Mean *			-40%					-23%						-21%						
										-26%										

⊠ Glass break.   ▢ Total failure, not measurable

ΔP in %

-100 -60 -30 -10 +10

measurement uncertainty of 2.9% according to EN 50380 (2003) on the 90% value. Some modules were not able to be measured due to a total electrical failure (grey) and four were mechanically destroyed due to glass breakage.

Only two modules passed the above mentioned threshold value resulting in a failure quote of 99%. The average deviation of all test specimens is -26%. An analysis of the power loss distribution shows a mean degradation of 40% of the first five modules at the negative string end, across all analysed strings. In contrast, the mean deviation of the five modules at the positive string end lies only at -21%. This tendency indicates very likely a potential-induced degradation (towards the negative string end) superimposed by a very prominent "normal" degradation (at all other module positions) far beyond the guaranteed values.

Figure 7 shows the EL-signal of four modules powered with current in forward mode. Inhomogeneous semiconductors with many failure patterns are affecting the modules from the edges inwards. For this module type, in its current state, it is hard to distinguish between production induced inhomogeneities and field-induced failure patterns. Figure 8 shows a picture taken on site where many modules with glass breakage are visible with the naked eye.

During the field measurement campaign 20 modules were selected for further in-depth laboratory analysis. To summarize the laboratory results:

- All investigated modules failed the guaranteed minimum power output (90% after 10 years) already in the sixth year of operation significantly with a mean deviation of -54% (including all failures, determined in the laboratory and not depicted);
- Burn marks (18% of all modules affected) at the current collector straps inside the modules indicate a too low specified or a too low reverse current overload protection (RCOP);
- 20% of all investigated modules (n=300) in the plant show glass breakage, most likely induced by the insufficient RCOP;
- A plant design failure in the form of an interconnection of six strings in parallel without string protecting diodes (knowing that this is common but not feasible for that module type) is fostering the two above mentioned module failures.

Moreover, accelerated stress tests in the climate chamber have confirmed PID susceptibility of all modules resulting in a development of TCO corrosion around the clamps. Figure 9 shows the test results as an evolution of the power output deviation compared to the label. The modules originate from different string positions: two modules from the positive string end (red) and three from the negative string end (black, illustrated as -/+End). After the initial laboratory power measurement, four modules were stressed during PID tests at negative bias and one module as a reference in damp heat (DH, dotted line)

Figure 7. EL pictures taken on-site.

Figure 8. Picture of a table in plant II.

without an applied voltage. The modules from the negative string end have a mean initial deviation of -43% whereas the modules from the positive string end have a mean initial deviation of -17%. The modules from the positive string end degraded further (A and B). The modules from the opposite string end regenerated, despite the negative potential during the exposure. The DH module (E) behaved like the modules from the positive string end.

It can be concluded that the modules are sensitive to PID due to the further power decrease and the visible TCO-corrosion around the clamps and edge region. The power output increase of the two test specimens can most likely be explained as an improvement of the semiconductor due to stabilization by high temperatures of 85°C during the climate chamber treatment (some manufacturers prescribe pre-conditioning before power measurements after dark storage in a warm environment, which was not the case here) and not due to a recovery process. Finally, the plant owner was advised to replace all modules in order to assure the economic viability of the plant.

Plant III (µc-Si)
Solar plant III was built with µc-Si modules and investigations were conducted in the laboratory. Figure 10 (left) shows the modules abnormalities with suspicion for TCO-corrosion (orange) and white areas (blue) indicating a low shadowing tolerance. For a further investigation of these issues and to validate the suspicion, eight modules were selected: two from the positive end of a string (A,C) and two from the negative end (B,D) all showing no TCO-corrosion; two more modules from the negative string end, already showing TCO-corrosion after two years of operationn (E,F) and two reference modules (G,H) (free from any degradation signs and from the positive string end). A summary of the module selection with the performed tests is shown in Table 2.

	Free of TCO-corrosion		Already affected with TCO-corrosion
	Take from + string end	Take from - string end	
(+1kV) PID	A	B	
(-1kV) PID	C	D	E,F
DH, HS	G,H		

Table 2. Module conditions and performed tests.

"A combination of field and laboratory tests increases the opportunities to receive precise and confident results and to come to the right conclusions"

The hot-spot tests revealed that the µc-Si TF modules are highly sensitive to shading. A brief partial shading leads to irreversible spots on the semiconductor (hot-spots) visibly as grey marks/white spots. During the test, no significant power loss could be found despite measured temperatures of maximum 80°C. The failures reported from the power plant could be reproduced during the laboratory test.

The PID test results are presented in Figure 11. Modules from a negative string position in the plant show partially visible TCO corrosion and an initial power deviation up to -18% (E,F). All investigated modules revealed significant further power degradation at negative bias resulting in power losses up to -55% (C to F). Furthermore, TCO-corrosion could also be proven as shown in the corner of the middle picture of Figure 10. The picture on the right hand side shows an example of an EL picture of module E after 500 hours' PID test exposed to negative bias. The module shows dark areas at the edges and corners in the EL picture. However, modules tested at positive bias reveal no power-related degradation processes but show visually a change of the semiconductor layers (fog-like). In contrast, an exposure to positive bias led to a power increase (up to labelled power). This was observed for the tested modules originating from a negative and positive string position due to a temperature regeneration effect (A,B). Accordingly for this module type, it can be stated that PID (such as TCO-corrosion) can be stopped by avoiding negative potential on site and an application of a proper grounding. Another opportunity would be a shift of the whole string potential further into the positive direction. Not shown are the results of modules G and H after the DH test. Both test specimens behaved in the same way as the positive PID tested modules indicating again that positive bias is not degrading the modules and that warm conditions (85°C) induce a regeneration process.

The presented results have shown that it can be challenging to differentiate between degradation mechanisms and temperature-driven power improvement of Si TF modules. This demonstrates the necessity to choose an appropriate module characterization procedure for reliable results and their correct interpretation. Consequently, it is necessary and recommended to follow the test specifications from the manufacturer of µc-Si modules for an evaluation of power output degradation. In this presented case, the procedure prescribes a regeneration at 90°C for 48 hours (e.g. damp heat chamber) followed by a light-induced degradation. This enables an evaluation of the power state of the modules before all treatments. Furthermore, it is important to distinguish between the "white-spot" phenomena and the TCO-corrosion. The authors presented this already elsewhere on the same module type [12].

Summary and conclusion

Field measurements (IV-curve tracing, EL and IR) have many positive benefits like analysis of large quantities of modules in the range of hundreds. Degradation effects at module level during operation can be detected and possible root causes investigated. One of the important advantages is that the modules are already performance-stabilized and no pre-conditioning, as with laboratory measurements, are necessary. Disadvantageous are the instable measurement conditions (intraday and seasonal) and particularly the high measurement uncertainties (5 to 10% for power output) [13].

Laboratory measurements are the environment-independent and more precise alternative solution but often limited due to financial constraints mostly resulting in low module quantities (low double-digit range). Nevertheless, using a representative and string-wise sample allows a validation of PID-related degradation. Despite higher accuracy (in this case 2.9%), pre-conditioning procedures due to dark storage (CdTe and CIGS) or seasonal power-output variations (Steabler-Wronski effect in silicon thin film), are mandatory. PID tests enable evaluation of the modules' sensitivity to this degradation mechanism, their regeneration potential and further risk to operate the modules in the plant at the given conditions. Table 3 summarizes the presented advantages and disadvantages between on-site and laboratory measurements.

A combination of field and laboratory tests increases the opportunities to receive precise and confident results and to come to the right conclusions. This enables the parties involved

to take measures against PID (e.g. negative pole grounding, regeneration or module replacement). A complete module replacement was necessary in two of the three presented projects.

The following recommendations are proposed to improve inspection methods of modules in operating plants:

- Further automatization is needed in failure detection and analysis field. Many measures were already implemented by monitoring service providers but an extension of automatization for module tests like electroluminescence would be very useful. A renouncement of IV-curve measurements could be taken into consideration as the good correlation of power output degradation with visibly failures on the EL images have shown in this article. This becomes even more critical as plant sizes continue to increase towards the GW range. The results provide evidence that a correlation between power drop and EL signal would lower inspection time, increase the number of inspected modules and lower the costs. This could be realized by performing only EL measurements without doing time intensive power measurements.

- Intense work towards a deeper understanding of mechanisms behind module failures of TF is necessary. Therefore, knowledge exchange along the whole value chain is essential.

To follow the presented recommendations, the PEARL project was established: "Performance and Electroluminescence Analysis on Reliability and Lifetime of Thin-Film Photovoltaics". The PEARL project aims to reduce the cost of electricity produced by thin-film PV power plants, by improving plant reliability, yield and prediction of the overall plant lifetime. For this purpose, large and small thin-film photovoltaic plants will be inspected by using particularly electroluminescence imaging. During the project, the applicability and understanding of electroluminescence imaging methods scaled to large-scale measurements on thin-film solar cells and modules will be improved. Furthermore, the objectives are to obtain knowledge about the appearance, behaviour and progression of failure mechanisms in thin-film PV plants. The gathered information will be used to increase the long-term profitability of thin-film photovoltaic projects by increasing operating yield, reducing operational and maintenance costs, improving accuracy of investment models and to improve bankability.

The PEARL TF-PV project is an international collaboration of industrial partners and research centres from Germany, Austria and the Netherlands, brought together via the Solar-era.net framework, namely: Forschungszentrum Jülich, Helmholz-Zentrum Berlin für Materialien und Energie (PVcomB), PI-Berlin, Austrian Institure of Technology, Crystalsol, TNO, ECN, TU-Delft, Solar Tester, KiesZon, eigenenergie.net and Straightforward. Interested

parties willing ro contribute to this project are invited to contact the authors!

	Field	Laboratory
Sample number	+ High	- Low
Costs	- Low	+ High
Measurement cond.	- Instable	+ Stable
Accuracy	- Low	+ High

Table 3. Evaluation of field and laboratory measurement advantages and disadvantages.
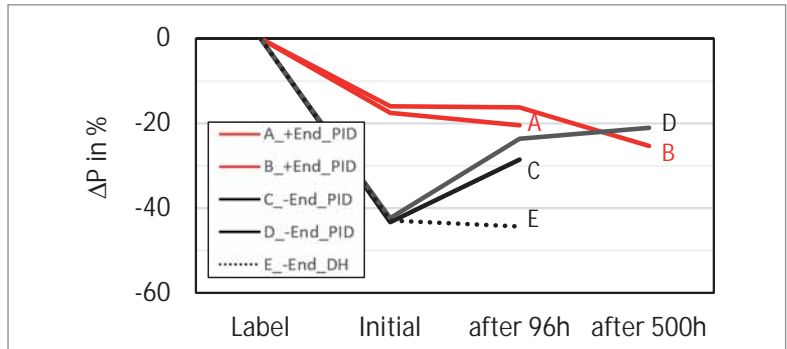

Figure 9. Module power evolution of CdTe modules from producer/plant II. The modules were taken from the negative (black) and the positive string end (red). After initial laboratory power measurement the modules were stressed at PID tests at negative bias and one module as a reference in damp heat (DH).
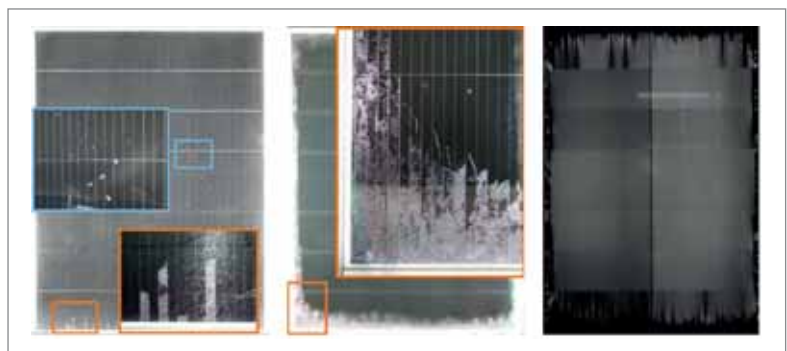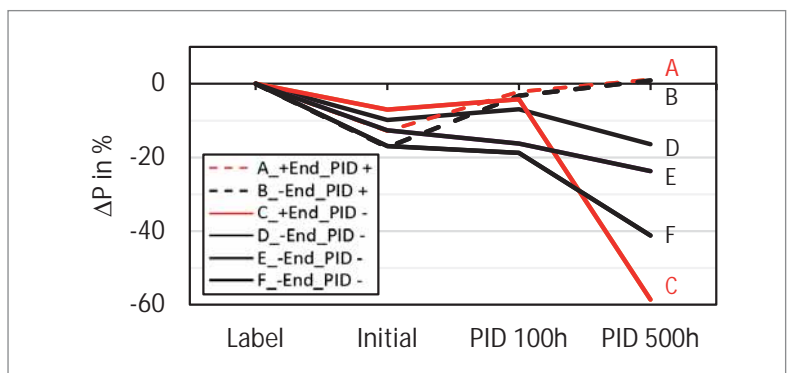

Figure 10. Left: Pictures of µc-Si module (E) of producer III with initial visual degradations showing TCO-corrosion (orange) and "white spots" (blue). Middle: TCO-corrosion after 500h PID(-) test. Right: Electroluminescence pictures after the test revealing dark areas around the edges indicating TCO-corrosion.

Figure 11. Module power evolution of µc-Si modules out of plant III. The modules were taken from different string positions. After initial power measurement in the laboratory, PID tests were conducted at positive and negative bias.

References
[1] P. Lechner, J. Schnepf, D. Geyer, R. Schaeffler, R. Wächter, T. Repmann, 2015, "Does the new IEC 62804-2 PID test procedure cover a service life of CIGS modules?", 32nd EU PVSEC, Hamburg.
[2] Technical specification IEC TS 62804-2 Ed.1, 82/1238/CD:2017-01
[3] S. Yamaguchi, S. Jonai, K. Hara, H. Komaki, Y. Shimizu-Kamikawa, 2015, "Potential-induced degradation of Cu(In,Ga)Se2 photovoltaic module", Japanese Journal of Applied Physics.
[4] P. Lechner, 2013, "PID Failure of c-Si and Thin-Film Modules and Possible Correlation with Leakage Currents", NREL PV Module Reliability Workshop.
[5] M. Atsushi, H. Yukiko, 2017, "Potential-induced degradation of thin-film Si photovoltaic modules", Japanese Journal of Applied Physics.
[6] M. A. Contreras, P. Hacke and I. Repins, 2016"Development of Cu (In,Ga)Se2 Test Coupons for Potential Induced Degradation Studies", Photovoltaic Specialists Conference (PVSC), 2016 IEEE 43rd.
[7] T. Weber, J. Berghold, F. Heilmann, M. Roericht, S. Krauter, P. Grunow, 2013, "Test sequence development for evaluation of potential-induced degradation on thin-film modules", 28th EU PVSEC, Paris.
[8] T. Weber, E. Benfares, S. Krauter, P. Grunow, 2010, "Electroluminescence on the TCO-corrosion of thin-film modules", 25th EU PVSEC, Valencia,
[9] S. Koch, T. Weber, C. Sobottka, A. Fladung, P. Clemens, J. Berghold, 2016, "Outdoor electroluminescence imaging of crystalline photovoltaic modules", 32nd EU PVSEC, Munich.
[10] IEC 61646 Ed. 2.0 (2008)
[11] IEC 61215-2, Ed.1.0 (2016)
[12] S. Wendlandt, S. Berendes, T. Weber, J. Berghold, S. Krauter and P. Grunow, 2016, "Shadowing investigations on thin-film modules", 32nd EU PVSEC, Munich.
[13] A. Preiss, U. Siegfriedt, T. Röder, P. Grunow, 2017, "Aktuelle Betrachtung der Messunsicherheit der Leistungsmessungen an PV-Modulen unter Feldeinsatzbedingungen, oder: Sind die 5% Unsicherheit (Pmax) wirklich die untere Grenze?", PV Symposium Bad Staffelstein.

About the authors

Thomas Weber studied environmental engineering at the University of Applied Science Berlin and completed his diploma with a topic of post annealing treatments of silicon thin-film solar cells at the Helmholtz-Center Berlin. Since June 2008 he has been working as a project manager at PI Berlin, specializing in TF PID and Electroluminescence. Since May 2014 he has been head of service unit module technology, R&D.

Steven Xuereb is a renewable energy professional who has sixteen years of experience both in the wind and solar industries. Currently he leads the PV Systems business unit at PI Berlin, focusing on delivering independent engineering services for large scale solar plants. Before joining PI Berlin, Steven spent eight years procuring and developing solar and wind projects in North America, Chile and South Africa for Airtricity and Mainstream Renewable Power. His experience in the industry includes greenfield development, acquisitions, contracts management, research and development, certification and service operations. He is a mechanical engineer with a master's degree in renewable energy from the Universities of Oldenburg and Kassel.

Cyril Hinz studied renewable energies at the University of Applied Science Berlin and completed his degree in 2016 with a master of science. Following his graduation, Hinz began working at PI Berlin as a project manager within the business unit PV Systems, conducting on-site measurements, and as a research associate within the R&D department with a specialization in 'regeneration of potential-induced degradation' and module cleaning.

Mathias Leers studied environmental engineering/renewable energy systems at the University of Applied Science Berlin and received his Master of Science degree in 2010. Mathias worked in the PI Laboratory before joining PI EXPERTS in 2011, where he was a project manager, involved in planning, expertise and outdoor measurements. Since 2014 the PI Experts are fully included into the PI Berlin PV System division.

Lars Podlowski is a technical executive in the solar industry. Since 1996 he has been working in PV module technology and manufacturing, and currently leads the R&D division at PI Berlin. Most of his career he spent at the former German PV pioneer SOLON where he served as CTO for 10 years. Prior to joining PI Berlin earlier this year Lars worked at First Solar, leading its high-efficiency c-Si module R&D team until First Solar closed the entire "Tetrasun" business unit in 2016. He holds a PhD in semiconductor physics from the Technical University Berlin.

Enquiries

Address: Wrangelstr. 100, 10997 Berlin, Germany
Phone: +49 30 814 52 64 111
E-mail: weber@pi-berlin.com; xuereb@pi-berlin.com, podlowski@pi-berlin.com

News

## JinkoSolar poised to hit 10GW annual shipment target, but what next?

When JinkoSolar released its Q3 results and guided full year 2017 module shipment figures, the company remained on track to overachieve on final quarter shipments, thereby becoming the first ever PV supplier to ship more than 10GW of modules in a calendar year.

If this landmark figure is reached, JinkoSolar will effectively have 10% market share, and it will have achieved one of the key goals set internally 12 months ago.

In the past four years, the company has moved from having 5% market-share in 2013 (with module shipments less than 2GW), to 2017 where 10% and 10GW has been the goal for its global sales team.

In February 2017, it was generally understood that JinkoSolar had set an internal goal for its sales team closer to 11GW, providing the first indication that hitting 10GW was seen as the real target, and one that would yield significant marketing kudos during 2018 and beyond.

Four issues prevail in dissecting JinkoSolar's rise from a 1-2GW module supplier to a 10GW player in 2017: Flexibility in cell and module supply to meet market-growth opportunities; Having a competitive module product offering at any given time; Maintaining gross margins in the 10-20% range; Having a global sales operations capable of winning opportunities in all key end-markets.

Credit: PV Tech
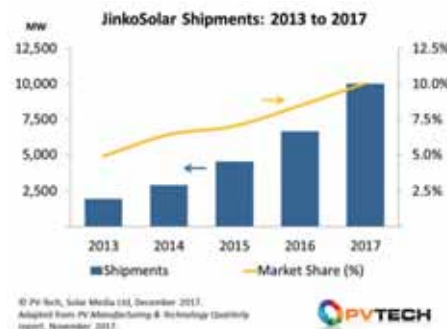
JinkoSolar is on track to surpass 10GW of shipments in 2017.

SHIPMENTS

JA Solar on track to increase module shipments by almost 50% in 2017

'Silicon Module Super League' (SMSL) member JA Solar reported cautious in-line financial results for the third quarter of 2017 but guidance for the fourth quarter indicates the company could increase module shipments by almost 50%, compared to the previous year.

The company has remained cautious about its business outlook all year, despite module shipments of 2,147.5MW in the second quarter of 2017. Although the record second quarter is not expected to be repeated again this year, third quarter module shipments of 1,582.5MW and fourth quarter shipment estimates of over 1,700MW underline significant shipment expectations of over 6,800MW in 2017, approximately a 48% increase over the previous year.

Importantly, based on JA Solar's capacity expansion plans in 2016 and 2017, shipments have remained in line with those expansions as the company ends 2017 with a nameplate capacity of around 7,000MW, highlighting very high utilisation rates despite the capacity increases.

Canadian Solar plans to reach over 10GW of module production in 2018

Canadian Solar reported stronger third quarter financial results than expected and increased full-year shipment and capacity expansion guidance, while guiding fourth quarter revenue in the record range of US$1.77 billion to US$1.81 billion.

Canadian Solar has now made four revisions to capacity expansion plans for 2017.

It completed the ramp up of a new multicrystalline silicon ingot casting workshop at Baotou, China, at the end of the third quarter of 2017, with a total annual capacity of 1,100MW, which included capacity relocated from its plant in Luoyang, China.

The company expects that its total worldwide module capacity would exceed 8,110MW by the end of 2017.

Subject to market conditions again, the company said it planned to add another 1,250MW of module capacity by the end of 2018, bringing nameplate capacity to 10.3GW.

Hanwha Q CELLS keeps on track to exceed 5.5GW of module shipments in 2017

'Silicon Module Super League' (SMSL) member Hanwha Q CELLS reported another in-line quarter and reiterated expectations of shipping 5.5GW to 5.7GW of modules in 2017.

Hanwha Q CELLS expects to ship 5.5-5.7GW of modules in 2017.

Credit: Hanwha QCELLS
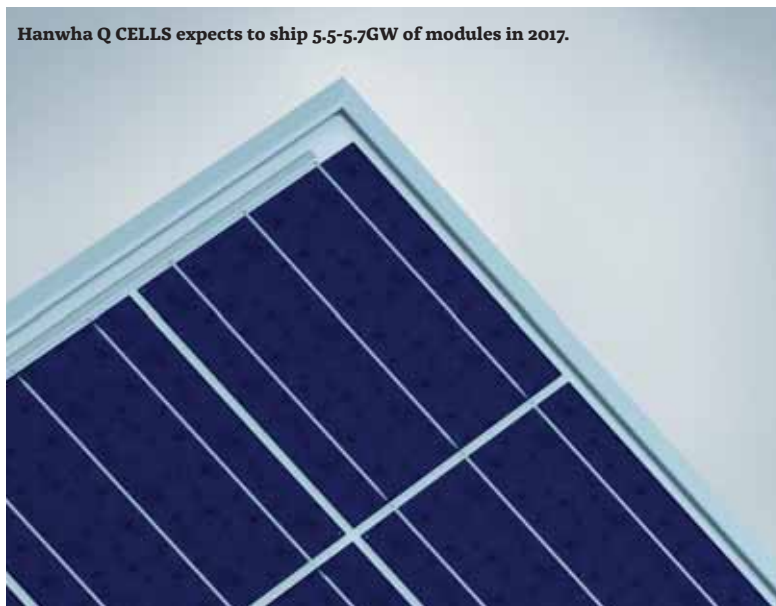
Having had margins impacted by module average selling price (ASP) declines in previous quarters, Hanwha Q CELLS noted higher wafer ASP's impacted margins in the third quarter of 2017.

Demand has remained strong and prices have continued to increase, despite polysilicon capacity increases.

The firm expected fourth quarter revenue in the range of US$610 million to US$630 million, indicating a stronger finish to the year with it highest quarterly revenue in 2017.

It also expected module shipments to be in the range of 5,500MW to 5,700MW. Shipment guidance has not changed all year. The company is not expected to gain market share against JinkoSolar, Trina Solar, Canadian Solar and JA Solar in 2017.

GET to focus on expanding solar module sales in emerging markets

Taiwan-based multicrystalline wafer producer Green Energy Technology (GET) is targeting solar module sales in emerging markets to boost revenue and return to profitability.

The strategic shift was outlined in reporting October 2017 wafer sales, which have gradually recovered since June. GET has launched its VPC certified light-weight module, which uses in-house produced wafers. The company has also secured its first module orders.

The lightweight modules are designed for a range of applications including floating solar. The modules are made by Gintung, a JV with solar cell producer Gintech.

GET reported sales for October 2017 of NT$ 1,191 million (US$39.4 million), up 4.7% from the previous month when revenue reached NT$1,137 million (US$37.6 million).

NEXT-GEN TECHNOLOGIES

Jolywood setting stage to more than double annual sales as IBC modules ramp

PV module materials and integrated n-type mono IBC (Interdigitated Back Contact) bifacial module manufacturer Jolywood (Suzhou) Sunwatt Co is expected easily to double annual revenue in 2017 after recently posting record third quarter sales.

Jolywood has been benefiting from the significant increase in PV module manufacturing capacity expansions since 2014 and growth in end-market demand in China and South East Asia.

However, significant growth in 2016 has been due to module backsheet material sales on the back of a 43% (53GW) increase in module output in China in 2017.

Jolywood is also starting to benefit from shipments of its high-performance IBC modules as the company started ramping its 2.1GW cell and module plant since the middle of the year.

In June 2017, the company secured an 800MW module purchase agreement to supply 315W n-type bifacial mono modules to COSCO Shipping Logistic with a winning bid valued at around RMB 2 billion.

MONDRAGON
ASSEMBLY

Risen Energy supplying multicrystalline half-cut cell modules to 'Top Runner' projects

China-based PV module manufacturer Risen Energy said that its latest module technology using multicrystalline half-cut cells with peak power output of 340-345W (72-cell), have achieved 'Top Runner' first-class certification by the China Quality Certification Centre (CQC) and shipments to projects have started.

The Top Runner certification meant Risen's new module had received high approval by a third-party certification agency with a national authority and that the level of the company's R&D had met the strict standards of the Top Runner certificate.

Risen's technical team had managed to add more length to the body of the module while keeping the same width, when using the half-cut cells.

The company said that the first batch of half-cut cell PV modules have been shipped to the Shanxi Yangquan PV Top Runner project. Risen is planning a high-volume of half-cut cell modules.

Mono-based PERC modules to drive bifacial market entry in 2018

The industry has shifted rapidly from a p-multi based market a couple of years ago, to one where mono PERC-based bifacial modules could become a mainstream product offering exiting 2018.

Mono-based solar modules are the route to higher efficiencies and panel power ratings, whether on n-type or p-type wafer substrates.

The industry is now moving into a period of mono-based PERC becoming more widely used in utility-based solar, a segment that has until now been largely dominated by 60 and 72-cell based p-type multi panels. Supply channels from China to India, and Vietnam to the US, have characterized the solar industry during 2016 and 2017.

Looking one step further than mono PERC (which is still largely a 2018-2019 mainstream entrance phenomenon), the speed at which glass/glass modules and bifaciality is moving with the major c-Si suppliers now suggests that almost all technology market forecasts will need to be adjusted very quickly.

Black & Veatch and RETC to establish bifacial solar module rankings

US-headquartered engineering and consultancy firm Black & Veatch along with engineering services, and certification testing lab, Renewable Energy Test Centre (RETC), will establish the first of its kind bifacial solar module ranking service.

The interest in bifacial technology has risen dramatically in a very short time as cell efficiencies have increased and costs have fallen.

Cherif Kedir, executive vice president of RETC said: "Bifacial modules are no longer a niche product. We are seeing increased interest from developers and project stakeholders in bifacial technologies and many module manufacturers are noticing. Advanced testing and results assessment customized for bifacial modules is critically needed to assess long-term bifacial module performance. The Black & Veatch-RETC bifacial module ranking will fill this gap."

The bifacial module ranking is designed to improve the understanding of current and upcoming commercial bifacial modules as a guide for developers, lenders and investors to generate quality-based finance and procurement strategies to ensure long-term project viability.

DISPOSAL

Japan issues guidelines on 'proper disposal' of used solar modules

The Japan Photovoltaic Energy Association (JPEA) has published voluntary guidelines on how to properly dispose of end-of-life solar PV modules. Installations of solar have risen sharply in Japan since 2012, and the country has regularly appeared in the top three markets worldwide for deployment. However, there has been a slowdown of late as the market started to focus on smaller-scale and rooftop systems. Due to the large amount of end-of-life modules expected in coming years, the association decided it is important to study in advance how to "smoothly" handle disposal of these PV materials.

Indeed, the National Institute of Advanced Industrial Science and Technology (NEDO) is already developing recycling technology.

Many local governments, waste disposers and industrial waste disposal companies are calling for more information on how to properly dispose of PV modules.

Manufacturers, importers, and distributors of PV modules have also been called on provide information on contained chemical substances in advance, to inform waste disposal companies such as removal contractors.

Japan has introduced voluntary PV module disposal guidelines

Credit: Flickr/Jeremy Levine

From bifacial PV cells to bifacial PV power plants – the chain of characterization and performance prediction

Christian Reise, Michael Rauer, Max Mittag & Alexandra Schmid, Fraunhofer Institute for Solar Energy Systems ISE, Freiburg, Germany

Abstract

Bifacial PV technology raises new challenges for the characterization and modelling of solar cells and modules, as well as for the yield predictions of power plants, as the contribution of the rear side can significantly affect the performance of these types of device. Reliable measurements and simulations are essential for gaining the trust of investors in this new and powerfully emerging technology. This paper covers the entire field of bifacial device characterization, from the additional demands on the measurement of bifacial solar cells and modules, through the modelling of cell-to-module losses, to the simulation of bifacial gains at the system level. An overview of different measurement set-ups and procedures for bifacial solar cells and modules is given, and the way in which the major influences can be controlled in order to achieve highly precise measurements is explained. With regard to yield predictions, the paper discusses how the existing models need to be extended to consider the additional site- and mounting-related factors that influence the available rear irradiance. It is shown that a combination of raytracing and electrical modelling allows accurate yield predictions of bifacial PV systems. The advanced tools presented in this paper for modelling cell-to-module losses and yield prediction outline the possibility for optimizing module and system design, and thus for increasing expected gains.

Introduction

Bifacial PV technology is currently seeing a remarkable boom, in both publications and advertisements as well as in real installation figures; this is no wonder, as fairly small changes to solar cell and module technology can lead to potential improvements of 5% or 10% in system output – a huge step compared with other evolutions in PV technology. The shift from monofacial modules to bifacial concepts, however, requires changes in materials, processes and set-ups. Simply replacing the solar cells would miss the point: the components, production and use of modules also need to change in order to successfully account for bifacial properties. The common module set-up using white backsheets, large junction boxes and module labels on the rear needs to be adapted. Component and material manufacturers have

reacted by making available edge connectors, thin glasses or transparent foils. The changeover from monofacial modules to bifacial ones in terms of module manufacturing is already under way but still a long way off. What industry and customers lack are not manufacturing solutions, equipment or components, but rather the results of brainwork: regulations, characterization processes and scientific models. How should the module power be stated on the label, and how can the additional gain of a bifacial module be determined? How is this gain to be measured and how can laboratory results be transferred to outdoor performance?

The industrial realization of bifacial module concepts has certainly outpaced existing characterization standards, but any gaps will soon be closed with the updated IEC 60904 standards. Unfortunately, there are some other remaining issues to be addressed, and the future optimization of bifacial modules and systems will be even more difficult than the optimization of monofacial modules. Scientists and R&D specialists are facing new challenges resulting from the second active side of the solar cell.

Realistic yield predictions of bifacial PV systems require precise device characterizations, a profound understanding of cell, module and system behaviour, and numerical models in order to include this knowledge in reliable projections. This paper covers the full characterization and modelling chain, beginning with the determination of PV cell properties via PV module power prediction and PV module characterization, and concluding with the prediction of bifacial gains in PV systems.

Accurate measurement of bifacial solar cells

The need for bifacial measurements is rather new, at both the cell and the module levels. A number of issues will be discussed at the cell level first; some of these issues will also show up again later at the module level.

The precise measurement of the illuminated current–voltage (I–V) characteristics is of central importance for solar cell and module

"The precise measurement of the illuminated current–voltage (I–V) characteristics is of central importance for solar cell and module manufacturers."

manufacturers. While the procedure for the measurement of conventional monofacial solar devices is well defined in the standards [1], discussions regarding the measurement of bifacial devices are still ongoing. Comprehensive overviews of measurement procedures under discussion have been recently reported [2–5]. These procedures are based either on both-side illumination of the device or on just front-side illumination with increased irradiance. The applicability of the procedures depends on cost, throughput and accuracy requirements, and can be different in laboratory and production line environments.

Measurements with double-sided illumination
One measurement procedure – which is very close to operational conditions of the bifacial device – is based on illuminating the device with an irradiance of 1,000W/m^2 from the front, and a reduced irradiance in the range of 0 to over 200W/m^2 from the rear. The measurement of the *I–V* characteristics is performed for at least three different rear irradiances, and the measured power of the bifacial device is then interpolated to rear irradiances of 100 and 200W/m^2. In addition to the front and rear *I–V* parameters at standard test conditions (STC), these power values will also be given in the measurement report [2–5].

There are different possibilities for realizing double-sided illumination of bifacial solar cells. One option is the application of an additional light source for the rear illumination. It has been shown that the front and rear light sources can be synchronized successfully for flash applications [6]. The interaction of front and rear illumination by light transmission from one side to the other side is not critical [7].

As an alternative to set-ups with two different light sources, facilities with one light source and mirrors are in use [8–10]. Two mirrors are thereby employed to deflect the light of one solar simulator to the front and the rear of the bifacial device, which is mounted in parallel to the direction of the light source. Such a two-mirror set-up is used at Fraunhofer ISE CalLab PV Cells for the precise measurement and characterization of bifacial solar cells (see Fig. 1). It has the advantage that it can be used as a replaceable module in an established offline flasher set-up.

A temperature regulation unit and an isolating enclosure are used for the two-mirror set-up in order to stabilize the temperature of the solar cell to 25±0.5°C. The uniformity of the front and rear irradiances in the solar cell plane was measured to be better than classification A [11]. The crosstalk caused by light passing from one side to the other was minimized to below the detection limit by installing non-reflective, moveable apertures, which can be moved very close to the edges of the solar cell on all sides. A class A spectrum of the front and rear illumination was ensured by adapting the

spectral filters in front of the flash lamp. Seven grating filters with transmittances in the range 10 to 40% are additionally available to reduce the irradiance onto the rear side of the solar cell in a spectrally neutral way [12]. In this way, a class A spectrum is maintained for irradiances below 1,000W/m^2 as well.

Up to now, it has not been clear which spectral distribution should be used for the rear illumination in measurements. When a bifacial device is operating in the field, the light reaching the rear side of the device is often not from direct sunlight, but from light which is reflected off the ground beneath the device. Since the ground reflectance can exhibit a significant spectral dependence, the spectral distribution of the rear illumination can differ significantly from the standard AM1.5g spectrum, which represents direct sunlight and is used for the illumination of the front side.

With a two-mirror set-up, both the standard spectrum and various spectral distributions can be implemented: spectrally neutral grating filters can be used for maintaining the standard spectrum, while other spectral distributions can be generated either by placing filters with distinct spectral dependence into the rear light path, or by replacing the rear mirror with reflectors having a defined reflectance.

To improve the measurement accuracy, it is important to consider the different front and rear spectral responsivities of the bifacial solar cell. This means that there are two different spectral mismatches for the front and rear sides, which is particularly critical if the front and rear spectral distributions differ. Further measurement errors can result from differences in the shading of the solar cell by the front and rear contact bars; this effect needs to be quantified and taken into account.

In conclusion, the two-mirror set-up developed at CalLab PV Cells fulfils the highest quality criteria (better than AAA classification) and enables the precise measurement of bifacial solar cells with double-sided illumination.

Measurements with single-sided illumination
The measurement procedure based on single-sided measurements has the advantage of requiring only minor changes to the available equipment. This procedure is also known as the *equivalent irradiance (G$_E$) method* [2–5]. An important point of this method – which needs special care – is the consideration of the additional current or power that would be generated by illumination of the rear side; therefore, in addition to measurements of front and rear *I–V* characteristics at STC under single-sided illumination, further front-side measurements at higher irradiances are performed. The bifaciality coefficients φ are calculated from the front and rear STC *I–V* parameters to quantify the differences in front and rear characteristics of the bifacial device. The rear irradiance is then weighted with

these coefficients to determine the additional front irradiance that is required in order to yield similar conditions with front-side illumination only. At least three different hypothetical rear irradiances are measured, and the results interpolated to rear irradiances of 100 and 200W/m^2.

In practice, conventional set-ups can still be used for the application of the G_E method with single-sided illumination; however, as these measurements are performed at irradiances of up to 1,200W/m^2, the set-ups may need to be upgraded. Several equipment manufacturers have adapted their solar simulators to meet these requirements [2,13–16]. A potential issue for industrial inline measurements with high throughput could be the determination of front and rear $I–V$ parameters at STC, which are needed for the calculation of the bifaciality coefficients of each cell. This requires either the solar cells to be flipped in between the measurements, or the use of a second solar simulator. A possible back-door solution could be to use the bifaciality φ of reference solar cells [3,5]; the applicability of this approach, however, needs to be carefully evaluated [6,7].

At CalLab PV Cells, the established and well-characterized steady-state solar simulator, which is customarily used for the calibrated measurement of conventional solar cells, is also used for measuring bifacial solar cells with single-sided illumination. A variety of measurement chucks with different reflectances and conductances are available for the mounting of the bifacial solar cells [17]. The simulator is operated at an increased lamp power to enable measurements to be taken at elevated irradiances.

Increasing the accuracy of measurements with single-sided illumination

Several correction procedures, such as the consideration of non-uniformity of irradiance or spectral mismatch correction, can be carried over from conventional measurements. However, there are also measurement uncertainties specific to bifacial solar cells; these need to be investigated carefully, and correction procedures need to be elaborated.

For the precise measurement of the fill factor of bifacial solar cells, it is important to consider the influence of the rear-contacting scheme [18]. Whereas conductive measurement chucks electrically contact the entire rear grid of the solar cells (busbars and fingers), non-conductive chucks contact only the busbars. Thus, differences in fill factor between the two measurement chucks occur: the higher the resistance of the metal fingers, the

larger the difference [18]. Although this effect also arises for conventional monofacial solar cells, it is much more pronounced for bifacial solar cells. By measuring the finger resistance, this effect can be quantified and taken into account.

It is furthermore important to ensure 'true' single-sided measurements. This means that unwanted contributions to the measured current by the current generated from the side that is actually non-illuminated needs to be minimized [2–4]. In the case of bifacial solar cells mounted on a measurement chuck, the most critical contribution comes from light that is transmitted through the solar cell, reflected at the measurement chuck and re-entering the solar cell through its rear side. This contribution of current is directly proportional to the long-wavelength reflectance of the measurement chuck [17], which enables the determination of the 'true' single-sided short-circuit current [3,5]: by measuring the short-circuit current of the bifacial solar cell with chucks of different reflectances, the current can be extrapolated to zero reflectance.

A large set of bifacial solar cells of different technologies has been measured at CalLab PV Cells on two chucks with very different long-wavelength reflectances. The correction procedure mentioned above was carried out to determine the respective extrapolated currents for each solar cell. Fig. 2 shows the relative deviations from these extrapolated currents for the entire set of solar cells.

From a calibration laboratory point of view, deviations exceeding 0.1% are relevant for I–V measurements. At CalLab PV Cells, a non-reflective chuck with a long-wavelength reflectance of 4% is therefore used to reduce the contribution of transmitted light to values below 0.1%$_{rel.}$. For solar cell sorting environments, higher deviations can possibly be tolerated. To keep deviations below 0.3%$_{rel.}$ for the solar cells investigated in this study, chucks with long-wavelength reflectances below 17% need to be used (see Fig. 2). By carefully adapting the chuck to the necessary measurement accuracy, the contribution by the non-illuminated side can thus be minimized.

In conclusion, for the precise measurements of novel solar cell types, such as bifacial solar cells, special care must be taken to avoid systematic measurements errors. Detailed and comprehensive investigations are necessary in order to develop sound measurement procedures and set-ups. Both approaches currently under discussion for the measurement of bifacial solar cells – measurements with single-sided illumination using the G_E method and measurements with bifacial illumination – can be performed at ISE CalLab PV Cells with high accuracy.

From bifacial cell to module efficiency

The cell-to-module (CTM) power ratio describes the ratio of the module power after module integration of the solar cells, to the sum of the power of the individual solar cells before integration. Optical and electrical gains and losses contribute to the CTM ratio [19,21]. This parameter is useful for assessing the losses caused by the integration of solar cells into modules. While the overall CTM ratio may be derived from a comparison of cell and module measurements, the roles of components and materials, as well as of new module concepts, can already be analysed and optimized with regard to power losses and efficiency in advance [22,24]. Of course, precise bifacial cell measurements as described above are a prerequisite for the successful completion of this task.

Introducing bifacial cells into PV modules means that existing models for CTM efficiency analysis or yield prediction [19] are no longer sufficient because of additional optical effects within the PV module, such as additional relevant internal reflections [20]. Conventional modules profit from backsheet reflection (Fig. 3, black) – i.e. light irradiating from the module front that reaches the cell front after internal reflections within the module. Bifacial modules feature three additional gains (Fig. 3, red), which also increase complexity in modelling [25]. In addition, gains resulting from a partial transparency and internal reflection occur in bifacial modules [25,26].

The power of bifacial cells naturally increases with additional irradiance from albedo reflection, but research also indicates that bifacial cells additionally profit from higher gains and internal reflection, as highlighted in Fig. 4 [25].

The additional light passing into the module and reaching the solar cell affects not only the optical CTM factors but also the electrical ones. The module current increases, and higher ohmic losses are a consequence. Alternatively, components (i.e. the cell interconnector ribbons) need to be adapted or new module topologies may be considered. Instead of serial cell-and-string interconnection,

Figure 1. Front-view image of the two-mirror set-up employed at ISE CalLab for measuring bifacial solar cells with double-sided illumination.
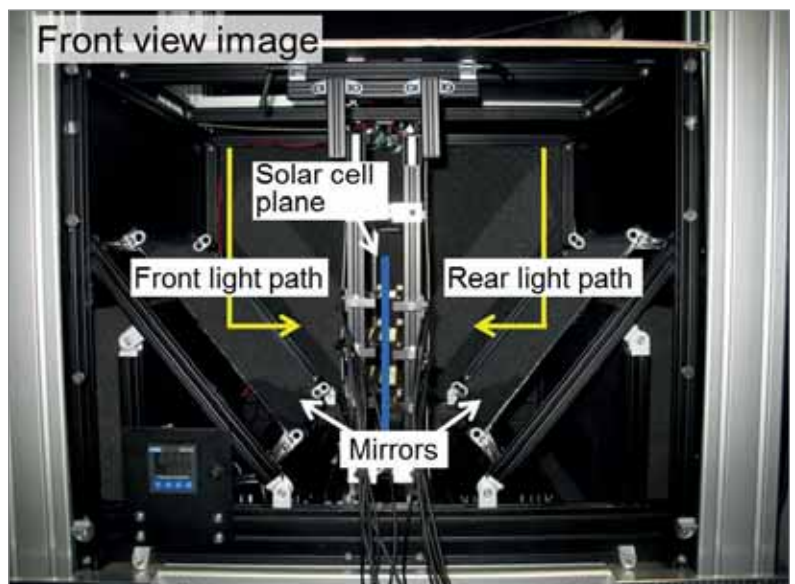
"The characterization of complete bifacial PV modules is a must for any product entering the PV market."

parallel circuits or networks might be used. In addition, a shifting of concepts away from ribbon-based interconnection of squared cells towards round-wire interconnection, half cells or shingling with bifacial cells will impact all types of CTM losses [27,28]. The possibilities are numerous, but the evaluation of all the concepts is difficult.

The different CTM factors influence each other and render the optimization of modules and components a non-trivial task. A holistic and flexible approach is necessary, and new models are required in order to successfully optimize bifacial modules. Fraunhofer ISE presented such an approach [19,22], and is currently extending and implementing models for bifacial solar cells into 'SmartCalc.CTM' – a software package to support CTM analyses and module optimization [22,29]. This tool allows virtual prototyping as well as supporting iterative development processes for several different module, cell and interconnection concepts. Adding the possibility to also optimize bifacial cells now supports the PV industry and allows the optimization of bifacial modules, given the increasing market share of bifacial cells.

Accurate measurement of bifacial PV modules

Following cell characterization and module design optimization, the characterization of complete bifacial PV modules is a must for any product

Figure 2. Relative deviation from 'true' single-sided short-circuit current resulting from light that is transmitted through the solar cell, reflected at the measurement chuck and re-entering the solar cell through its rear side. A large set of bifacial solar cells was measured on measurement chucks with different reflectances for this purpose.
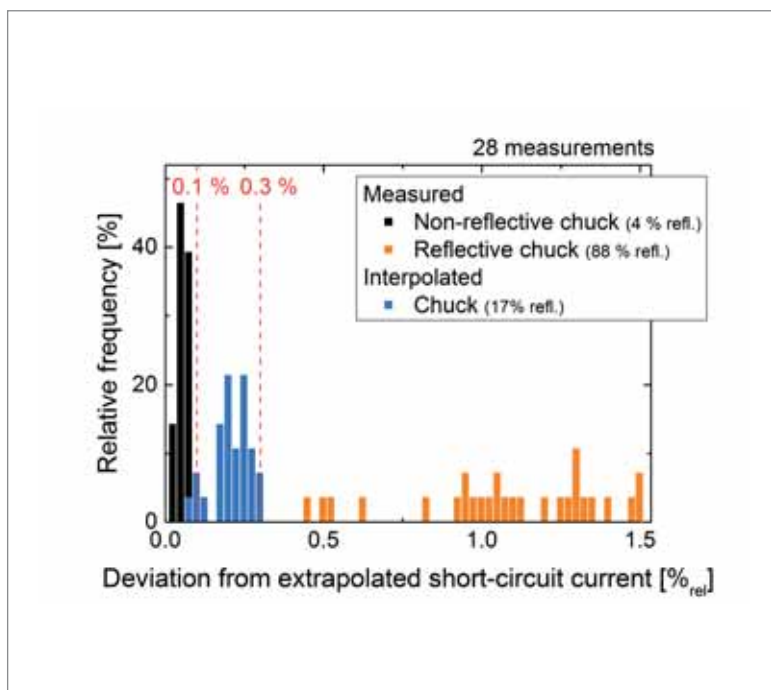
entering the PV market. Here, similar challenges to those associated with cell measurements discussed above will be encountered, and, accordingly, various methods are currently under discussion for this very purpose.

Since the existing standards for the I–V measurement of PV devices neither consider gains arising from rear irradiation, nor define the measurement conditions for the rear side of the module, it is often not clear how the nominal power of a particular commercial module is determined. The labelled values often refer to front-side measurement under STC, while the irradiance condition on the rear side is not specified. Depending on whether the rear side was covered or open to incident stray light, or measured with a proprietary (i.e. non-standardized) reflector behind the module, the resulting measured power can vary by several per cent. Many datasheets state values for the boost in bifacial power: these are mostly extrapolated from front-side STC values, assuming a linear power boost, or they are determined by more advanced calculations. Values for rear-side efficiency or bifaciality are usually not mentioned, despite this information being needed to estimate bifacial gains for the specific installation conditions. In any case, the comparability and meaningfulness of datasheet values is not very satisfactory.

Set-ups for double-sided illumination

The easiest way to obtain additional rear irradiance in the I–V measurement of bifacial modules is to place a reflective material behind the module. The light transmitted through the module and stray light incident on the reflector will be reflected onto the rear side of the module. The resulting quality of the rear irradiance is highly dependent on the material properties of the reflector (specularity and spectral distribution) and the distance between module and reflector, as well as on the module transmission. With this method, the achievable light intensity and homogeneity is limited and influenced by the module under test.

An alternative method is to place a second light source behind the module; this way, the rear intensity is tuneable independently of front-side intensity, and the light quality can be well defined. Homogeneity and spectral match are only determined by the light source and are not influenced by module properties. Some companies are already offering sun simulators with double-sided illumination. With the exception of table flashers, sun simulators for modules typically have a very large footprint: the fact that for this kind of set-up the footprint is doubled for bifacial illumination, along with the additional costs, might discourage module manufacturers from upgrading their sun simulators.

Another option for creating a defined rear irradiance is to split up the light from the sun simulator and direct it simultaneously onto both
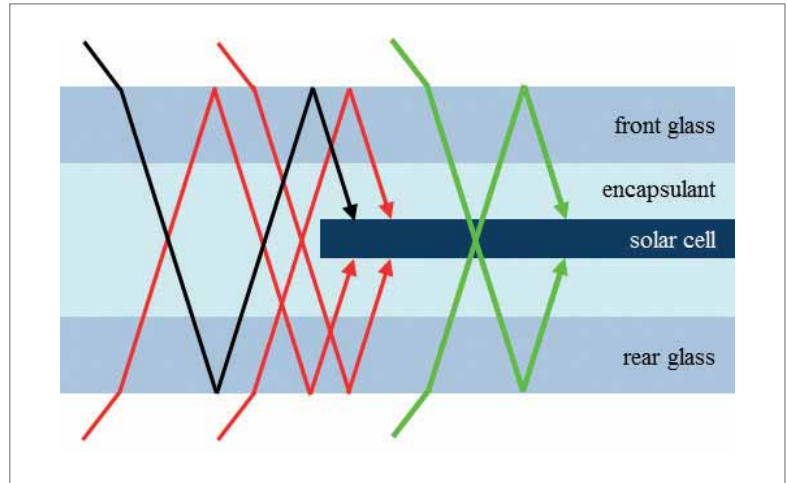
sides of the module by using mirrors. A schematic of this set-up is shown in Fig. 5.

At CalLab PV Modules, a mirror set-up has been developed, enabling bifacial illumination of full-size modules of up to 1m × 2m, with an irradiation quality of better than AAA. Two mirrors at a 45° angle to the lamp direct the light of the solar simulator simultaneously onto both sides of the module, as described above for bifacial PV cells. The mirrors are constructed from a silver-coated reflector sheet, with a reflectance of over 95% in the wavelength range from 300 to 1,200nm, so that the reflected spectrum remains of A+ quality. The reflector sheets are attached to glass panes in order to achieve a smooth surface for maintaining homogeneity of irradiance. The lamp power can be adjusted between 100 and 1,000W/m^2, and by inserting attenuation filters the rear intensity can be reduced. The attenuation filters used for this work are made of woven wire mesh, a material which demonstrates spectrally neutral transmission and good spatial homogeneity on large areas, as reported in Santamaria et al. [12]. The currently available transmissions are 20, 35 and 55%. With this variable light intensity and variable front-to-rear intensity, typical irradiation conditions for different installation geometries (e.g. south, east–west) can be simulated.

At the moment, most module producers and labs only have the possibility of taking measurements under single-sided irradiance. It has not so far been proved that measurements under single-sided and bifacial irradiance produce the same results, and so these approaches will be compared, on the basis of measurements of different commercial bifacial modules, in the following sections.

I–V measurement under single-sided illumination

For a basic characterization of bifacial modules, it is necessary to measure each side separately at STC, with the other side being protected from incident stray light. For all single-sided measurements in this work, the rear side of the module was covered by a black curtain. The spectrally weighted reflection of the material is 4.3% and is fairly constant over the relevant wavelength range between 300 and 1,200nm. Along the long edges of the module, a mask prevents light from passing by the module, so that the incident light on the rear cover is limited solely to the light transmitted through the module and to that passing by the short edges of the module. In this way the electrical module parameters of each side are determined with maximum precision. With these results, the bifaciality φ of current and power, which is defined as the ratio of the rear-side value to the front-side value, can be calculated. The single-sided STC parameters are also the basis for yield simulations of bifacial PV systems [30].

Figure 3. Schematic of cover reflection gains in modules with bifacial cells and transparent rear cover.

Single-sided vs. bifacial measurement

When comparing the front-side measurement under elevated irradiance (the G_E method) with the measurement under real bifacial irradiance, the question is: to what extent does the light-incident side influence the results? As shown in Schmid et al. [31], the role of the light-incident side for short-circuit current I_{sc} and open-circuit voltage V_{oc} can be described by the bifaciality φ for I_{sc}, while the fill factor FF is determined by different influences.

In the comparison of single-sided and bifacial measurements of commercial modules, it is important to also consider the shape of the $I–V$ curves. Most bifacial modules have distorted rear $I–V$ curves, as a result of partial shading by the junction box, cabling, frame or label, or because of cell sorting according to front-side current only. An example of typical $I–V$ curves is shown in Fig. 6. Since in the G_E method a module $I–V$ curve is measured only under elevated front irradiance, the distortion of the rear $I–V$ curve will not be detected, as can be observed in Fig. 6. While the $I–V$ curve of the G_E measurement is as smooth as that of the front-side STC measurement, the $I–V$ curve for the bifacial measurement is affected by the partial shading of the rear side of the module. Depending on the rear intensity and the severity of the distortion, this can lead to a deviation between measured power and FF for G_E and bifacial measurements.

Fig. 7 shows measured FFs for different illumination conditions for a typical module. FF_{FRONT} and FF_{REAR} refer to single-sided irradiance in 100W/m^2 steps between 100 and 1,000W/m^2. FF_{BIFA} refers to symmetrical irradiance for the front and rear sides. Additionally, the FFs for the G_E and the bifacial measurement, corresponding to 1,000W/m^2 front and 200W/m^2 rear intensities, are shown. The x axis is scaled to I_{sc} instead of irradiance, in order to enable a comparison to be made of the FF at the same current level.

In the case of measurements under single-sided illumination on the front and rear sides, a higher FF for the rear-side illumination was found. This higher FF is not just related to the fact that the lower rear
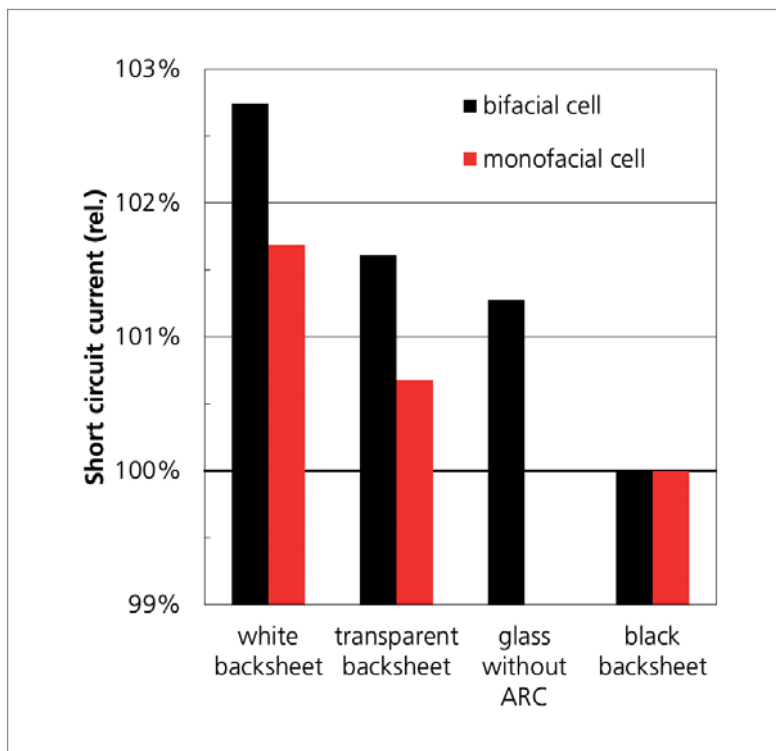
Figure 4. Short-circuit current gain of monofacial and bifacial solar cells (different manufacturers) in four-cell modules with different rear-cover materials and 2mm cell spacing. (Front-side irradiance only, mask used, normalized to I_{sc} measured with a black backsheet.)
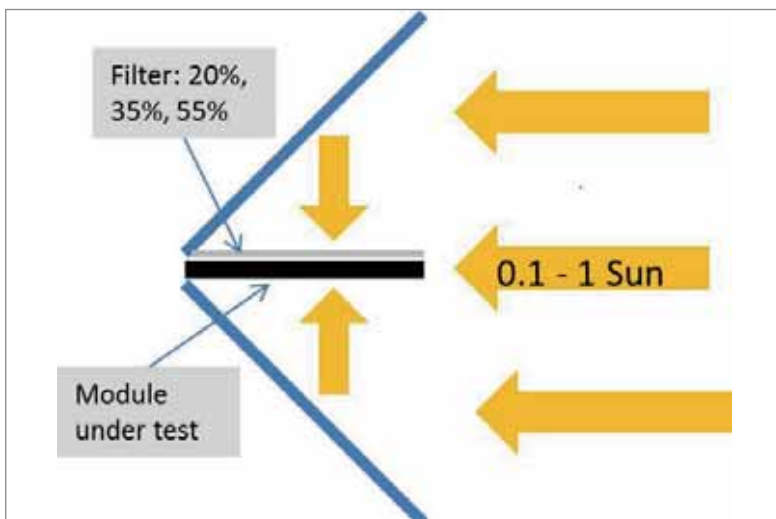

Figure 5. Schematic of a possible bifacial measurement set-up: two mirrors at a 45° angle to the lamp simultaneously direct the light onto both sides of the module

current leads to a smaller series resistance loss. Even when comparing the front and rear fill factors for the same current level, as shown in the graph in Fig. 7, the rear fill factor is significantly higher. The mean difference in *FF* between front and rear illumination was found to be 0.3% for commercial modules at the same current level. This affects the *FF* in the bifacial measurement as opposed to the

"The well-known algorithms for the calculation of irradiance at the front side of a module are not adequate for bifacial applications."

reduction in *FF* due to partial shading mentioned earlier. As can be seen in the graph, the *FF* under bifacial irradiance is typically found to be higher than in the measurement under G_E.

The deviation of measured P_{MPP} was calculated for all bifacial modules measured with the bifacial set-up and with the G_E method. With irradiance conditions of 1,000W/m² on the front side and 200W/m² on the rear side, the mean deviation was 0.5%, ranging from a minimum deviation of 0.24% to a maximum of 0.9%. The difference is strongly influenced by the distortion of the rear *I–V* curve. As these effects can only be determined by true bifacial measurements, it is recommended not to count on G_E measurements alone when reliable results are needed.

Bifacial PV power plants
Finally, all the knowledge gathered about bifacial PV cells and modules is utilized when a bifacial PV power plant's performance is to be predicted or assessed. Again, there are some differences compared with the well-established procedures for monofacial PV systems.

The additional energy delivered by bifacial PV modules is commonly (but not accurately) called *bifacial gain (BG)*. Compared with solar cell development steps which just increase STC power per area, the yield gain produced by the rear-side contribution of bifacial PV modules is no longer a pure module property. The *BG* depends heavily on the amount and distribution of the irradiation reaching the rear module surface. Moreover, in contrast to the front side of the module, the availability of rear-surface irradiance depends on a greater number of system-related factors, such as:

· Mounting geometry (module height, module tilt angle, row-to-row distances)
· Ground albedo and its homogeneity
· Mounting structure (which also influences the homogeneity of rear-side irradiance)

As the amount of irradiation available to the rear side of a bifacial module is strongly influenced by system properties, the final bifacial gain too is essentially regarded as a system property. In a first step, the irradiance gain from the rear surface of the module may be expressed as optical bifacial gain:

$BG_{OPT} = G_{REAR} / G_{FRONT}$

Unfortunately, the rear side of a bifacial PV module is less efficient than the front side. Typical ratios of rear-side to front-side efficiency (called *bifaciality φ*) range from 60 to 95%. Consequently, the rear-side electricity production of any module will not be directly proportional to the optical gain, but will instead be reduced by the bifaciality factor, which leads to the bifacial gain of the module:

$BG_{MOD} = φ \, G_{REAR} / G_{FRONT}$

Finally, the additional electricity production may differ from BG_{MOD}, as the system response is not completely linear (especially if clipping effects from inverter or grid power limitations come into play). This final BG_{SYS} value may only be derived from two simulation runs – one with bifacial modules and one with monofacial modules with identical properties:

$$BG_{SYS} = E_{REAR} / E_{FRONT} = (E_{BIFA} - E_{MONO}) / E_{MONO}$$

These steps are detailed in the next two sections, while some typical results for BG will be given in a subsequent section.

Estimation of optical gain and module gain

The well-known algorithms for the calculation of irradiance at the front side of a module are not adequate for bifacial applications; Fraunhofer ISE has therefore developed appropriate methods and tools on the basis of 'Radiance', a backward raytracing software package. Radiance, developed at the Lawrence Berkeley Labs, USA, is a powerful lighting simulation software; it has been in use within the daylighting research and application community for several decades, and offers excellent flexibility in the description of surface properties and structural geometry. The Radiance calculation scheme uses absolute properties of radiance and irradiance in suitable physical units of W/m^2sr or W/m^2. Models of the natural sun and sky light sources are provided via the gendaylit tool, which creates a complete sky radiance distribution for any reasonable pair of global and diffuse horizontal irradiance parameters G_{HOR} and D_{HOR} given as input values. Radiance can both render images and provide numerical values of local irradiance as 'seen' by virtual irradiance sensors. A comparison with monitoring data from real bifacial PV plants ensures the accuracy of the simulation results. A model validation in particular was presented in Reise et al. [30].

Other approaches use the radiosity method, which is well known from computer graphics rendering. Based on a radiative energy balance between many neighbouring surface elements, this method is much faster than raytracing, although not as accurate, and requires a larger number of test cases for validation. Both the raytracing and radiosity methods may be used to calculate look-up tables, representing the relationship between BG and a small number of geometry parameters, such as tilt angle, row distance and height above ground.

In the case in question, a raytracing model considers all details of the PV module mounting geometry (module type, fixed or varying module tilt angle, row-to-row distance, components of the mounting structure). For a realistic estimation of bifacial gains, the calculations are typically carried out for a module in the centre of a large homogeneous generator section.

Using the raytracing tool, the calculation of the irradiation levels is performed for each time step of the meteorological input data and for both

sides (front and rear) of each of the 60 or 72 solar cells within a module. These individual irradiance values are then aggregated to front- and rear-side module irradiance values. From these values, the optical bifacial gain BG_{OPT} and the module bifacial gain BG_{MOD} may be calculated. At the same time, an effective irradiation on the module is known:

$$G_{EFF} = G_{FRONT} + \varphi \, G_{REAR}$$

Finally, G_{EFF} serves as the input to the calculation of PV power generation and all related losses using 'Zenit', Fraunhofer ISE's own modelling tool for PV power plants. In fact, using G_{EFF} here is quite similar to the G_E concept explained above for PV module characterization.

Estimation of system level gain

In this calculation, as in a standard yield estimation, both module-related and BOS-related losses are addressed. The most important losses are:
- Reflection losses due to non-normal incidence of irradiation.
- Efficiency losses (or gains) due to the deviation from STC.
- Conduction losses on both DC and AC (low and medium voltage) sides.
- Inverter losses (device efficiency and, if applicable, power limitations).
- Transformer losses (when feeding into the medium- or high-voltage grid).

System-level bifacial gains are then determined from two separate model runs, using time series of G_{FRONT} or G_{EFF} as input. This appears to be a somewhat incorrect comparison, as no-one would operate a bifacial module with a covered rear surface. However, from a modelling point of view, the output of a monofacial module is simply

Figure 6. I–V curves of a typical commercial module under front-side irradiance and under rear-side irradiance (STC conditions), compared with bifacial and G_E irradiance corresponding to a rear irradiance of 200W.
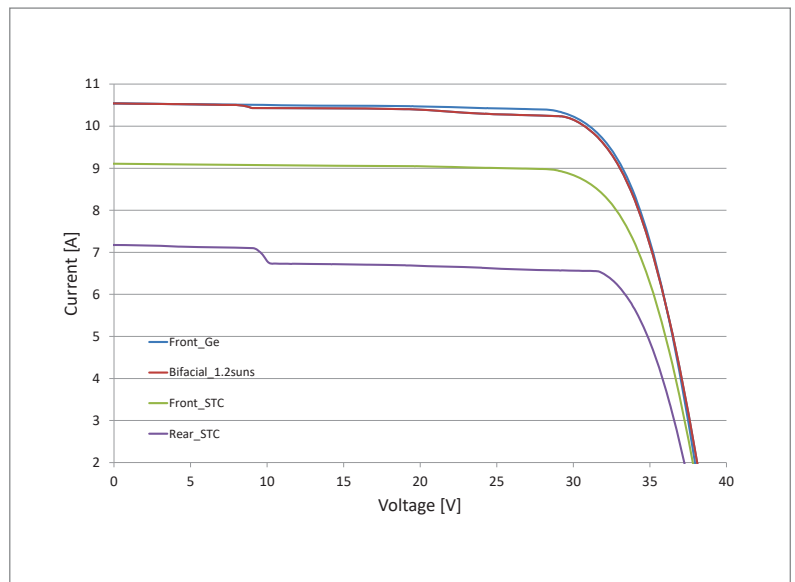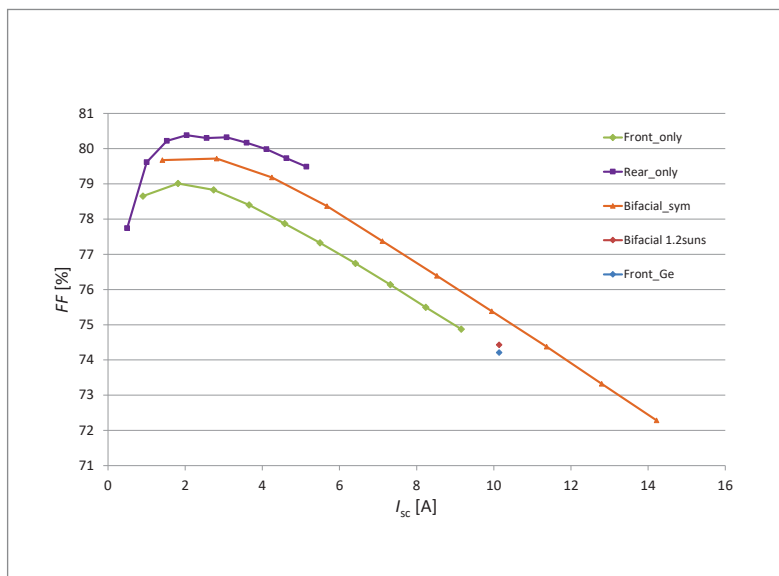
Figure 7. FFs measured for front-side, rear-side and bifacial irradiance, with respect to I_{sc}. Additionally the FFs for the G_E and bifacial measurements with 200W rear intensity are shown.

related to that of a bifacial one featuring the same front-side STC power. A number of important effects, such as increased module operating temperature, or the results of a more-or-less correct inverter sizing are clearly reproduced when applying the G_E or G_{EFF} method to a standard yield-prediction model.

Representative results

With commercial bifacial PV projects, the module mounting will probably follow, and somehow adapt, traditional installation schemes. However, when seeking optimized yields, some design contradictions may occur:

- For rooftop systems, increased module height (for higher rear-surface irradiance) will also increase wind loads, demanding more stable and expensive mounting structures.
- For many systems, increased row-to-row distance will increase not only optical gains, but also all costs related to the area requirements.
- Artificially increased albedo (for both ground-mounted and rooftop systems) will also increase maintenance (cleaning) efforts.

Since 2009, Fraunhofer ISE has been extending its yield-prediction service to bifacial PV systems. A number of studies have been prepared since then, covering single commercial projects as well as parameter studies for bifacial PV systems. Table 1 presents a number of representative results for BG_{MOD}, as extracted from a number of studies for sites in Central Europe.

Type	Height [m]	Tilt angle [°]	Albedo	GCR	BGMOD [%]	Notes
Ground mounted	0.7m	30	0.20	0.43	5	(1)
Ground mounted	1.0m	30	0.20	0.40	8	(2)
Ground mounted	0.5m	30	0.20	0.40	9	(3)
Ground mounted vertically	0.0m	90	0.20	0.00	9	(4)
Ground mounted vertically	0.0m	90	0.20	0.20	−17	(5)
Rooftop	0.1m	20	0.40	0.40	6	(6)
Rooftop	0.3m	20	0.40	0.40	11	(6)
Rooftop	0.3m	20	0.60	0.40	16	(6)

Notes: (1) three modules stacked in landscape mode; (2) one module in landscape mode, calculated w/o mounting structure; (3) two modules stacked in portrait mode; (4) single row, gain vs. 30° south monofacial; (5) multiple rows, gain vs. 30° south monofacial; (6) calculated w/o mounting structure.

Table 1. Predicted yield values for typical large-scale bifacial PV system configurations (GCR = ground cover ratio = module area/ground area).

Ground-mounted systems in a traditional geometric configuration on grass or similar natural surfaces deliver bifacial gains between 5 and 9%. The *BG* depends mainly on row-to-row distance, but also, less importantly, on mounting height. For dense PV systems, bifacial gains may at least compensate for the mutual shading that occurs between module rows.

Bifacial modules mounted vertically should yield module bifacial gains close to the bifaciality factor (*BF*), since both module surfaces receive the same amount of irradiation. However, from a commercial point of view, the output of vertical bifacial systems will be comparable to that of monofacial systems in a standard layout (e.g. 30° tilted towards the south). Single rows then demonstrate a gain of around 9%, while multiple rows lead to a loss of some 17% for a specific configuration.

Bifacial PV systems installed on flat roofs may yield gains in the range 6 to 16%. In contrast, here the *BG* depends primarily on the (typically low) mounting height, and, to a lesser extent, on the row-to-row distance. Rooftop systems have the option to substantially increase albedo and *BG* by using bright roofing membranes.

Conclusions

All in all, with larger commercial systems, realistic bifacial gains are expected to range from 5 to 15%. Ground-mounted systems on natural (non-desert) surfaces will probably stay below 10%, while rooftop systems offer the potential for higher gains through the use of highly reflecting roofing materials.

"With larger commercial systems, realistic bifacial gains are expected to range from 5 to 15%."

References
[1] IEC 60904-1:2006, "Photovoltaic devices – Part 1: Measurement of photovoltaic current-voltage characteristics".
[2] Fakhfouri, V. et al. 2016, "IEC 60904-1-2: Measurement of current-voltage characteristics of bifacial photovoltaic devices", Presentation, 3rd bifi PV Worksh., Miyazaki, Japan.
[3] Fakhfouri, V. et al. 2017, "IEC 60904-1-2: Measurement of current-voltage characteristics of bifacial photovoltaic devices", Presentation, 4th bifi PV Worksh., Constance, Germany.
[4] Kopecek, R. & Libal, J. 2017, "Complex problems require simple solutions: How to measure bifacial devices correctly?", *Photovoltaics International*, 37th edn, pp. 105–112.
[5] Fakhfouri, V. 2017, "IEC standard for power rating of bifacial PV devices", Special report bifacial technologies, standards and systems, *PV-Tech Power*, pp. 20–21.
[6] Ramspeck, K. et al. 2016, "Measurement concepts for bifacial PV-devices – What is really required?", Presentation, 3rd bifi PV Worksh., Miyazaki, Japan.
[7] Ramspeck, K. et al. 2017, "Measurement techniques for bifacial solar cells", Presentation, 4th bifi PV Worksh., Constance, Germany.
[8] Soria, B. et al. 2012, "Characterization of bifacial modules of different architectures", Presentation, 1st bifi PV Worksh., Constance, Germany.
[9] Edler, A. et al. 2012, "Flasher setup for bifacial measurements", Presentation, 1st bifi PV Worksh., Constance, Germany.
[10] Schmid, A. et al. 2016, "Characterization and testing of bifacial modules", *Proc. 32nd EU PVSEC*, Munich, Germany.
[11] IEC 60904-9:2007, "Photovoltaic devices – Part 9: Solar simulator performance requirements".
[12] Santamaria, A.A. et al. 2014, "Assessment of uncalibrated light attenuation filters constructed from industrial woven wire meshes for use in photovoltaic research", *Proc. 29th EU PVSEC*, Amsterdam, The Netherlands, p. 3214.
[13] h.a.l.m. electronics, "cetisPV-IUCT-2400" and "cetisPV-IUCT-Q", Tech. spec.
[14] [https://www.spiresolar.com/news/spire-solar-simulators-bifacial-ready/].
[15] [http://wavelabs.de/wp-content/uploads/Data_sheet_SINUS-220.pdf].

[16] [https://ecoprogetti.com/sun-simulator-for-solar-panel-testing-in-led-class-aaa/].

[17] Hohl-Ebinger, J. et al. 2010, "Bifacial solar cells in STC measurement", *Proc. 25th EU PVSEC*, Valencia, Spain, p. 1358.

[18] Rauer, M. et al. 2016, "Monofacial IV measurements of bifacial silicon solar cells in an inter-laboratory comparison", *Proc. 32nd EU PVSEC*, Munich, Germany.

[19] Haedrich, I. et al. 2014, "Unified methodology for determining CTM ratios: Systematic prediction of module power", *Sol. Energy Mater. Sol. Cells*, Vol. 131, pp.14–23.

[20] Guerrero-Lemus, R. et al. 2016, "Bifacial solar photovoltaics – A technology review", *Renew. Sustain. Energy Rev.*, Vol. 60.

[21] Wirth, H. et al. 2016, *Photovoltaic Modules: Technology and Reliability,* Berlin: De Gruyter.

[22] Mittag, M. et al. 2017, "Systematic PV module optimization with the cell-to-module (CTM) analysis software", *Photovoltaics International*, 36th edn.

[23] Mittag, M. et al. 2017, "Cell-to-module (CTM) analysis for photovoltaic modules with shingled solar cells", *Proc. 44th IEEE PVSC*, Washington DC, USA.

[24] Mittag, M. et al. 2017, "Electrical and thermal modeling of junction boxes", *Proc. 33rd EU PVSEC*, Amsterdam, The Netherlands.

[25] Mittag, M. et al. 2017, "Analysis of backsheet and rear cover reflection gains for bifacial solar cells", *Proc. 33rd EU PVSEC*, Amsterdam, The Netherlands.

[26] Singh, J. et al. 2015, "Comparison of glass/glass and glass/backsheet PV modules using bifacial silicon solar cells", *IEEE J. Photovolt.*, Vol. 5.

[27] Woehrle, N. et al. 2017, "Solar cell demand for bifacial and singulated-cell module architectures", *Photovoltaics International*, 36th edn.

[28] Klasen, N. et al. 2017, "Shingled cell interconnection: Aiming for a new generation of bifacial PV-modules", *Proc. 7th Worksh. Metalliz. Interconn. Cryst. Sil. Sol. Cells.*

[29] [http://www.cell-to-module.com].

[30] Reise, C. et al. 2015, "Realistic yield expectations for bifacial PV systems – An assessment of announced, predicted and observed benefits", *Proc. 31st EU PVSEC*, Hamburg, Germany.

[31] Schmid, A. et al. 2017, "IV measurement of bifacial modules: Bifacial vs. monofacial illumination", *Proc. 33rd EU PVSEC*, Amsterdam, The Netherlands.

....

About the authors

Christian Reise received a diploma and a Ph.D. in physics from the University of Oldenburg, Germany. He has been with Fraunhofer ISE in Freiburg since 1994, and has expertise in the fields of energy meteorology, energy-efficient buildings, numerical simulation, and PV system technology. He is currently working in the PV power plant group, concerned with the quality assurance of MW-scale PV systems.

Michael Rauer received his diploma degree in physics in 2009 from the Albert Ludwig University of Freiburg, and his Ph.D. in 2014 from the University of Constance, both in collaboration with Fraunhofer ISE. In 2015 he was awarded the SolarWorld Junior Einstein Award for his work on screen-printed aluminium contacts. He currently works at the CalLab PV Cells laboratory on the measurement of novel silicon solar cell concepts.

Max Mittag studied industrial engineering and management at the Freiberg University of Mining and Technology. In 2010 he completed his diploma thesis at Fraunhofer ISE and joined the photovoltaic modules department, where his current work includes cell-to-module efficiency analysis and the development new photovoltaic module concepts.

Alexandra Schmid received her diploma degree in physics from the TU Karlsruhe in 2006, with a diploma thesis on solar cell process development carried out at Fraunhofer ISE. She then worked on the characterization of solar cells and solar cell production processes at centrotherm, before rejoining Fraunhofer ISE in 2013. At the CalLab PV Modules test laboratory, she is involved in the development of measurement procedures for new technologies, such as bifacial or thin-film modules.

....

Enquiries

Christian Reise
Fraunhofer Institute for Solar Energy Systems ISE
Heidenhofstrasse 2
79110 Freiburg, Germany

Tel: +49 (0)761 4588 5282
Email: christian.reise@ise.fraunhofer.de

Advertisers and web index

To advertise within Photovoltaics International, please contact the sales department: Tel +44 (0) 20 7871 0122

THE INDISPENSABLE GUIDE FOR MANUFACTURERS IN SOLAR

NEXT ISSUE:

- Wet processing tools
- IBC mass production
- Calculating bifacial gain

Photovoltaics International contains the latest cutting edge research and technical papers from the world's leading institutes and manufacturers.

Divided into six sections – Fab & Facilities, Materials, Cell Processing, Thin Film, PV Modules and Market Watch – it is an essential resource for engineers, senior management and investors to understand new processes, technologies and supply chain solutions to drive the industry forward.

An annual subscription to **Photovoltaics International**, which includes four editions, is available at a cost of just $199 in print and $159 for digital access.

Make sure you don't miss out on the ultimate source of PV knowledge which will help your business to grow!

SUBSCRIBE TODAY: **www.photovoltaicsinternational.com/subscriptions**

SNEC 2018 PV POWER EXPO
Dialogue & Conference & Exhibition

www.snec.org.cn

12th (2018) International Photovoltaic Power Generation Conference & Exhibition

May 28-30, 2018

Shanghai New International Expo Center
(2345 Longyang Road, Pudong District, Shanghai, China)

关注SNEC微信   Follow us at WeChat

◎Asian Photovoltaic Industry Association / Shanghai New Energy Industry Association
◎Show Management: Follow Me Int'l Exhibition (Shanghai), Inc.
 Add：Room 902, Building No. 1, 2020 West Zhongshan Road, Shanghai 200235, China
Tel：+86-21-33561099 / 33561095 / 33561096   Fax：+86-21-33561089
◎For exhibition: info@snec.org.cn   For conference: office@snec.org.cn

PV 3.0, 360W+

About LONGi Solar

A world leading mono-crystalline solar module manufacturer for achieving best LCOE (levelized cost of electricity) solutions.

LONGi Solar is a world leading manufacturer of high-efficiency mono-crystalline solar cells and modules. The Company is wholly owned by LONGi Group. LONGi Group (SH601012) is the largest supplier of mono-crystalline silicon wafers in the world, with total assets above $2.7 billion. (2016)

Armed and powered by the advanced technology and long standing experience of LONGi Group in the field of mono-crystalline silicon, LONGi Solar has shipped approximately 2.5GW products in 2016. The Company has its headquarters in Xi'an and branches in Japan, Europe, North America, India and Malaysia.

With Strong focus on R&D, production and sales & marketing of mono-crystalline silicon products, LONGi Solar is committed to providing the best LCOE solutions as well as promoting the worldwide adoption of mono-crystalline technology.

en.longi-solar.com

LONGi Solar